CCS Chemistry

MINI REVIEW

Received: Mar. 4, 2025 | Accepted: Apr. 16, 2025 | Published: June 28, 2025

A Cyclodextrin Odyssey in the Stoddart Group: From Syntheses to Applications

Yong Wu[1*†], Enxu Liu[2†], Changxia Shi[3*†] & J. Fraser Stoddart[2,4,5,6,7,8*]

[1]*Key Laboratory of Drug-Targeting and Drug Delivery System of the Education Ministry and Sichuan Province, Sichuan Engineering Laboratory for Plant-Sourced Drug, and Sichuan Research Center for Drug Precision Industrial Technology, West China School of Pharmacy, Sichuan University, Chengdu 610041,* [2]*Department of Chemistry, The University of Hong Kong, Hong Kong SAR 999077,* [3]*Beijing National Laboratory for Molecular Sciences, Laboratory of Polymer Physics and Chemistry, Institute of Chemistry, Chinese Academy of Sciences, Beijing 100190,* [4]*Department of Chemistry, Northwestern University, Evanston, Illinois 60208,* [5]*Center for Regenerative Nanomedicine, Northwestern University, Chicago, Illinois 60611,* [6]*Stoddart Institute of Molecular Science, Department of Chemistry, Zhejiang University, Hangzhou 310027,* [7]*ZJU-Hangzhou Global Scientific and Technological Innovation Center, Hangzhou 311215,* [8]*School of Chemistry, University of New South Wales, Sydney, New South Wales 2052*

[*]*Corresponding authors: yongwu@scu.edu.cn; cxshi@iccas.ac.cn; stoddart@hku.hk;* [†]Y. Wu, E. Liu, and C. Shi contributed equally to this work.

Cite this: *CCS Chem.* **2025**, 7, 1935–1971
DOI: 10.31635/ccschem.025.202505711

Cyclodextrins (CDs)—a class of cyclic oligomers of glucopyranosyl units featuring hydrophilic rims and hydrophobic cavities—have captured the imagination of scientists for over a century. Among all naturally occurring and wholly synthetic macrocycles, CDs have established their credentials as phenomenal compounds that have made vital scientific and technological impacts on a variety of disciplines, such as the chemical, materials, environmental, biological, food, cosmetic, and medical sciences. In this minireview, we look back upon the Stoddart group's 56-year journey of adventure and achievements in relation to CDs. Advances we have made in the chemical syntheses of CD derivatives, analogues, and enantiomers are summarized. The integration of CDs and their derivatives as nanoscale building blocks for the (non)covalent functionalization of surfaces, nanotubes, and polymers, as well as in the construction and applications of chemically modified molecules and supermolecules—for example, CD-based second-sphere coordination complexes, CD metal–organic frameworks, and CD-based mechanically interlocked molecules—are presented. Our exploration in CD science and technology highlights the versatility of CDs in both fundamental and applied sciences, suggesting that there is still ample room for future discoveries.

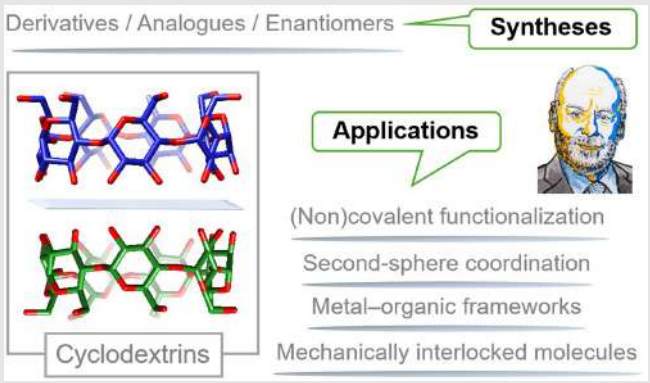

Keywords: chemical synthesis, drug release, gold separation, host–guest chemistry, hydrophobic interactions, mechanically interlocked molecules, metal–organic frameworks, (non)covalent functionalization, second-sphere coordination, supramolecular chemistry

DOI: 10.31635/ccschem.025.202505711
Citation: *CCS Chem.* **2025**, 7, 1935–1971
Link to VoR: https://doi.org/10.31635/ccschem.025.202505711

Introduction

Macrocycles,[1] which are either available from natural sources or can be obtained by unnatural product synthesis, lie at the heart of research in host–guest[2] and supramolecular[3] chemistry. The covalently linked structures of these macrocycles dramatically reduce their conformational flexibilities, enabling them bind guests by means of a collection of noncovalent interactions[4] without incurring large losses in conformational entropy. The selective binding of guests within the cavities of macrocycles mimics the ligand–receptor interactions found ubiquitously in biological systems and allows scientists to manipulate the physical, chemical, and biological properties of guest molecules with unprecedented precision and selectivity. It was for the development and use of certain types of macrocycles—which include but are not limited to crown ethers, cryptands, cavitands, and spherands—that Pedersen,[5] Lehn,[6] and Cram[7] were jointly awarded the Nobel Prize in Chemistry in 1987.

Although the past decades have witnessed[8–22] rapid growth in the number of wholly synthetic macrocycles, the century-old, naturally occurring cyclodextrins (CDs) have remained[23–26] the most popular class with more than 2,000 publications appearing in the scientific literature each year.[27] Despite the fact that CDs (α and β) were first discovered serendipitously by Villiers[28] early in 1891 as unwanted byproducts from a culture medium of *Bacillus amylobacter* grown on starch, it took some 80 years, up until the 1970s, for scientists to characterize the chemical structures, determine suitable approaches for product purification, elucidate the enzyme's mechanism of action, improve and scale up the enzyme-mediated synthetic protocol, clarify their excellent biocompatibility, and most importantly of all, uncover their remarkable ability to form inclusion complexes with a wide variety of substrates. Over this period, seminal contributions, from hypotheses to experimental demonstrations, have been made by pioneers including Schardinger,[29] Pringsheim,[30] Karrer,[31] Freudenberg,[32] French,[33] Cramer,[34] Casu,[35] Bender,[36] Saenger,[37] Breslow,[38] and Szejtli,[39] to mention just a few names.

Currently, the best known (Figure 1a) and studied α-, β-, and γ-CDs are homologous cyclo-oligosaccharides consisting, respectively, of six, seven, and eight

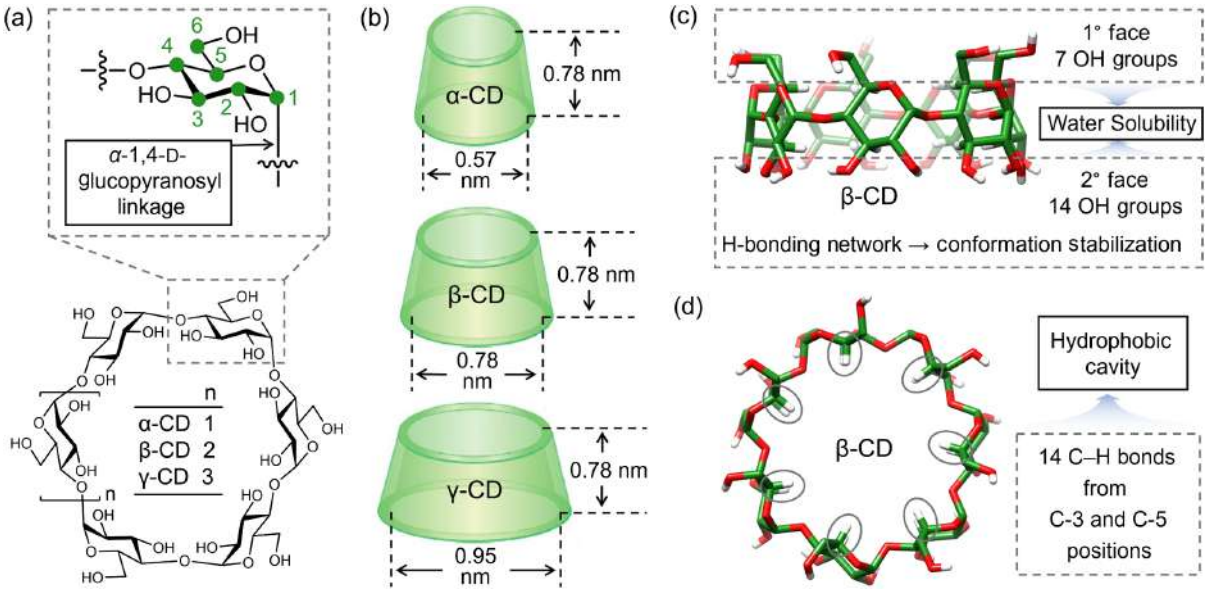

Figure 1 | *Structural features of α-, β-, and γ-CDs, which belong to the point group C_6, C_7, and C_8, respectively. (a) Structural formulas of α-, β-, and γ-CDs, featuring six, seven, and eight α-1,4-linked D-glucopyranosyl units, respectively. (b) Graphical representations of α-, β-, and γ-CDs showing the depths and diameters of their cavities. (c) A side-on view of β-CD as a stick representation showing that all primary and secondary OH groups are distributed around the 1° and 2° faces, respectively. The stabilization of the relatively rigid truncated cone-shaped conformation resulting from intramolecular hydrogen-bonding networks formed between OH groups at the 2° faces. The existence of 21 OH groups causes β-CD soluble in water. (d) A plan view of β-CD as a stick representation showing that 14 C–H bonds from C-3 and C-5 positions are pointing inwards, causing the central cavity to be hydrophobic. The crystal structures shown in (c, d) have been redrawn from Cambridge Crystallographic Data Centre (CCDC) deposition number 674965. Hydrogen atoms on C-1, C-2, C-4, and C-6 positions and solvent molecules have been omitted for the sake of clarity. C green, H white, O red.*

DOI: 10.31635/ccschem.025.202505711
Citation: *CCS Chem.* **2025**, 7, 1935–1971
Link to VoR: https://doi.org/10.31635/ccschem.025.202505711

glucopyranosyl units which are linked solely by α-1, 4-D-glucopyranosyl bonds. The most stable conformations of CDs are relatively rigid truncated cones (Figure 1b), which are stabilized (Figure 1c) by intramolecular hydrogen-bonding networks formed between hydroxyl (OH) groups at their secondary (2°) faces. On account of the existence of numerous OH groups distributed around the two rims and many C–H bonds from C-3 and C-5 positions pointing inwards, respectively, CDs are molecules (Figure 1c,d) with both hydrophilic exteriors and hydrophobic cavities. These structural features of CDs endow them with unusual properties relating to molecular recognition—courtesy of noncovalent interactions such as hydrophobicity,[40] hydrogen bonding,[41] and van der Waals[42] interactions—to form water soluble inclusion complexes with small molecules and portions of larger compounds. The ability of CDs to host various guests is the reason for their widespread adoption in subsequent academic research and industrial applications.

In addition to their inclusion complex-forming propensities, CDs have shown themselves to be able to promote or catalyze chemical reactions on both covalently and noncovalently bound substrates. These catalytic properties, reminiscent of the prerogative of enzymes, has fired the imagination of many scientists to develop[43–46] enzyme mimics and analogues based on native CDs and their derivatives. On account of their inherently stable chiralities, which result in chiral discrimination when binding and complexing with enantiomers, CDs have also found broad applications in chiral recognition and separations.[47–49] Of particular note, the use of CDs and their derivatives as chiral selectors in high-performance liquid chromatography (HPLC), gas chromatography, and capillary electrophoresis has played[50,51] a dominant role in enantiomeric analysis and separations. These CD-based analytic and separation techniques form the basis of a number of well-established practices in the modern pharmaceutical, agrochemical, and food industries.

CDs can be mass-produced on an industrial scale of more than 10,000 metric tons[52] per year through enzymatic modification of one of the most abundant natural polysaccharides, that is, amylose in starch, making them ten-a-penny nowadays. The facile availability and excellent biocompatibility[53] of CDs have allowed them to be consumed by humans as ingredients of food, cosmetics, and drugs.[24,27,54] As the only class of hosts that has been credited the "generally recognized as safe" status by the U.S. Food and Drug Administration, CDs and their derivatives are widely used as excipients in the formulation of 130 approved drugs.[55,56] Additionally, CD derivatives can serve as (potential) active pharmaceutical ingredients, for example, in the blockbuster drug sugammadex,[57,58] and a number of drug candidates such as adamgammadex,[59,60] HPβCD,[61] and UDP-003,[62] to meet some of the unmet medical needs in clinical practice.

Aside from the abovementioned applications, CDs have also played crucial roles in numerous research niches such as photochemistry and photophysics,[63–65] environmental chemistry,[66,67] polymer chemistry,[68–70] molecular imaging,[71,72] and gene delivery.[73,74] Almost every aspect of CDs, both fundamental and applied, has been reviewed[23–27,29–39,43–48,50–56,63,67,75–113] by us as well as by other groups over the past decades, and so this minireview focuses on the Stoddart group's 56-year journey of adventures in relation to CDs. This review emphasizes (1) the design and syntheses of CD derivatives, analogues, and enantiomers, (2) the use of CD derivatives for the (non)covalent functionalization of surfaces, nanotubes, and polymers, and (3) the integration of CDs and their derivatives as nanoscale building blocks in the construction and applications of chemically modified molecules and supermolecules—for example, CD-based second-sphere coordination complexes, CD metal–organic frameworks (CD-MOFs), and CD-based mechanically interlocked molecules (MIMs). We hope that this review article—which provides a comprehensive landscape of how rational design, serendipity, extensive collaborations, as well as our long-term interest and persistence in CD science and technology, have all contributed to the field—will serve as an inspiration to attract and encourage more researchers to explore the unknown of CDs.

Syntheses of Cyclodextrin Derivatives, Analogues, and Enantiomers

The scope of native CDs for diverse research and application purposes is hampered by a number of structural features, not least of all (1) the lack of chemically useful functional groups, that is, only one type of functional, i.e., OH groups, is present; (2) the lack of monosaccharide diversity of the cyclo-oligosaccharide skeleton, which results in a challenge to perturbate the innate structural features of CDs; and (3) the long-standing lack of available enantiomeric CDs, which restrains their full potential, particularly when the stereochemistry and chirality become considerations. In order to release CDs from these structural straightjackets, considerable efforts by the Stoddart group have been devoted to making (1) CD derivatives with site-selective modifications; (2) CD analogues containing a range of different monosaccharides; and (3) most recently, three mirror-image CDs, or L-CDs, as we prefer to call them. In this section, we will present, one by one, the motivations, general considerations, and simplified synthetic routes related to meeting the challenges posed by (1), (2), and (3).

DOI: 10.31635/ccschem.025.202505711
Citation: *CCS Chem.* **2025**, 7, 1935–1971
Link to VoR: https://doi.org/10.31635/ccschem.025.202505711

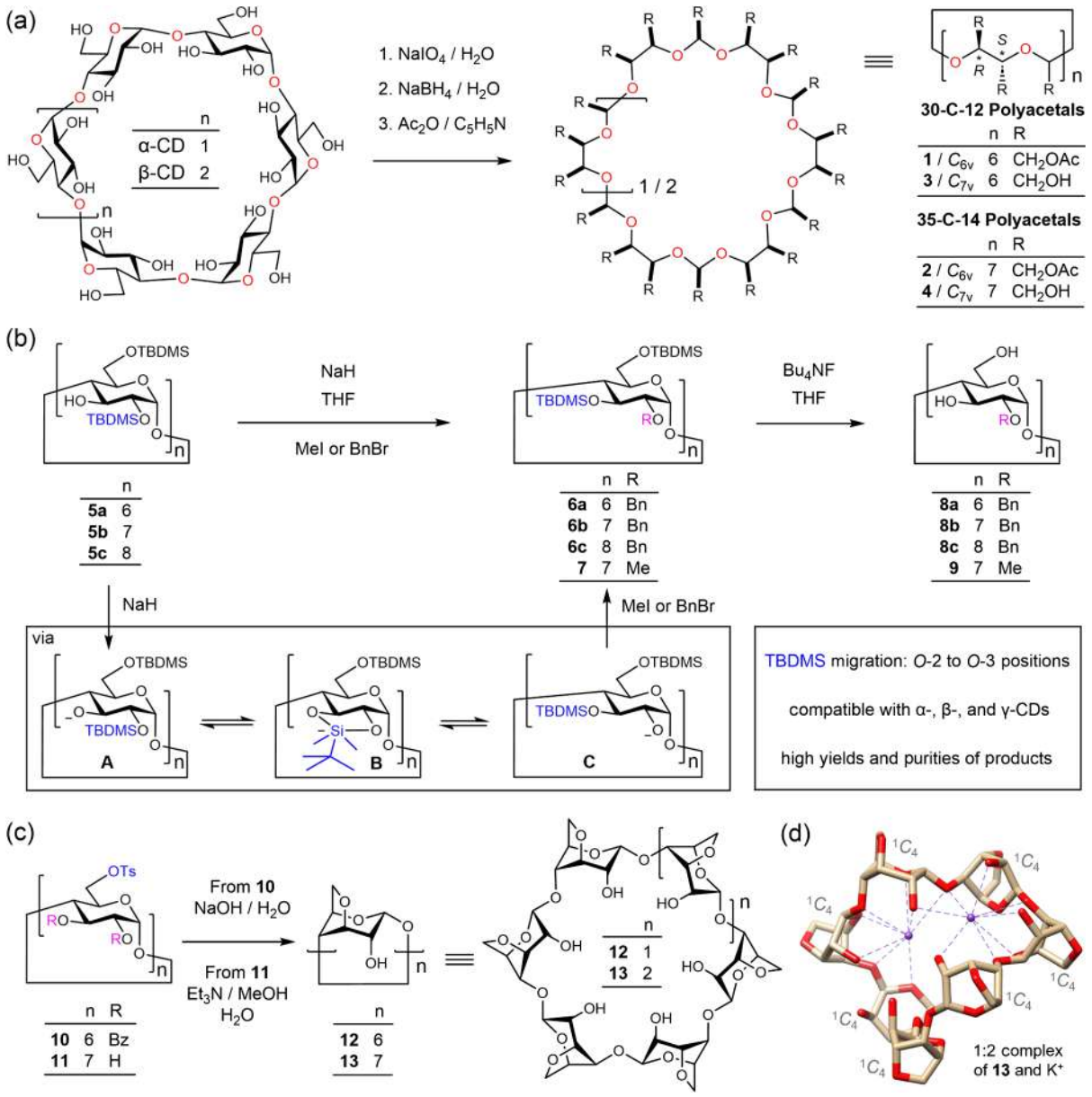

Figure 2 | *(a) Syntheses of 30-crown-12 and 35-crown-14 polyacetals from α- and β-CDs, respectively, through a three-step procedure. (b) Selective per-2-O-alkylation of α-, β-, and γ-CDs featuring a silyl group-migration (O-2 to O-3) mechanism. (c) Syntheses of per-3,6-anhyro-α- and β-CDs (**12**, **13**) from tosylates (**10**, **11**), respectively, under basic conditions. (d) Crystal structure of a 1:2 complex of **13** and K^+ ions. All sugar units of **13** adopt $^1C_4$ conformations. The crystal structure shown in (d) has been redrawn from CCDC deposition number 1251319. Hydrogen atoms and solvent molecules have been omitted for the sake of clarity. C brown, O red, K purple.*

Cyclodextrin Derivatives

Selective chemical modifications on native CDs, which result in affecting their solubilities in water and other solvents, in addition to tuning their host–guest properties for improved chiral recognition and enzyme mimicry, have attracted considerable research interest by other researchers.[47,85,86] While most synthetic efforts aimed at making CD derivatives have led to the production of a large number of compounds preserving their native cyclo-oligosaccharide skeletons, our first encounter with CDs resulted (Figure 2a) in the syntheses of heterocyclic ring compounds, that is, achiral [30]crown-12 and [35] crown-14 polyacetals. Turning the clock back over half a century, it was in the late 1960s—when Stoddart was pursuing research with Dr Walter Szarek[114] at Queen's University under the auspices of a National Research Council of Canada Postdoctoral Fellowship—that the

DOI: 10.31635/ccschem.025.202505711
Citation: *CCS Chem.* **2025**, 7, 1935–1971
Link to VoR: https://doi.org/10.31635/ccschem.025.202505711

groundbreaking research by Pedersen[8,9] related to making of large-sized rings, that is, crown ethers, was published in the *Journal of the American Chemical Society*. Inspired by Pedersen's seminal research, Stoddart realized that α- and β-CDs can serve as ideal precursors to access, respectively, 30- and 35-membered heterocyclic rings **1** and **2** following a three-step procedure.[115,a] Some 30 years later, the synthesis of heterocyclic ring **1** was repeated by Lichtenthaler and coworkers[116] in order to produce a per-hydroxymethylated [30]crown-12 polyacetal (**3**) for the investigation of its molecular geometry in the solid state as well as in solution.

The OH groups on the primary (1°) faces of CD tori are more reactive than the OH groups on the 2° faces. As a result, mono- and per-functionalization on the 1° faces of CDs are relatively straightforward and reliable.[117–123] Selective functionalization on the 2° faces, which requires the distinguishing of reactivities between the 2-OH and 3-OH groups, has, however, proved to be much more challenging.[85,86,124] For instance, when following a previously reported[125–127] protocol to perform selective 2,6-*O*-methylation of β-CD, the product, that is, per-2,6-di-*O*-methyl-β-cyclodextrin (DM-β-CD), we obtained was found[128–130] to be less than 70% pure. The main impurity was identified[128,b] as an unsymmetrical overmethylated cyclodextrin derivative (DM+1)-β-CD. These early investigations by the Stoddart group underscore the importance of synthesizing chemically modified CDs with sufficient purity using reliable methods.

In 1995, the Stoddart group described[131] a novel approach (Figure 2b) to the synthesis of some chemically modified CDs, that is, per-2-*O*-alkylated derivatives. This approach takes advantage of the migratory property of *tert*-butyldimethylsilyl (TBDMS) groups as substituents attached to the C-2 positions of α-, β-, and γ-CD derivatives. Specifically, per-2,6-di-*O*-*tert*-butyldimethylsilyl CDs (**5a, 5b**, and **5c**) react with alkyl or benzyl halides under strongly basic conditions to produce per-2-*O*-alkylated-3,6-di-*O*-silylated derivatives (**6a, 6b, 6c**, and **7**), which can be subjected to desilylation to afford regio-specifically the per-2-*O*-alkylated derivatives (**8a, 8b, 8c**, and **9**). In the proposed mechanism, the site-selective per-2-*O*-alkylation is dependent on a two-step process, in which (1) TBDMS groups of intermediates **A** migrate from *O*-2 to *O*-3 positions, via the formation of transition states **B**, to generate intermediates **C** and (2) alkylation of the *C*-2 positions of the more reactive intermediates **C** takes place under kinetic control. The protocol is not only compatible with α-, β-, and γ-CDs but also gives products of high yields and purities. The reliability and practicality of this protocol have been showcased subsequently by others[132] in the syntheses of a library of 2-*O*-substituted CD derivatives for the development of new reversal agents for the neuromuscular blocker rocuronium bromide.

Selective modifications of the OH groups of CDs may result[133] in the interconversion of D-glucopyranosyl units from $^4C_1$ to $^1C_4$ chair conformations, offering the opportunity to tune their host–guest chemistry. One example of this kind was reported[134,135] by the Stoddart group in 1991. When compounds **10** and **11** are treated (Figure 2c) with base, the oxygen atoms at C-3 positions attack—only if the D-glucopyranosyl rings adopt $^1C_4$ conformations—the C-6 positions where tosyl groups act as leaving groups. All the six-membered rings (Figure 2d) in the resulting per-3,6-anhydro-CDs (**12**, **13**) adopt $^1C_4$ conformations.[136] On account of the fact that these CD derivatives are rich in well-oriented oxygen atoms in their cavities, they can act as hosts for both ammonium ions and metal cations, as revealed[135,136] by fast atom bombardment mass spectrometry and X-ray crystallography (Figure 2d) carried out on single crystals of 1:2 complexes of **13** and K^+. Coincidentally, research by Gadelle and Defaye,[137] which employed halides as the leaving groups at C-6 positions to produce the same compounds **12** and **13**, was published, together with the research by the Stoddart group, as back-to-back communications[134,137] in *Angewandte Chemie* in 1991.

Cyclodextrin Analogues

During the last two decades before the end of the 20th century, growth in synthetic carbohydrate chemistry was rapid in order to meet the increasing demand of glycobiology for homogeneous oligosaccharides and glycoconjugates. With a growing number of new glycosylation methods[138,139] and glycan assembly strategies[140] available, carbohydrate chemists were able to access many complex oligosaccharides and polysaccharides employing de novo synthesis. In particular, the syntheses[141,142] of some unnatural cyclo-oligosaccharides from saccharides other than D-glucopyranose opened up the possibility of building new cyclo-oligosaccharide skeletons that could potentially exhibit their own distinctive host–guest chemistry. Encouraged by the successful syntheses of D-manno- and L-rhamno-oligosaccharides reported, respectively, by Ogawa and coworkers[143–145] and Nishizawa and coworkers,[146–148] the Stoddart group attempted and completed[141,149,150] the syntheses (Figure 3) of a series of CD analogues composed of alternating D- and L-sugars.

In contrast to the common stepwise syntheses of linear precursors followed by cycloglycosylation strategy often used[143–148,151] in the preparation of cyclo-oligosaccharides, the Stoddart group's synthetic routes towards a number of CD analogues (**20**–**24**, **26**, **27**, and **29**) relied[141] on polycondensation–cyclization or cyclo-oligomerization strategy. Our group employed[150] a disaccharide **19**, which bears a trityloxy group as the glycosyl acceptor function in the D-rhamnopyranosyl residue and a

DOI: 10.31635/ccschem.025.202505711
Citation: *CCS Chem.* **2025**, 7, 1935–1971
Link to VoR: https://doi.org/10.31635/ccschem.025.202505711

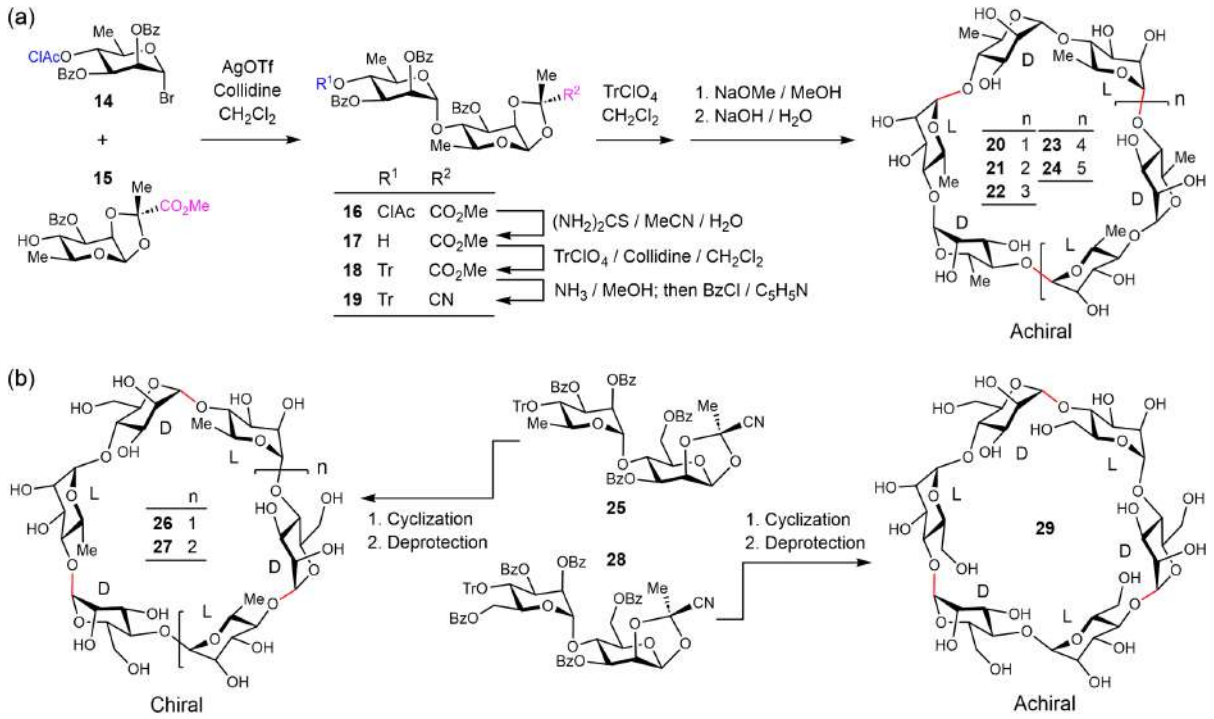

Figure 3 | *(a) Syntheses of achiral cyclic hexa- to tetradecasaccharides **20**–**24** employing a polycondensation–cyclization strategy in which disaccharide **19** serves as the monomer. (b) Syntheses of cyclo-oligosaccharides **26**, **27**, and **29** from disaccharide monomers **25** and **28**, respectively. While both cyclohexasaccharides **26** and cyclo-octasaccharide **27** are chiral, cyclo-octasaccharide **29** is achiral.*

1,2-*O*-cyanoethylidene group[152] as the glycosyl donor function in the L-rhamnopyranosyl residue, as the monomer (Figure 3a). Disaccharide **19** was obtained through a condensation reaction between a D-rhamnosyl bromide **14** and a L-rhamnosyl acceptor **15** bearing a 1,2-*O*-methoxycarbonylethylidene group as a latent[153–155] leaving group, followed by a three-step protecting group manipulation. The crucial polycondensation of monomer **19** in dilute solution proceeded smoothly and gave a series of homologous compounds, which were subject to global protection to produce five CD analogues, that is, cyclic hexa- to tetradecasaccharides **20**–**24** with alternating D- and L-rhamnopyranosyl residues.

It is worth noting that the products, composed only of even numbers of sugar residues, were obtained for the simple reason that a disaccharide was chosen as the monomer. The same synthetic strategy (Figure 3b) as that described for the syntheses of compounds **20**–**24**, was employed[149,150] for the construction of another two CD analogues, one pair (**26**/**27**) consisting of alternating D-mannopyranosyl and L-rhamnopyranosyl residues, the other (**29**) consisting of alternating D- and L-mannopyranosyl residues. In sharp contrast to the polycondensation of monomer **19**, which gave cyclic oligomers of up to a 14-mer, relatively smaller rings were obtained as the main products (**26**/**27**/**29**) in the polycondensations wherein disaccharide **25** or **28** was employed as the monomer.

For a number of these synthetic D/L cyclo-oligosaccharides, for example, **21**, **22**, **27**, and **29**, single crystals suitable for X-ray crystallographic analysis were obtained, and their solid-state structures were solved. In all cases, the crystallographic analyses revealed that these new CD analogues adopt cylindrical conformations (Figure 4a,c,e)—a distinctive feature when compared with those truncated cone-shaped conformations of natural CDs. The secondary OH groups are located at both rims, and as a result, these CD analogues are absent of the so-called 1° and 2° faces. In addition, when compared with large-ring CDs, for example, δ-CD with nine D-glucopyranosyl units and ε-CD with 10 D-glucopyranosyl units, whose conformations are much distorted,[75] cyclodecasaccharide **22** can maintain its cylindrical conformation in the solid state (Figure 4c,d). The packing of these cylindrical molecules in the crystal lattices of **21**, **22**, and **27** forms infinite stacks, creating[149,150,156] nanotube-like arrangements (Figure 4b,d,f), reminiscent of the supramolecular nanotubes formed by cyclic peptides composed of alternating D/L amino acids reported by Ghadiri et al.[157]

DOI: 10.31635/ccschem.025.202505711
Citation: *CCS Chem.* **2025**, 7, 1935–1971
Link to VoR: https://doi.org/10.31635/ccschem.025.202505711

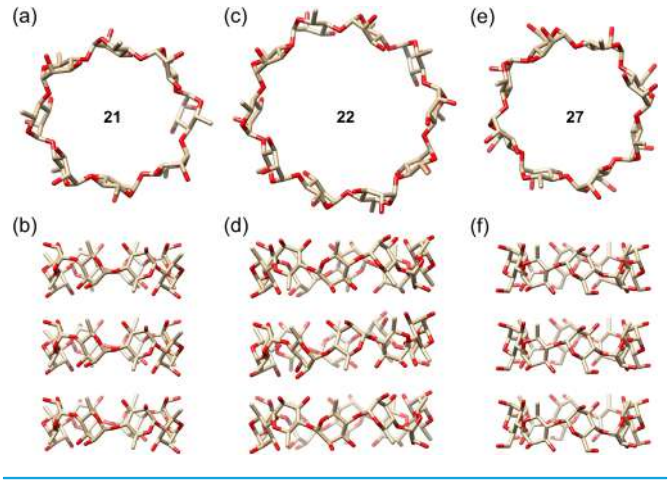

Figure 4 | *Plan views of (a) cyclooctasaccharide **21** and (c) cyclodecasaccharide **22** with alternating D- and L-rhamnopyranosyl residues, as well as (e) cyclo-octasaccharide **27** with alternating D-mannopyranosyl and L-rhamnopyranosyl residues as stick representations showing their cylindrical conformations. Side-on views of discrete stacks of (b) **21**, (d) **22**, and (f) **27** as stick representations showing nanotube-like superstructures. The crystal structures shown in (a/b), (c/d), and (e/f) have been redrawn from CCDTBDC deposition numbers 1221815, 100130, and 1265649, respectively. Hydrogen atoms and solvent molecules have been omitted for the sake of clarity. C brown, O red.*

Cyclodextrin Enantiomers

One of the most striking features of naturally occurring CDs, that is, D-CDs, compared to other types of canonical supramolecular hosts,[1] is that they are compounds with inherently stable chiralities. Indeed, it is this feature that forms the basis of numerous applications in areas such as chiral recognition, separation science, chemical reactions/catalysis, and in the creation of chiral materials. Clearly, the fact that mirror-image versions of D-CDs were previously unavailable has limited the realization of their full potential. More importantly, since D-CDs have found countless applications in biological systems that are composed of overwhelmingly homochiral biomolecules, the availability of mirror-image CDs, that is, L-CDs, would provide scientists with a unique opportunity to investigate[158–160] their roles at the interface with biology, for example, in drug delivery systems or as active pharmaceutical ingredients.

In order to address this fundamental research niche, the Stoddart group recently achieved[161,162] the synthesis for the first time of the three L-CDs—namely, α-, β-, and γ-L-CDs, which contain (Figure 5) six, seven, and eight L-glucopyranosyl units, respectively. In contrast to most synthetic cyclooliosaccharides[141] linked mainly by 1,2-*trans* glycosidic bonds, the production of the L-CDs requires the construction of multiple contiguous 1,2-*cis* glycosidic linkages, which constitutes a long-standing challenge in carbohydrate chemistry.[163]

In order to meet this challenge head on, two specifically designed monosaccharide building blocks, that is, **30** and **31**, both of which bear benzoyl (Bz) groups at their C-6 positions, were employed. The construction of α-L-glucopyranosidic linkages takes advantage (Figure 5a) of the remote anchimeric assistance[164–168] of these Bz groups, aided and abetted by a β-face shielding effect provided by Et_2O. The condensation of **30** and **31** in the presence of *p*-TolSOTf, which was generated in situ from *p*-TolSCl and AgOTf in Et_2O, produced (Figure 5a) a disaccharide donor **32** with complete α-selectivity. Removal of the TBDMS groups on **32** gave a disaccharide acceptor **33**, which was employed in a donor preactivation-based, three component one-pot glycosylation,[169–173] resulting in a linear hexasaccharide **34** without the need to isolate the intermediate linear tetrasaccharide. Further elongation of the glycan chain through coupling reactions with one and two monosaccharide acceptors **31**, generated linear hepta- and octasaccharides **35** and **36**, respectively. Removal of the TBDMS groups on **34**, **35**, and **36**, followed by cyclizations, gave the fully protected derivatives of α-, β-, and γ-L-CDs—namely, **40**, **41**, and **42**. Global deprotection produced (Figure 5b) the three L-CDs on half-gram scales in no more than eight steps from simple and readily available monosaccharide building blocks **30** and **31**.

An X-ray crystallographic investigation of a β-D- and β-L-CD cocrystal revealed that the two enantiomers self-sort into layered assemblies in which two adjacent layers are composed of the same enantiomers (Figure 6a). The stacking of both enantiomers along the *c*-axis in an alternating DDLL manner results (Figure 6b,c) in nanotube-like arrangements. This crystallographic packing of enantiomeric CDs raises the question: what would the effect be if racemic CDs, instead of D-CD by itself, were used in applications such as drug formulations? As expected, L-CDs are much more biostable than their natural counterparts, as revealed[174] in a recent in vitro investigation, suggesting that they might have a unique role to play in biochemistry and biomedicine. In vivo experiments continue to be carried out, however, in order to shed light on the absorption, distribution, metabolism, excretion, and toxicity profiles of these wholly synthetic L-CDs.

(Non)covalent Functionalization of Surfaces, Nanotubes, and Polymers

Selectively modified CDs are attractive nanoscale building blocks that can be incorporated onto surfaces, nanotubes, and polymers resulting from either covalent or

DOI: 10.31635/ccschem.025.202505711
Citation: *CCS Chem.* **2025**, 7, 1935–1971
Link to VoR: https://doi.org/10.31635/ccschem.025.202505711

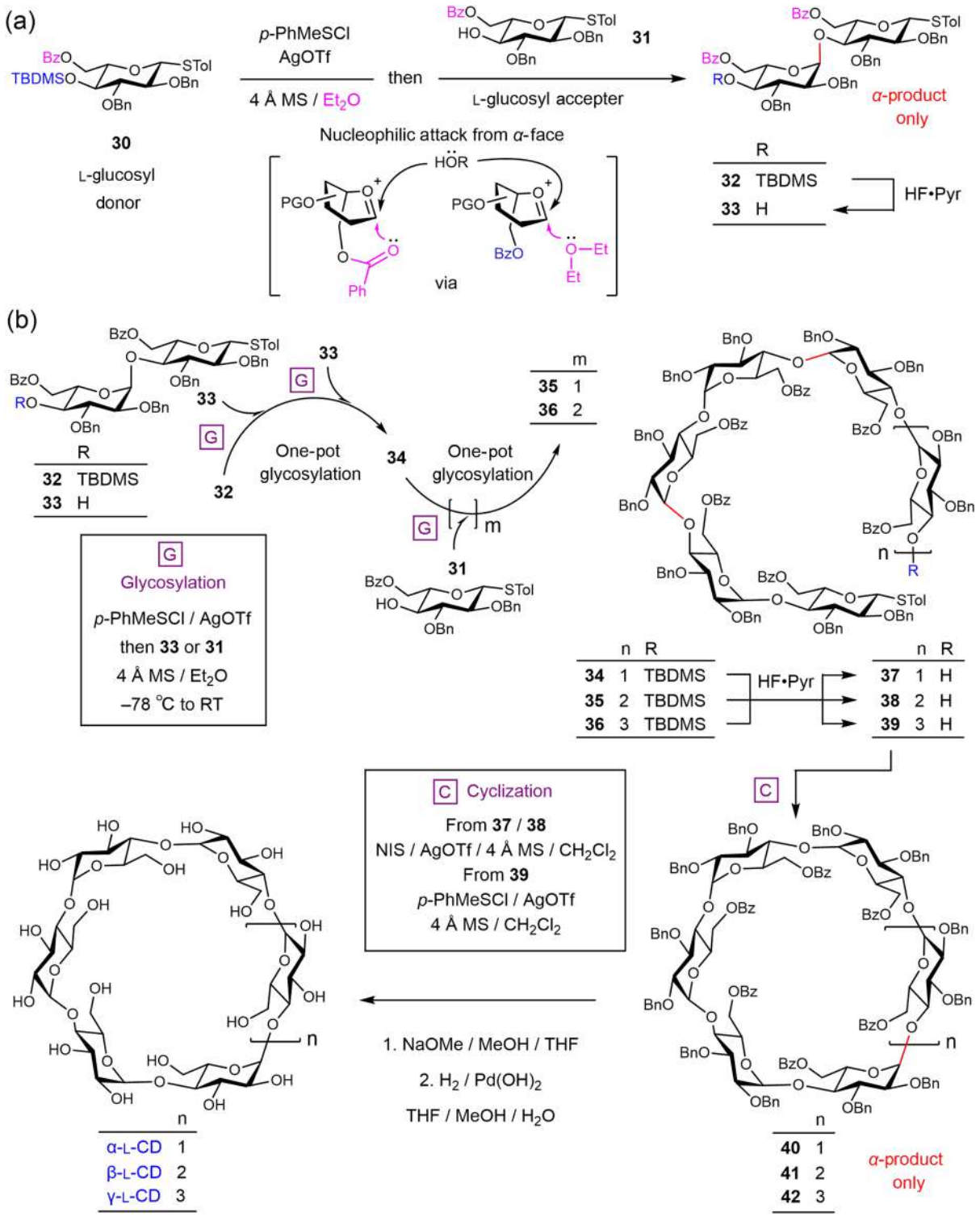

Figure 5 | *(a) Syntheses of disaccharides **32** and **33** from monosaccharide building blocks **30** and **31** employing a highly diastereoselective α-L-glucopyranosyl glycosylation followed by the removal of TBDMS groups. (b) Syntheses of α-, β-, and γ-L-CDs from building blocks **31**, **32**, and **33** featuring one-pot glycosylations, protecting group manipulations, cyclizations, and global deprotections.*

noncovalent bonding interactions (NCIs) in order to achieve tailored properties and functions. In this context, the Stoddart group has employed[175–179] (1) thiolated β-CD (T-β-CD) for the covalent functionalization of gold surfaces in collaboration with Angel Kaifer at the University of Miami, (2) pyrene-modified β-CD (P-β-CD) for the

DOI: 10.31635/ccschem.025.202505711
Citation: *CCS Chem.* **2025**, 7, 1935–1971
Link to VoR: https://doi.org/10.31635/ccschem.025.202505711

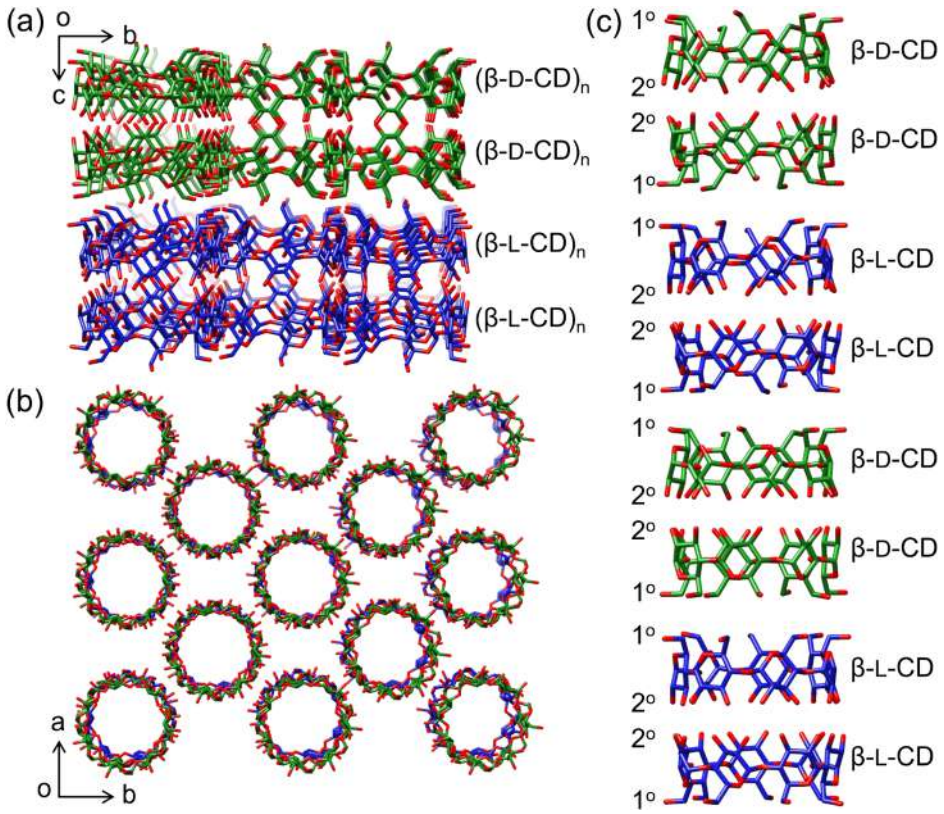

Figure 6 | *Solid-state superstructures of the β-D- and β-L-CD cocrystal as stick representations viewed along (a) the a-axis and (b) the c-axis. (c) A side-on view of a discrete stack of β-D- and β-L-CDs as a stick representation showing an alternating DDLL packing pattern. Adapted with permission from ref 161. Copyright 2024 Springer Nature.*

noncovalent modification of single-walled carbon nanotubes (SWNTs) in collaboration with George Grüner at the University of California, Los Angeles (UCLA), and (3) deoxycholic acid-modified β-CD (D-β-CD) for the reversible noncovalent modification of an azobenzene-branched poly(acrylic acid) (ABP) copolymer.

Covalent Functionalization of Surfaces

Chemisorption of organosulfur compounds on gold surfaces is a well-known phenomenon[180,181] that leads to the

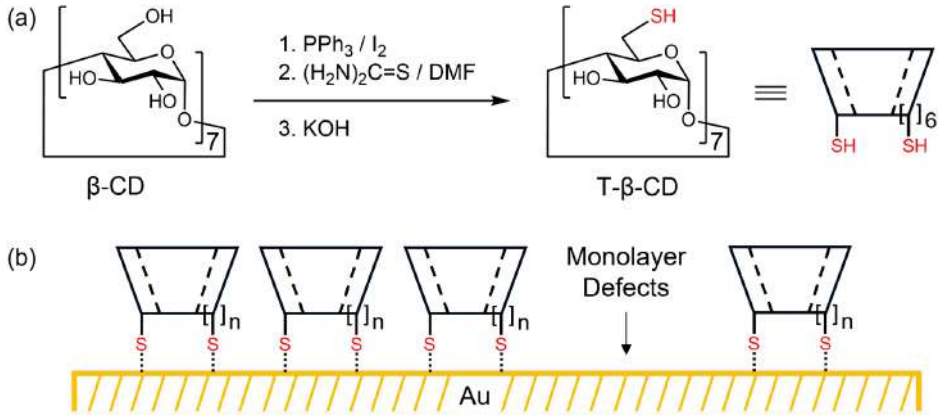

Figure 7 | *(a) Synthesis of T-β-CD from β-CD. (b) Schematic representation of the chemisorption of T-β-CD onto a gold surface employing a maximum of seven thiolate–gold covalent bonds per receptor molecule, achieving an estimated surface coverage in the range 64%–75%.*

DOI: 10.31635/ccschem.025.202505711
Citation: *CCS Chem.* **2025**, 7, 1935–1971
Link to VoR: https://doi.org/10.31635/ccschem.025.202505711

formation of self-assembled monolayers exhibiting highly organized molecular structures. In order to introduce well-defined binding sites to monolayers so as to investigate the interfacial binding properties of the resulting monolayer assemblies, T-β-CD—a β-CD derivative (Figure 7a) in which all primary OH groups are substituted with thiol groups—was prepared[175] from β-CD. T-β-CD chemisorbs strongly onto gold surfaces, employing a maximum of seven thiolate–gold bonds per receptor molecule, achieving (Figure 7b) an estimated surface coverage in the range 64%–75%. Although this covalent functionalization results in imperfect monolayers in which a significant portion of the gold surface remains uncovered, these defects can be eradicated by treating the monolayers with a combination of ferrocene and pentanethiol.[175] Ferrocene, which is an excellent guest for β-CD, occupies the monolayer binding sites, thereby guiding pentanethiol to occupy and seal the defective areas of the monolayer. Gold electrodes modified by this approach demonstrated robust binding properties when exposed to aqueous solutions containing low concentrations (<60 μM) of ferrocene: voltammetric responses indicate[175] the expected reversible oxidation of CD-bound ferrocene. The dynamic nature of interfacial ferrocene complexation was confirmed[175] by competition experiments employing *m*-toluic acid (mTA), wherein the voltammetric signals of the CD-bound ferrocene gradually diminished with increasing concentrations of mTA.

Noncovalent Functionalization of Nanotubes

SWNTs are recognized[182] for their biocompatibility, appropriate size, and heightened sensitivity to minor electrical changes, demonstrating significant potential for the electronic detection of biological entities and simple gases. Despite these advantages, the insolubility of SWNTs in most organic solvents and the challenges associated with handling these complex carbon nanostructures significantly hinder their practical applications. Consequently, there is a substantial demand for low-cost, industrially viable methods to modify the structures and properties of SWNTs so as to extend their usability.[183] Among various strategies, noncovalent functionalization of SWNTs contributes significantly to preserving their intrinsic properties while markedly enhancing their solubility.[176]

In order to incorporate CDs into the noncovalent functionalization of SWNTs, P-β-CD—a β-CD derivative in which a pyrene functionality is attached to its 1° face—was synthesized and coated onto SWNTs as a result of [π···π] interactions.[177] The resulting P-β-CD-SWNT hybrids were employed (Figure 8a,b) in the fabrication of SWNT/field-effect transistor (FET) devices, which can function as chemical sensors capable of detecting nonfluorescent organic molecules selectively in aqueous environments by means of β-CD-mediated molecular recognition. This noncovalent functionalization of SWNTs with P-β-CD enhances their interactions with organic molecules, resulting in detectable changes in the electrical properties of SWNT/FET devices.

As a proof-of-concept investigation,[177] we selected (Figure 8a) five organic compounds—namely, 1-adamantanol (1-ADA), 2-adamantanol (2-ADA), 1-adamantanecarboxylic acid (1-ACA), sodium cholate (SC), and sodium deoxycholate (SD)—as test substrates. These substrates are known to bind β-CD to form inclusion complexes with different binding affinities, while they are not expected to interact directly with the SWNTs. The electrical conductance of the device exhibited high

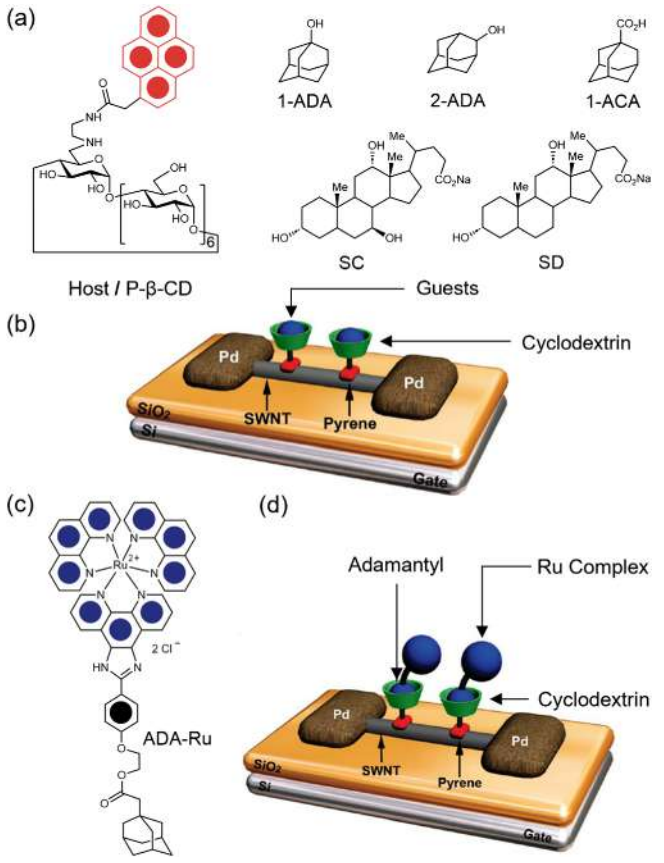

Figure 8 | *(a) Structural formulas of P-β-CD and the five guests—namely, 1-ADA, 2-ADA, 1-ACA, SC, and SD. (b) Schematic representation of the P-β-CD-decorated SWNT/FET device showing how P-β-CD-decorated SWNT hybrids interact with guests when they are being sensed in the FET device. (c) Structural formula of the ADA-Ru complex. (d) Schematic representation of the P-β-CD-decorated SWNT/FET device showing how P-β-CD-decorated SWNTs interact with ADA-Ru complexes when they are being sensed in the FET device. (b and d) Adapted with permission from ref 176. Copyright 2009 American Chemical Society.*

DOI: 10.31635/ccschem.025.202505711
Citation: *CCS Chem.* **2025**, 7, 1935–1971
Link to VoR: https://doi.org/10.31635/ccschem.025.202505711

sensitivity to these guest molecules, varying significantly with changes in their surface adsorption. The shifts in transistor characteristics correlated directly with the complex formation constants (K_S) between P-β-CD and these guests, enabling both selective and quantitative detection of organic molecules in aqueous solutions. The K_S values for the complexation of P-β-CD with these guest molecules follow the sequence: 1-ADA > 2-ADA > 1-ACA > SD > SC, with the highest one of 44,200 ± 2000 M^{-1} for 1-ADA and the lowest one of 4370 ± 2004 M^{-1} for SC.

When exposed to substrate molecules, which can be encapsulated within the cavities of β-CD with moderate K_S values and do not have appreciable interactions with the SWNTs, the transistor characteristics of the SWNT/FET devices shift toward negative gate voltages. These voltage shifts are strongly dependent on the K_S values between these guests and P-β-CD and follow a linear relationship. It is hypothesized that the changes in transistor characteristics, specifically conductivity (G), result from alterations in carrier concentration (n) on account of a charge-transfer process from P-β-CD to the SWNTs or from changes in carrier mobility (μ) caused by potential scattering and SWNT deformation. As G is defined by the formula $G = n\mu e$, where e is the electron charge, transistor measurements of the transfer characteristics in the SWNT/FET devices effectively discern between changes in carrier concentration and variations in carrier mobility. The experimental data demonstrates that the electrical conductance of the P-β-CD-decorated SWNTs is responsive to specific organic molecules and varies markedly with alterations in their surface adsorption. This platform holds substantial promise for practical applications in environmental monitoring, medical diagnostics, and gene-chip technologies.[184]

Additionally, we have utilized (Figure 8c,d) the P-β-CD-decorated SWNT/FET device as a tunable photosensor[178] in aqueous solutions to detect a luminescent ruthenium complex, that is ADA-Ru. In this SWNT/FET device, the P-β-CD, which was coated onto the SWNT surfaces, functions as a sensing host, while the ADA-Ru acts as a sensing guest. The host–guest interactions between P-β-CD and ADA-Ru result in the formation of an inclusion complex, in which the adamantyl moiety of ADA-Ru inserts into the cavity of P-β-CD, facilitating a charge-transfer process between the ADA-Ru and the P-β-CD-SWNT hybrid to occur in aqueous solutions. Experimental findings revealed significant changes in electrical conductance of the device in response to light. Upon exposure to light with an intensity (I) of 40 W m^{-2} and excitation wavelength (λ_{ex}) of 280 nm, the transfer curve of the SWNT/FET device shifts toward a negative gate voltage by approximately 1.6 V, and its sheet resistance increases rapidly, indicating a charge-transfer process from P-β-CD to the SWNTs upon illumination. Conversely, in the presence of the ADA-Ru complex, the transfer curve shifts toward a positive gate voltage by about 1.9 V, and the sheet resistance decreases gradually under illumination (I = 40 W m^{-2}, λ_{ex} = 490 nm), suggesting a charge-transfer process from the P-β-CD-SWNT hybrid to the ADA-Ru complex. This photoresponsive charge-transfer process is fully recoverable upon removal of the light source, showcasing the device's potential for applications in tunable light detection and advanced photovoltaic devices such as artificial eyes and photovoltaic devices.

Noncovalent Functionalization of Polymers

Drawing on prior research[185–187] showing that in aqueous solutions, β-CD displays a strong binding affinity for *trans*-azobenzene units and virtually no affinity for *cis*-azobenzene units, it has been suggested that β-CD/azobenzene inclusion complexes have the capacity to form light-responsive supramolecular hydrogels. In order to explore this possibility,[179] D-β-CD and an ABP copolymer (Figure 9a) were synthesized. The interaction dynamics between D-β-CD and the *trans*/*cis* configurations of azobenzene units in the ABP copolymer were examined thoroughly using UV/Vis spectroscopy, circular dichroism, and ^{1}H rotating-frame Overhauser enhancement spectroscopy so as to shed light on the mechanism which drives a light-responsive reversible gelation process. The results confirmed that the *trans*-azobenzene units are bound strongly within the cavities of D-β-CD whereas the *cis*-azobenzene units do not bind at all. The formation of supramolecular inclusion complexes between D-β-CD and the *trans*-azobenzene units leads to a hydrogel. Upon exposure to UV light at 355 nm, the hydrogel transitions efficiently to the sol phase on account of the photochemical conversion of *trans*-azobenzene units to their *cis* configurations, causing the dissociation of the resulting *cis*-azobenzene units from D-β-CD. This transition can be reversed (Figure 9b), restoring the original hydrogel structure, by exposure to visible light at 450 nm. The swelling ratio (8.7 ± 0.7) for fresh hydrogel samples remain stable throughout multiple gel-to-sol and sol-to-gel transition cycles, indicating the excellent reversibility of the gelation process.

Cyclodextrin-Based Second-Sphere Coordination Complexes

The role of macrocyclic ligands in the formation of coordination complexes can generally be divided into two categories—one is as first-sphere ligands that link directly to metal centers and the other is as second-sphere ligands that bind to the first-sphere ligands of coordination complexes through NCIs.[188–191] Beginning in the early 1980s, the Stoddart group, in collaboration with Howard Colquhoun at the ICI Corporate Laboratory,

DOI: 10.31635/ccschem.025.202505711
Citation: *CCS Chem.* **2025**, 7, 1935–1971
Link to VoR: https://doi.org/10.31635/ccschem.025.202505711

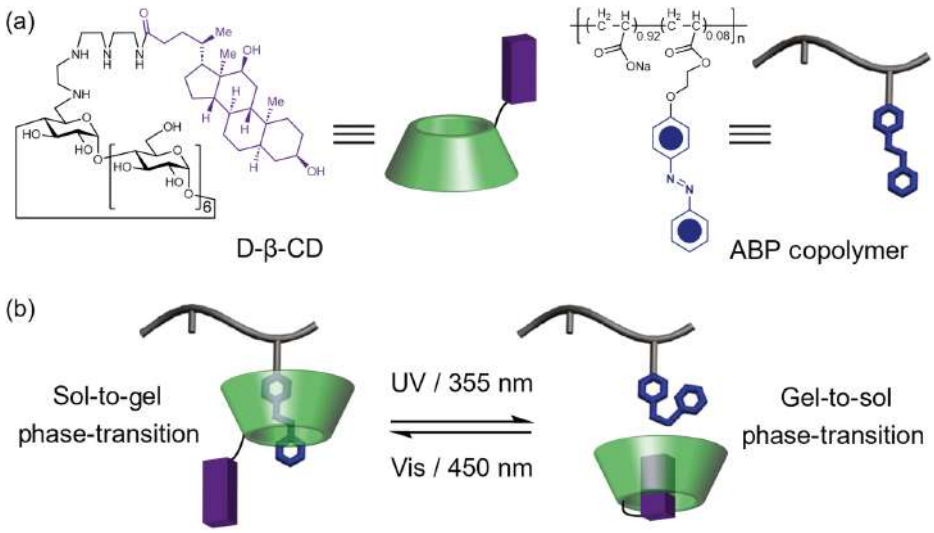

Figure 9 | *(a) Schematic representations of the structural formulas for D-β-CD and the ABP copolymer. (b) Reversable supramolecular inclusion between D-β-CD and azobenzene units in the ABP copolymer triggered by UV/Vis light, allowing the sol-to-gel and gel-to-sol phase-transition cycles.*

investigated[192–196] into the nature of second-sphere coordination complexes formed from transition metal complexes and macrocyclic crown ethers. Following these initial investigations, the Stoddart group has reported[197–203] a number of second-sphere coordination complexes wherein CDs and their derivatives act as second-sphere ligands for organometallic compounds in aqueous media.

In 1985, the Stoddart group discovered[197] that a 1:1 crystalline adduct can be formed from α-CD and a cationic transition metal complex, that is, $[Rh(cod)(NH_3)_2][PF_6]$ (cod = 1,5-cyclooctadiene). Although $[Rh(cod)(NH_3)_2][PF_6]$ undergoes slow hydrolysis of its ammine ligands in an α-CD-containing aqueous solution, good-quality single crystals of the 1:1 adduct, that is, $[Rh(cod)(NH_3)_2$•α-CD], have been obtained and characterized (Figure 10a–c) by X-ray crystallography. In the solid state, the cod ligand inserts partially into the α-CD cavity, and the complex tilts to allow the two ammine ligands to form N–H···O hydrogen bonds ([N···O] = 3.24, 3.25, 3.31, 3.46 Å) with four secondary OH groups from two of the six α-D-glucopyranosyl units in the receptor. While the adduct does exist in D_2O, as revealed by ^1H nuclear magnetic resonance (NMR) spectroscopy, it decomposes slowly over time as ammonia is released from the first coordination sphere. Substituting the two ammine ligands with a bidentate en ligand (en = $H_2NCH_2CH_2NH_2$) yielded a rhodium complex that is stable in α-CD-containing aqueous solutions. A binding constant (K_a) between α-CD and $[Rh(cod)(en)][PF_6]$ was determined to be 520 ± 80 mol^{-1} kg from a quantitative ^1H NMR spectroscopic analysis of the concentration dependence of $[Rh(cod)(en)$•α-CD$][PF_6]$ in D_2O.

In addition, a neutral antitumor drug carboplatin, that is, diammine-1,1-cyclobutanedicarboxylatoplatinum(II) $[Pt(NH_3)_2(CBDCA)$ (CBDCA = cyclobutane-1,l-dicarboxylato)], was found[198] to be able to form a 1:1 adduct with α-CD in water with a standard free energy change

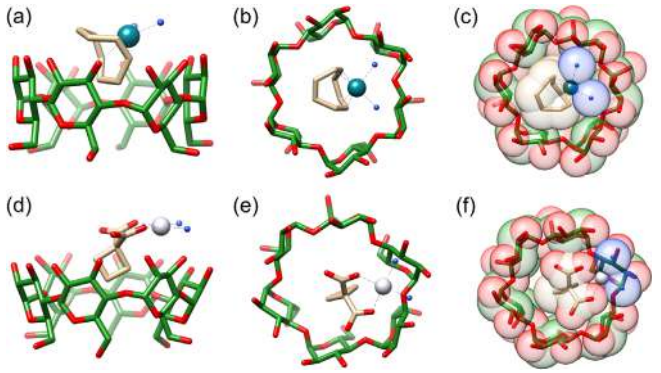

Figure 10 | *Side-on views of the 1:1 second-sphere adducts (a) $[Rh(cod)(NH_3)_2$•α-CD] and (d) $[Pt(NH_3)_2(CBDCA)$•α-CD] shown as stick representations. Plain views of (b) $[Rh(cod)(NH_3)_2$•α-CD] and (e) $[Pt(NH_3)_2(CBDCA)$•α-CD] shown as stick representations. Plan views of (c) $[Rh(cod)(NH_3)_2$•α-CD] and (f) $[Pt(NH_3)_2(CBDCA)$•α-CD] shown as stick representations with the corresponding semitransparent space-filling representations superimposed upon them. The crystal structures shown in (a/b/c) and (d/e/f) have been redrawn from CCDC deposition numbers 1136980 and 1138168, respectively. Hydrogen atoms and solvent molecules have been omitted for the sake of clarity. C green or brown, O red, N blue, Rh cyan, Pt grey.*

DOI: 10.31635/ccschem.025.202505711
Citation: *CCS Chem.* **2025**, 7, 1935–1971
Link to VoR: https://doi.org/10.31635/ccschem.025.202505711

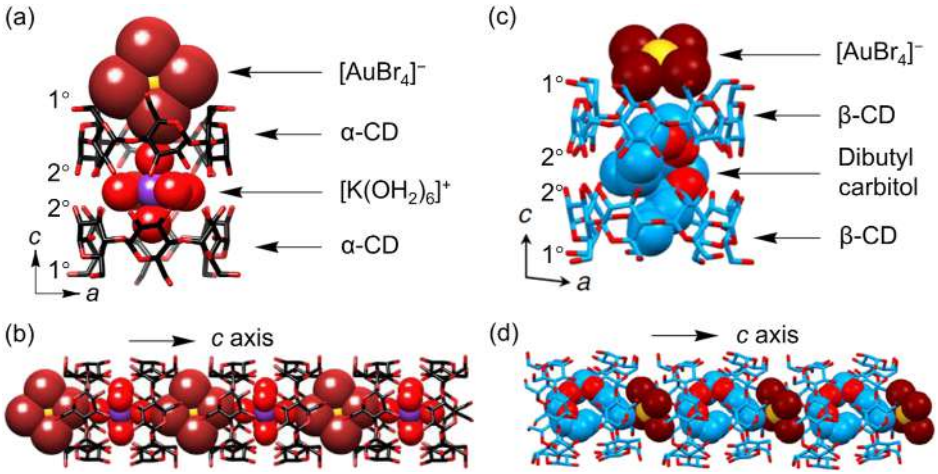

Figure 11 | *(a) Stick and space-filling representation of a 1:2 second-sphere adduct formed from KAuBr4 and α-CD. (b) Stick and space-filling representation of the one-dimensional nanostructure extending along the c-axis, featuring a continuous channel formed by α-CD tori occupied by alternating $[K(OH_2)_6]^+$ and $[AuBr4]^-$ ions. (c) Stick and space-filling representation of the $HAuBr_4$•DBC ⊂ 2β-CD quaternary complex. (d) Stick and space-filling representation of the one-dimensional nanostructure extending along the c-axis in which the β-CD tori form a continuous channel occupied by alternating DBC and $[AuBr_4]^-$ anions. (a, b) Adapted with permission from ref 206. Copyright 2013 Springer Nature. (c, d). Adapted with permission from ref 208. Copyright 2023 Springer Nature.*

($-\Delta G^0$) ranging from 10.4 to 13.0 kJ mol^{-1} at 22–25 °C, as revealed by microcalorimetry and ^1H NMR spectroscopy. Slow cooling (from 80 °C to room temperature) of an α-CD-containing aqueous solution saturated with respect to the platinum complex resulted[199] in single crystals suitable for X-ray diffraction (XRD) analysis. The solid-state structure of $[Pt(NH_3)_2(CBDCA)$•α-CD] reveals (Figure 10d–f) that the adduct is stabilized by the penetration of the cyclobutane ring of carboplatin into the α-CD cavity, resulting in the two ammine ligands to form N–H···O hydrogen bonds ([N···O] = 2.94, 3.14 Å) with secondary OH groups on neighboring α-D-glucopyranosidic units of α-CD. The formation of second-sphere coordination complexes between α-CD and carboplatin has prompted others[204] to develop microencapsulated carboplatin-hydroxypropyl α-CD complexes that were shown to be effective against experimental brain tumors.

While the use of CDs as second-sphere ligands to bind to first-sphere coordination complexes was investigated[197–203] intensively by the Stoddart group at the University of Sheffield in the 1980s, our research in this direction did not get its second wind until the early 2010s. The revisiting[205] of CD-based second-sphere coordination started with an accidental result obtained by Zhichang Liu during an attempt to make a CD-MOF from γ-CD and $KAuBr_4$. Instead of producing an extended framework, γ-CD and $[K(OH_2)_6][AuBr_4]$ cocrystalline into a bamboo-like one-dimensional superstructure. More surprisingly, upon mixing an aqueous solution of $KAuBr_4$ with an aqueous solution of α-CD, a shiny pale brown precipitate forms spontaneously. X-ray crystallographic analysis of single crystals, which were grown from a dilute aqueous solution of $KAuBr_4$ and α-CD by the slow vapor diffusion method, revealed[206] a 1:2 second-sphere adduct between $KAuBr_4$ and α-CD (Figure 11a), structuring into a one-dimensional polymeric $\{[K(OH_2)_6][AuBr_4] \subset (\alpha\text{-CD})_2\}_n$ superstructure (Figure 11b). In this superstructure, the first-sphere ligands—H_2O and $AuBr_4^-$—are encapsulated by the α-CD tori, which pack alternately in head-to-head and tail-to-tail arrangements to form one-dimensional channels. The octahedral $[K(OH_2)_6]^+$ is sandwiched between the 2° faces of two α-CD tori, resulting in an unusual encapsulation in which hydrophilic fully hydrated K^+ ions are buried inside in the hydrophobic CD channels by means of second-sphere coordination. In contrast, the hydrophobic $AuBr_4^-$ anion, exhibiting square-planar coordination, is encapsulated between the 1° faces of two α-CD tori, each primarily occupied by a $AuBr_4^-$ ligand. The hydrophobic effect, augmented by [C–H···Br–Au] hydrogen bonding interactions between the $AuBr_4^-$ anion and the H-5 and H-6 atoms on the 1° faces of the α-CD tori, drives the second-sphere coordination of α-CD with $AuBr_4^-$ ion. Additionally, within the one-dimensional α-CD channel, the alignment of two first-sphere coordination complexes with alternating positive and negative charges contributes to the stabilization of the overall superstructure as a result of attractive electrostatic interactions.

The coprecipitation process involving α-CD and $KAuBr_4$ is featured by its high selectivity. No precipitation (Figure 12a) was formed when α-CD was replaced by either β- or γ-CD, as these larger CDs are unable to

DOI: 10.31635/ccschem.025.202505711
Citation: *CCS Chem.* **2025**, 7, 1935–1971
Link to VoR: https://doi.org/10.31635/ccschem.025.202505711

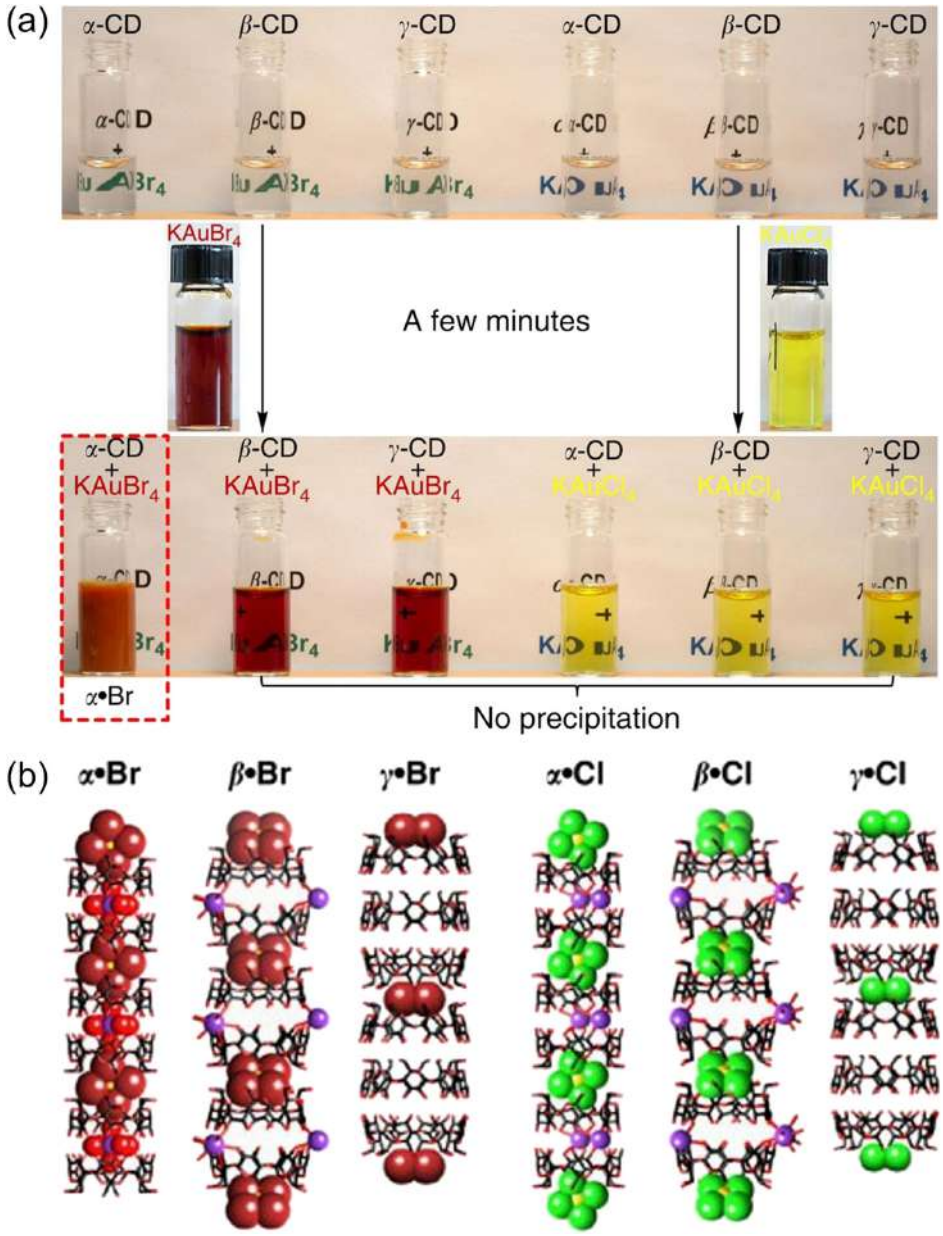

Figure 12 | *(a) Selective coprecipitation from α-CD and $KAuBr_4$. The brown precipitate formed spontaneously when adding an aqueous solution of $KAuBr_4$ into an α-CD-containing aqueous solution. (b) Stick and space-filling representations of the solid-state superstructures of α-CD•$KAuBr_4$, β-CD•$KAuBr_4$, γ-CD•$KAuBr_4$, α-CD•$KAuCl_4$, β-CD•$KAuCl_4$, and γ-CD•$KAuCl_4$. The main reason for the coprecipitation between α-CD and $KAuBr_4$ is that they form a one-dimensional polymeric $\{[K(OH_2)_6][AuBr_4] \subset (\alpha\text{-CD})_2\}_n$ superstructure. Adapted with permission from ref 206. Copyright 2013 Springer Nature.*

encapsulate the $[K(OH_2)_6]^+$ counterion complex, nor do they promote the formation of a low-solubility superstructure with $KAuBr_4$. They do, however, facilitate the formation of more soluble complexes (Figure 12b). Similarly, the use of $KAuCl_4$ with α, β, or γ-CD does not result in coprecipitation (Figure 12a), although more soluble complexes (Figure 12b) are once again obtained. The selective precipitation of $KAuBr_4$ with α-CD remains effective even in the presence of other coordination complexes, such as PtX_4^{2-} and PdX_4^{2-} (where X = Cl/Br), highlighting the specificity of this α-CD-mediated coprecipitation method. The efficiency of gold recovery is notably influenced by the counterions associated with $AuBr_4^-$, with the K^+ ion yielding the highest precipitation rate, approximately 80%. In contrast, using Na^+, Rb^+, and Cs^+ results[207] in significantly lower recovery rates of 0%, 41%, and 61%, respectively. In the crystal structures of these latter complexes, the hydrated counterions are absent, with the

DOI: 10.31635/ccschem.025.202505711
Citation: *CCS Chem.* **2025**, 7, 1935–1971
Link to VoR: https://doi.org/10.31635/ccschem.025.202505711

alkali metal ions instead being coordinated by the oxygen atoms of the glucopyranosyl residues of α-CD. Temperature also plays a crucial role in the recovery yield, as lower temperatures reduce the solubility of the adducts, thereby enhancing the efficiency of gold recovery. For instance, the gold recovery yield increased to 94% when the coprecipitation was performed at 0 °C.

In order to develop a laboratory-scale gold recovery process, an expedient coprecipitation method was tested on two types of gold-bearing scrap alloys, composed of 58 wt % gold and 42 wt % other metals, including Zn, Cu, and Ag. Initially, the alloys were dissolved in a mixture of concentrated HBr and HNO_3 and then neutralized with aqueous KOH. The addition of α-CD to these neutralized solutions resulted in immediate coprecipitation, even in the presence of competing metal ions such as Zn^{2+} and Cu^{2+}. The precipitated adduct, encapsulating the recovered gold, was isolated by filtration and subsequently reduced using sodium metabisulfite ($Na_2S_2O_5$), yielding metallic gold. The gold recovery from the two scrap samples achieved[206] yields of 89% with a purity of 97% and 92% with a purity of 95%, respectively. For scaling to industrial levels, $KAuBr_4$ can be synthesized in situ using either a solution of KBr, Br_2, and H_2O, or KBr, O_3, and H_2O_2.

In an effort to advance the molecular recognition process between α-CD and $KAuBr_4$ into a viable gold-recovery technology, a startup company, Cycladex, was established in 2014. This company was launched to commercialize this innovative process that is not only economically viable but also environmentally friendly. The Cycladex method provides numerous advantages over the traditional cyanide-based gold recovery methods, such as significantly faster leaching times and improved gold recovery efficiencies. Additionally, this method markedly reduces the environmental footprint associated with gold extraction, lowers operational costs, and diminishes capital expenditures, establishing it as a superior and sustainable alternative in the gold extraction industry.

Although the marriage of α-CD with $KAuBr_4$ provides a more environmentally friendly alternative compared to the traditional cyanide process, several limitations remain to overcome: (1) A high gold concentration ($[KAuBr_4] > 6$ mM) in the leaching solution is required. (2) Additional potassium ions are necessary. (3) High acidity in the leaching solution inhibits the formation of coprecipitates. (4) Gold recovery efficiency drops below 80% at room temperature. (5) The cost of α-CD remains relatively high. Therefore, the development of more efficient and cost-effective gold separation technologies that are practical for industrial applications is both significant and necessary.

In this context, the Stoddart group disclosed recently an additive-induced gold separation paradigm[208] based (Figure 11c,d) on the precise control of the reciprocal transformation of second-sphere coordination adducts formed between β-CD and $[AuBr_4]^-$ anions. Mechanistic investigations revealed that the additives promote rapid assembly of β-CD and $[AuBr_4]^-$ anions by driving the anions from the inner cavity to the 1° faces of two β-CD tori, while the additives occupy the space between the 2° faces, forming infinite one-dimensional supramolecular polymers that precipitate from aqueous solutions as cocrystals. A broad range of common organic solvents can serve as additives, with those having higher boiling points yielding superior gold-recovery efficiencies. Notably, a gold-recovery efficiency of 99.8% was achieved when dibutyl carbitol (DBC) was used as the additive. This rapid cocrystallization process is highly selective for $[AuBr_4]^-$ anions, with no precipitate observed in the presence of metal cations or structurally similar anions, such as $[PdBr_4]^{2-}$ and $[PtBr_4]^{2-}$. A laboratory-scale gold-recovery protocol has also been established,[208] achieving 94% gold recovery directly from a leaching solution of gold-bearing scrap with gold concentrations as low as 9.3 ppm. Compared to our previously established protocol using α-CD, the additive-induced polymerization with β-CD offers several advantages: (1) Gold recovery can be achieved at low concentrations (9.3 ppm) with enhanced efficiencies (>94%). (2) The process eliminates the need for additional potassium ions. (3) Coprecipitation can be directly carried out in acidic leaching solutions, eliminating the need for neutralization. (4) Additionally, β-CD is less costly than α-CD.

In the traditional cyanide process for gold extraction, a critical step involves the extraction of $Au(CN)_2^-$ ions from activated carbon into an aqueous medium under rigorous conditions,[209–211] including elevated temperatures (95–140 °C), high pressures (70–400 kbar), and concentrated cyanide and hydroxide solutions. There is a burgeoning demand for the development of novel technologies that facilitate this process under much less severe conditions. In response, we demonstrated[212] that the second-sphere coordination between α-CD and $KAu(CN)_2$ can facilitate (Figure 13a) the gold stripping process from activated carbon. Single-crystal XRD analysis revealed that aqueous solutions of α-CD and $KAu(CN)_2$ give 1:1 and 2:1 adducts when a slow evaporation protocol and a slow diffusion of EtOH vapor are employed, respectively. In both instances, the stabilization of the adducts in the solid state is facilitated through numerous [C–H···π] and [C–H···anion] interactions, where the cyanide ligands in the primary coordination sphere interact with the α-CD in the secondary sphere. Moreover, the K^+ counterions serve to bridge the α-CD tori within the crystal structure by forming coordinative [K^+···O] bonds with glucopyranosyl residues (Figure 13b).

In aqueous environments, the formation of a 1:1 adduct between $KAu(CN)_2$ and α-CD was substantiated through ^{1}H NMR titration and isothermal titration calorimetry. The binding affinity for this complex was quantified to be

DOI: 10.31635/ccschem.025.202505711
Citation: *CCS Chem.* **2025**, 7, 1935–1971
Link to VoR: https://doi.org/10.31635/ccschem.025.202505711

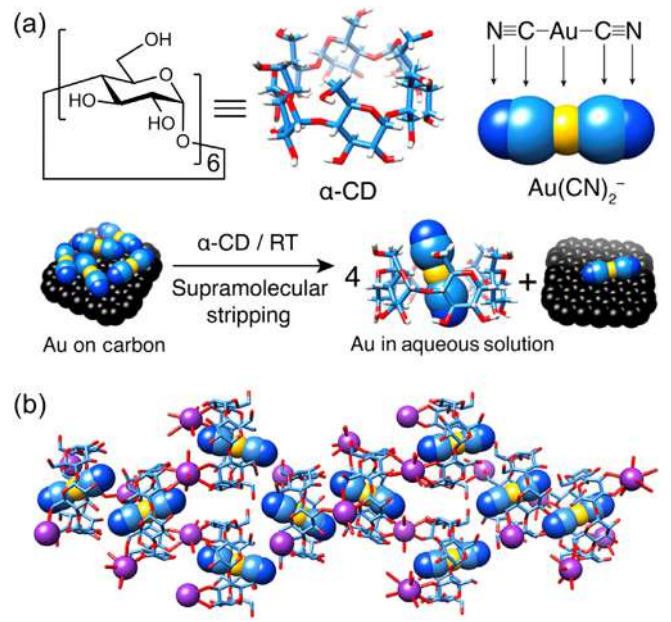

Figure 13 | *(a) Graphical illustration of gold stripping from the surface of activated carbon into aqueous solution employing α-CD. (b) Stick and space-filling representation of the crystal packing between $KAu(CN)_2$ and α-CD, showing the relative positions of K^+ cations and $Au(CN)_2^-$ anions with respect to α-CD tori. Adapted with permission from ref 212. Copyright 2021 American Chemical Society.*

approximately 10^4 M^{-1}. The formation of this adduct is primarily enthalpy-driven, effectively compensating for a slight entropic penalty. Notably, the interaction between $KAu(CN)_2$ and α-CD exhibits high selectivity. The use of β-CD or γ-CD resulted in lower binding affinities, approximately 10^2 and 10^1 M^{-1}, respectively. Although $KAg(CN)_2$ also forms a 1:1 adduct with α-CD in aqueous solution, its binding affinity is notably lower by an order of magnitude compared to that of $KAu(CN)_2$. This characteristic of second-sphere coordination offers a novel application for the efficient stripping of gold from activated carbon at ambient temperatures, specifically targeting $Au(CN)_2^-$ in the presence of $Ag(CN)_2^-$. Such specificity renders the carbon-in-pulp process[209–211] highly effective, particularly for the extraction of gold from ores with substantial silver content.

Cyclodextrin Metal–Organic Frameworks

Metal–organic frameworks (MOFs), a term introduced by Yaghi et al.[213] in 1995, represent a broad category of porous, crystalline materials consisting of organic struts and metal-containing inorganic clusters—or SBUs, structural bonding units. While the past three decades have witnessed[214] explosive growth in the preparation, characterization, and applications of MOFs, the vast majority of MOFs reported in the literature are composed of organic struts derived from nonrenewable petrochemical feedstocks and transition metals, giving rise to inevitable toxicological concerns when it comes to biological and medical applications.[215] In recent years, there are continuous efforts in preparing biocompatible MOFs, ideally from naturally occurring biomolecules and nontoxic metal ions.[216,217]

In 2010, Ronald Smaldone in the Stoddart group at Northwestern University (NU) serendipitously discovered[218,219] the formation of a new class of biocompatible MOFs—namely CD-MOFs—while exploring the possibility of forming a 2:1 host–guest complex from two dipotassium azobenzene-4,4′-dicarboxylate and one γ-CD as the first step in an attempt to prepare Borromean rings with three different rings. Upon diffusing MeOH vapor into an aqueous solution of the two precursors over approximately five days, orange, cubic single crystals (Figure 14a) were obtained. As revealed by XRD analysis, the 2:1 complex was not formed. Instead, only the γ-CD tori, coordinated with K^+ ions, crystallized in the form of millimeter-sized cubes, while the counterions, azobenzene-4,4′-dicarboxylate, were disordered. On realizing the critical role of the alkali metal ions in the formation of this extended framework, Smaldone established that, by employing this slow vapor diffusion protocol, CD-MOF-1 can be synthesized using one equivalent of γ-CD and eight equivalents of KOH.

Single-crystal XRD analysis revealed that CD-MOF-1 crystallizes in a cubic cell of space group *I*432. Each unit cell (3.1 nm edge) is made of six γ-CD tori (Figure 14b) held together through coordination of K^+ ions to primary OH groups and the endocyclic oxygen atoms on the 1° faces (Figure 14c) of alternating D-glucopyranosyl units on the γ-CD tori, which results in the formation of a spherical pore (Figure 14d) with inner diameter of 1.7 nm. The packing of $(\gamma\text{-CD})_6$ cubes, which are connected through coordination of K^+ ions to the C-2 and C-3 OH groups on the outwardly directed 2° faces (Figure 14c) of the other four alternating D-glucopyranosyl units, leads to an infinite body-centered cube interconnected with channels (Figure 14e) formed from tail-to-tail γ-CD pairs aligned in all three dimensions.

CD-MOF-1, which is made from γ-CD and KOH, constitutes the first example[220,c] of highly crystalline CD-MOF to be obtained. Applying the same vapor diffusion method as that employed in the preparation of CD-MOF-1, isostructural CD-MOF-2 and CD-MOF-3 can be prepared, respectively, simply by switching the source of metal ions from KOH to RbOH and CsOH.[221,d] In addition, edible[222] CD-MOFs were prepared on a large scale by vapor diffusion of 190-proof grain alcohol into an aqueous solution containing distilled water, food-grade γ-CD, and a food preservative, namely potassium

DOI: 10.31635/ccschem.025.202505711
Citation: *CCS Chem.* **2025**, 7, 1935–1971
Link to VoR: https://doi.org/10.31635/ccschem.025.202505711

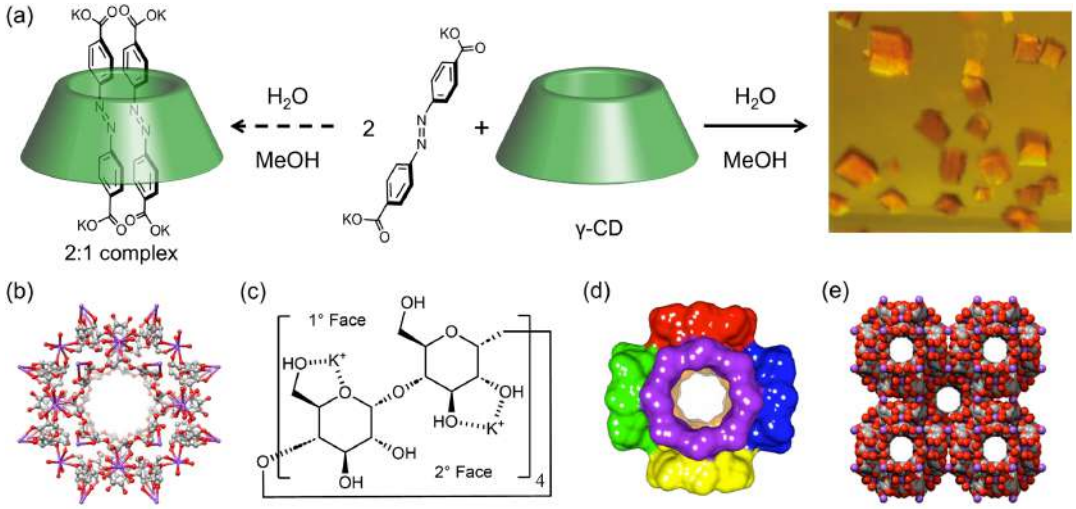

Figure 14 | *(a) Attempts to form a 2:1 complex in aqueous mixture between dipotassium azobenzene-4,4′-dicarboxylate and γ-CD resulting in the formation of cubic crystals of an extended framework, i.e., CD-MOF-1. (b) Ball-and-stick representation of the solid-state structure of the cubic $(\gamma\text{-CD})_6$ representing the unit cell (3.1 nm edge) of CD-MOF-1. (c) A configurational representation of the structure of the maltosyl repeating unit in γ-CD, showing the alternating coordination of K^+ ions to the 1° and 2° faces of a γ-CD. (d) The cuboidal orientation of the six γ-CD tori showing the 1.7 nm sized spherical pore at the center of each $(\gamma\text{-CD})_6$ repeating motif. (e) Space-filling representation of the extended solid-state structure, illustrating the body-centered cubic packing arrangement of the $(\gamma\text{-CD})_6$ repeating motifs. (b, d, e) Adapted with permission from ref 218. Copyright 2010 John Wiley and Sons.*

benzoate. Following our initial work on synthesizing CD-MOFs, a wide range of CD-MOF analogues and other types of carbohydrate-based extended frameworks—employing various combinations of cyclo-oligosaccharides and metal salts—have been made and characterized[223–241] by the Stoddart group as well as by other research groups.

Over the years, CD-MOFs have emerged as an attractive class of green, extended framework materials owing to their low cost, facile availability, robust crystallinity, permanent porosity, stable homochirality, and excellent biocompatibility. On account of their ability to host a variety of guest molecules, including gases, (bio)active molecules, drugs, nanoclusters, and nanoparticles, CD-MOFs have found a wide range of applications in CO_2 adsorption,[242–244,e] syntheses of metal-based nanoparticles and gel particles,[245–247] sensing,[248–250] information storage,[251] separations,[252,253] trapping of reactive intermediates,[254] catalyst supports,[255] circularly polarized luminescent materials,[256,257] nanoreactors,[258,259] protein encapsulation,[260] and drug delivery.[261–263] In the remaining part of this section, we will confine our discussion to some of our most recent advances in employing CD-MOFs to (1) create circularly polarized luminescent materials and (2) promote selective chemical transformations. For other content in relation to CD-MOFs, either synthetic or applied, we refer readers to some recently published review articles.[100,101,264–267]

CD-MOF-Based Circularly Polarized Luminescent Materials

While the existence of ordered chiral environments within CD-MOFs renders them ideal hosts to encapsulate organic dyes for light-emitting applications, investigations in this direction have not been carried out until recently.[256,257] In 2022, the Stoddart group employed[257] three achiral polycyclic aromatic fluorophores—namely, 1-pyrenecarboxylic acid, 9-anthracenecarboxylic acid, and perylene-3,9-dicarboxylic acid—in the construction of three fluorophore-loaded CD-MOFs by cocrystallization of these fluorophores with γ-CD in the presence of KOH. Although significant quantities of fluorophores were included in these CD-MOFs as revealed by ^{1}H NMR spectroscopic analyses of digested samples, single-crystal XRD did not reveal the presence of any guests in the anthracene- and perylene-containing CD-MOFs, suggesting that the fluorophores in both CD-MOFs are disordered extensively. Nonetheless, in a pyrene-loaded γ-CD-containing hybrid framework (CD-HF), that is, $PyC^- \subset$ CD-HF, the crystal structure assumed a new trigonal space group ($P3_221$) instead of the common cubic $I432$ space group found in the case of the other two fluorophore-loaded CD-MOF-1.

The solid-state superstructure of $PyC^- \subset$ CD-HF revealed[257] that each $(\gamma\text{-CD})_2$ tunnel hosts two π-stacked PyC^- guests, with an average distance of approximately

DOI: 10.31635/ccschem.025.202505711
Citation: *CCS Chem.* **2025**, 7, 1935–1971
Link to VoR: https://doi.org/10.31635/ccschem.025.202505711

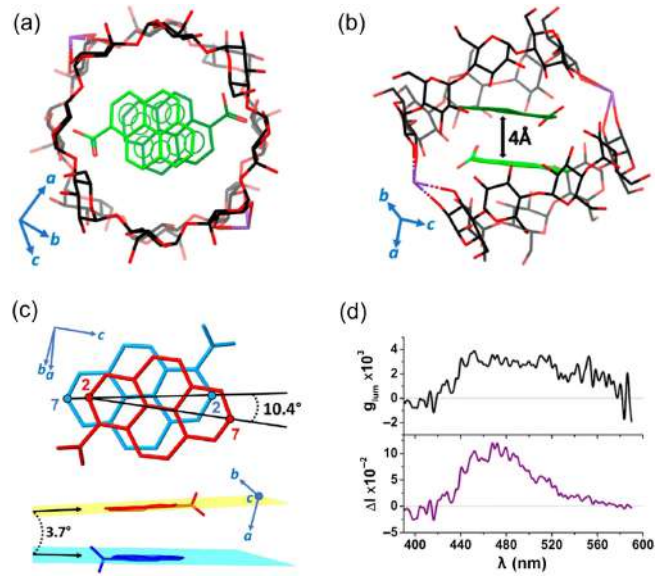

Figure 15 | *(a) Graphical illustrations of π-stacked PyC⁻ anionic dimers encapsulated by (γ-CD)$_2$ tunnels showing (b) an average distance of ca. 4 Å between the two aromatic planes, which subtend (c) a relative rotation of of 10.4° and an angle of 3.7°. (d) g_{lum} (black trace) and ΔI (violet) values measured for PyC⁻ ⊂ CD-HF crystals in MeOH suspension with an light-emitting diode excitation source of λ_{ex} = 300 nm. Adapted with permission from ref 257. Copyright 2022 American Chemical Society.*

4 Å between the two aromatic planes (Figure 15a,b). The aromatic planes of these π-stacked PyC⁻ anions subtend a relative rotation of 10.4° and an angle of 3.7° (Figure 15c), thus breaking the centrosymmetry and resulting in a chiral dimeric structure. Further analysis of the superstructure demonstrated[257] that the inclusion of PyC⁻ anions and their NCIs with γ-CDs in CD-HF causes geometrical changes in the tori that influence their assembly, leading to the formation of a trigonal CD-HF with a helical chirality.

The spatially oriented arrangements of fluorophores within PyC⁻ ⊂ CD-HF crystals resulted[257] in specifically generated photophysical and chiroptical properties, such as the controlled emergence of circularly polarized luminescence (CPL) emission. When a suspension of the PyC⁻ ⊂ CD-HF crystals in MeOH was used for the measurement of CPL activity, a constant and reliable signal (Figure 15d) for g_{lum} = +3.5 × 10^{-3}—where g_{lum} is the dimensionless luminescence dissymmetry ratio—was recorded. Of note, this g_{lum} value is in the same range as that of a few γ-CD-based circularly polarized luminescent materials described by Yang and coworkers[65] and Liu and coworkers.[256] This research achieved a complete understanding of the mechanism of chirality transfer from chiral hosts to encapsulated achiral fluorophores at a molecular level, an attribute which is indispensable for the development of more efficient CPL emitters.

CD-MOF-Based Nanoreactors

CDs have long been touted as artificial enzymes[43–46] that promote or catalyze chemical reactions on bound substrates within their nanosized cavities. On account of the fact that CD-MOFs contain countless nanoconfined binding sites capable of preorganizing certain substrates in a well-defined manner through a collection of NCIs including electrostatic, hydrogen-bonding, hydrophobic, and van der Waals interactions, it follows that CD-MOFs hold the potential to serve as nanoreactors for selective chemical transformations. In this context, the Stoddart group recently demonstrated[258] a highly efficient [4+4] photodimerization of 1-AC⁻—where 1-AC⁻ is the negatively charged conjugate carboxylate of 1-anthracenecarboxylic acid—under UV light irradiation with excellent regioselectivity and good enantioselectivity.

Prior to carrying out [4+4] photodimerizations, 1-AC⁻ was encapsulated inside CD-MOF-1 employing an anion-exchange protocol. Upon UV light (370 nm) irradiation of the anthracene-load crystals, that is, 1-AC⁻ ⊂ CD-MOF-1, 1-AC⁻ underwent[258] photodimerization to produce four possible regioisomers (Figure 16a)—namely, the *anti*-head-to-tail (*anti*-HT), the *anti*-head-to-head (*anti*-HH), the *syn*-head-to-tail (*syn*-HT), and the *syn*-head-to-head (*syn*-HH). The main product was identified as the *anti*-HH with a calculated yield of 85% based on a quantitative ^{1}H NMR spectroscopic analysis. The overall yields of other regioisomers were, however, calculated to be only 8%, suggesting that the regioselectivity is as high as 91%. A closer examination of the *anti*-HH using chiral HPLC revealed that the (–)-*anti*-HH constitutes the major enantiomer in an enantiomeric excess of 79%. The excellent regioselectivity and good enantioselectivity for the photodimerization of 1-AC⁻ within CD-MOF-1 were ascribed[258] to a two-step process (Figure 16b,c)—(1) 1-AC⁻ was diffused into CD-MOF-1 and trapped in active sites, that is, the (γ-CD)$_2$ tunnel, in a highly preorganized manner through multiple NCIs acting in concert, and (2) the selective photodimerization of 1-AC⁻ gives energetically the most favorable products, that is, (–)-*anti*-HH, which are extruded from the (γ-CD)$_2$ tunnel and reside in the (γ-CD)$_6$ cubic cavity. This proposed mechanism is supported by both a solid-state superstructure of 1-AC⁻ ⊂ CD-MOF-1 and theoretical calculations.

The versatility of CD-MOFs to harbor selective chemical transformations has also been vindicated by a site-selective C–H functionalization.[259] In this investigation (Figure 17a–g), an anionic benzophenone guest, that is, 2-benzoylbenzoate (2-BZ⁻), was incorporated into the (γ-CD)$_2$ tunnel of CD-MOF-1 through anion exchange. Upon photoirradiation, the photoexcited 2-BZ⁻ abstracts the hydrogen atoms from C(sp^3)–H bonds by means of hydrogen atom transfer. As a result of a substrate preorganization provided by a nanoconfinement

DOI: 10.31635/ccschem.025.202505711
Citation: *CCS Chem.* **2025**, 7, 1935–1971
Link to VoR: https://doi.org/10.31635/ccschem.025.202505711

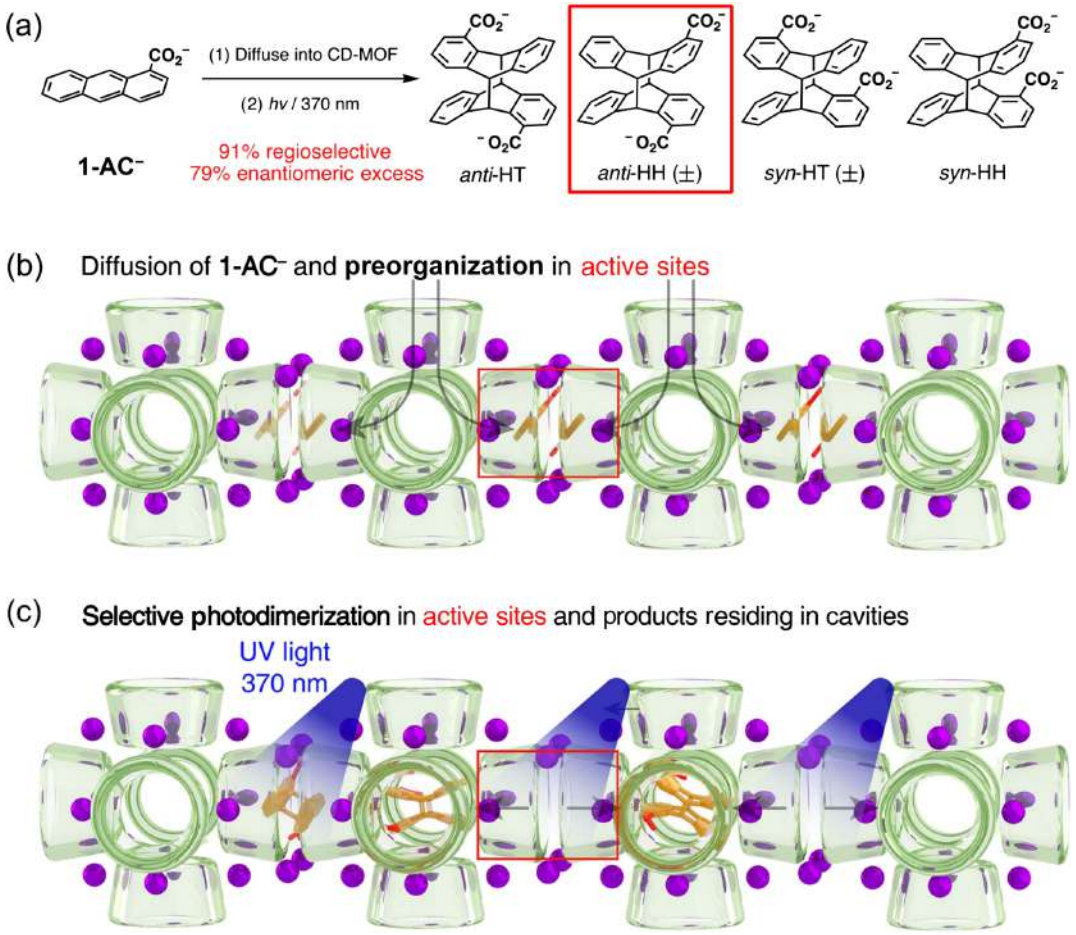

Figure 16 | *(a) Photodimerizations of 1-AC⁻ encapsulated inside CD-MOF-1 produce anti-HH (±) in excellent regioselectivity and good enantioselectivity. (b) A proposed mechanism involves the preorganization of 1-AC⁻ in active sites, i.e., the (γ-CD)$_2$ tunnel, followed by selective photodimerization in active sites and subsequent products residing in the (γ-CD)$_6$ cubic cavity. Adapted with permission from ref 258. Copyright 2021 American Chemical Society.*

environment within CD-MOF-1, the photoexcited 2-BZ⁻ reacts selectively with one of the two C(sp^3)–H hydrogen atoms on the C-6 atom of γ-CD, triggering subsequent intramolecular condensation to form a pair of BZ-functionalized γ-CDs—namely, (*RS*)-BZ-6′-γ-CD and (*RR*)-BZ-6′-γ-CD—in 20% yield with a diastereoisomeric ratio (dr) of 5.2:1. The observed site selectivity of this photoinitiated C–H functionalization was attributed,[259] based on theoretical calculations, to a less steric hindrance associated with C-6-functionalized (γ-CD)$_2$ tunnels in CD-MOF-1 compared with C-3 and C-5.

Cyclodextrin-Based Mechanically Interlocked Molecules

CD-based host–guest complexes are suitable templates for the syntheses of MIMs[268,269] such as catenanes and rotaxanes. The resulting mechanically interlocked structures have attracted[94–98] considerable research interest for several reasons, which include, but are not limited to, the following: (1) CD-based MIMs can be obtained at low cost using an easily relied-upon self-assembly protocol. (2) CD-based MIMs are good examples for the investigation of orientational mechanostereoisomerism on account of the fact that CDs lack mirror symmetries.[270] (3) CDs are water soluble and biocompatible, making them ideal components for MIM construction, particularly when it comes to applications in aqueous and biological environments.[271] In this section, we will discuss our continuous efforts in (1) the syntheses of CD-based catenanes and rotaxanes, (2) the elaboration of CD-based polypseudorotaxanes in order to mimic the multivalent protein–carbohydrate interactions, and (3) the use of CD-based (pseudo)rotaxanes as nanovalves for controlled drug release.

Syntheses of Cyclodextrin-Based Catenanes and Rotaxanes

The first successful syntheses[272,f] of CD-based catenanes were accomplished[273,274] in the Stoddart research

DOI: 10.31635/ccschem.025.202505711
Citation: *CCS Chem.* **2025**, 7, 1935–1971
Link to VoR: https://doi.org/10.31635/ccschem.025.202505711

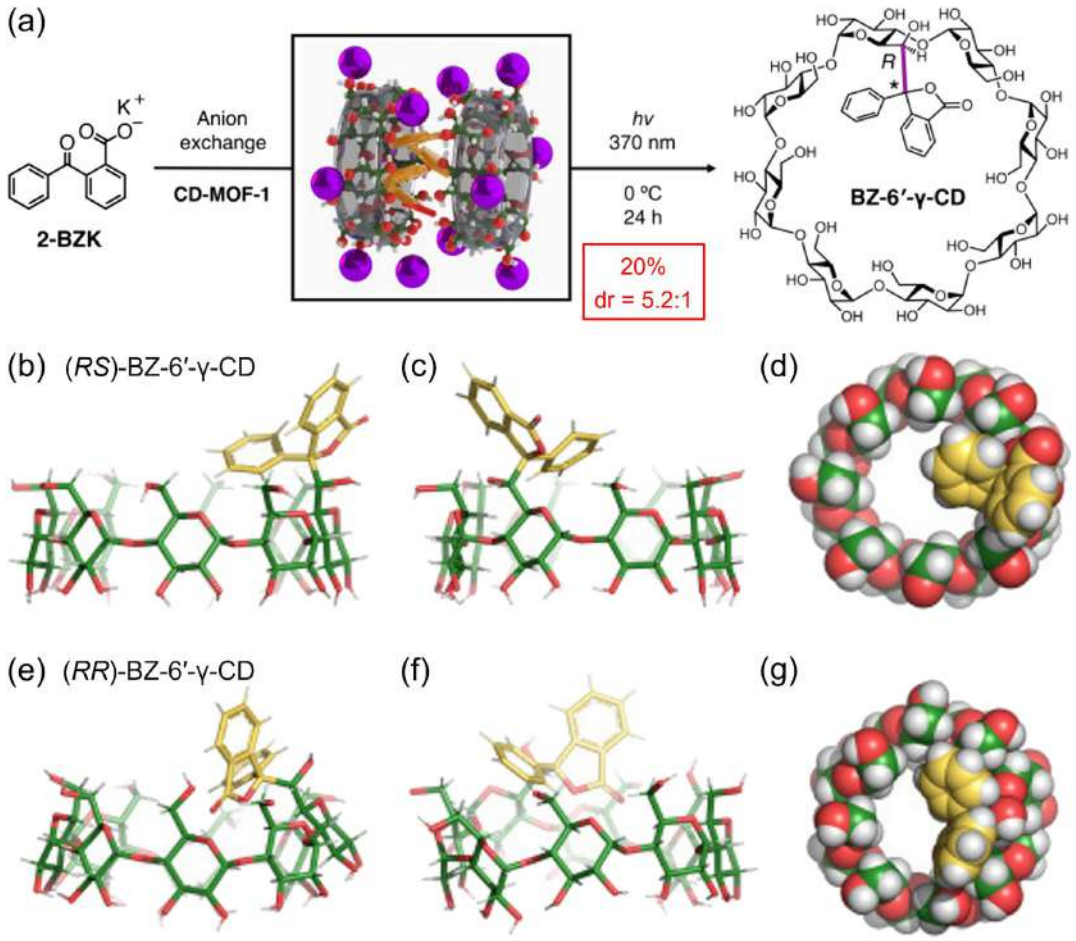

Figure 17 | *(a) Photoinitiated C–H functionalization in CD-MOF-1 proceeds in exclusive site-selectivity, resulting in a pair of diastereoisomers—namely, (RS)-BZ-6′-γ-CD and (RR)-BZ-6′-γ-CD. Solid-state structures of (RS)-BZ-6′-γ-CD shown as (b, c) stick representations and (d) space-filling representation. Solid-state structures of (RR)-BZ-6′-γ-CD shown as (e, f) stick representations and (g) space-filling representation. Adapted with permission from ref 259. Copyright 2024 Cell Press.*

laboratory at the University of Birmingham in the early 1990s. The syntheses involve (Figure 18) the threading of DM-β-CD with a molecular dumbbell **43** consisting of a hydrophilic aromatic core and two poly(ethylene glycol) (PEG)-based side chains, both terminated by amino groups. The rigid aromatic core entices the guest molecule into the CD cavity in aqueous solutions mainly through hydrophobic interactions, while the PEG chains serve as flexible water-soluble spacers, facilitating macrocyclization and enhancing the water solubility of the resulting complexes. Both terminal amino groups on the bound substrate can react with terephthaloyl chloride in a basic aqueous solution containing DM-β-CD, leading to cyclization and the formation of a series of structurally different catenanes. Chromatographic separation revealed four distinct catenanes: two [2]catenanes —namely, **44** and **45**, one incorporating a monomeric macrocycle in 3% isolated yield and the other a dimeric one in 0.8% isolated yield, as well as two isomeric [3] catenanes—namely, **46** and **47**. In addition to these catenanes, free macrocycles and polyamides were identified invariably as major side products.

The two [3]catenanes exist as a pair of head-to-tail/head-to-tail (**46**) and head-to-head/tail-to-tail (**47**) orientational mechanoisomers, as revealed by both the corresponding ^{1}H and ^{13}C NMR spectra. The synthetic macrocyclic component in **46** has averaged C_2 symmetry, whereas in **47**, it has averaged D_2 symmetry. The difference in symmetry types of macrocyclic components in **46** and **47** allow both isomers to be identified[273] unambiguously by NMR spectroscopic analyses. For example, the bitolyl methylene group in **46** can be identified in the ^{1}H NMR spectrum ($CDCl_3$) as two singlets at δ = 4.59 and 4.65, whereas one singlet was observed at δ = 4.62 for theses protons in **47**. One of these catenanes **44** provided[273] single crystals suitable for X-ray

DOI: 10.31635/ccschem.025.202505711
Citation: *CCS Chem.* **2025**, 7, 1935–1971
Link to VoR: https://doi.org/10.31635/ccschem.025.202505711

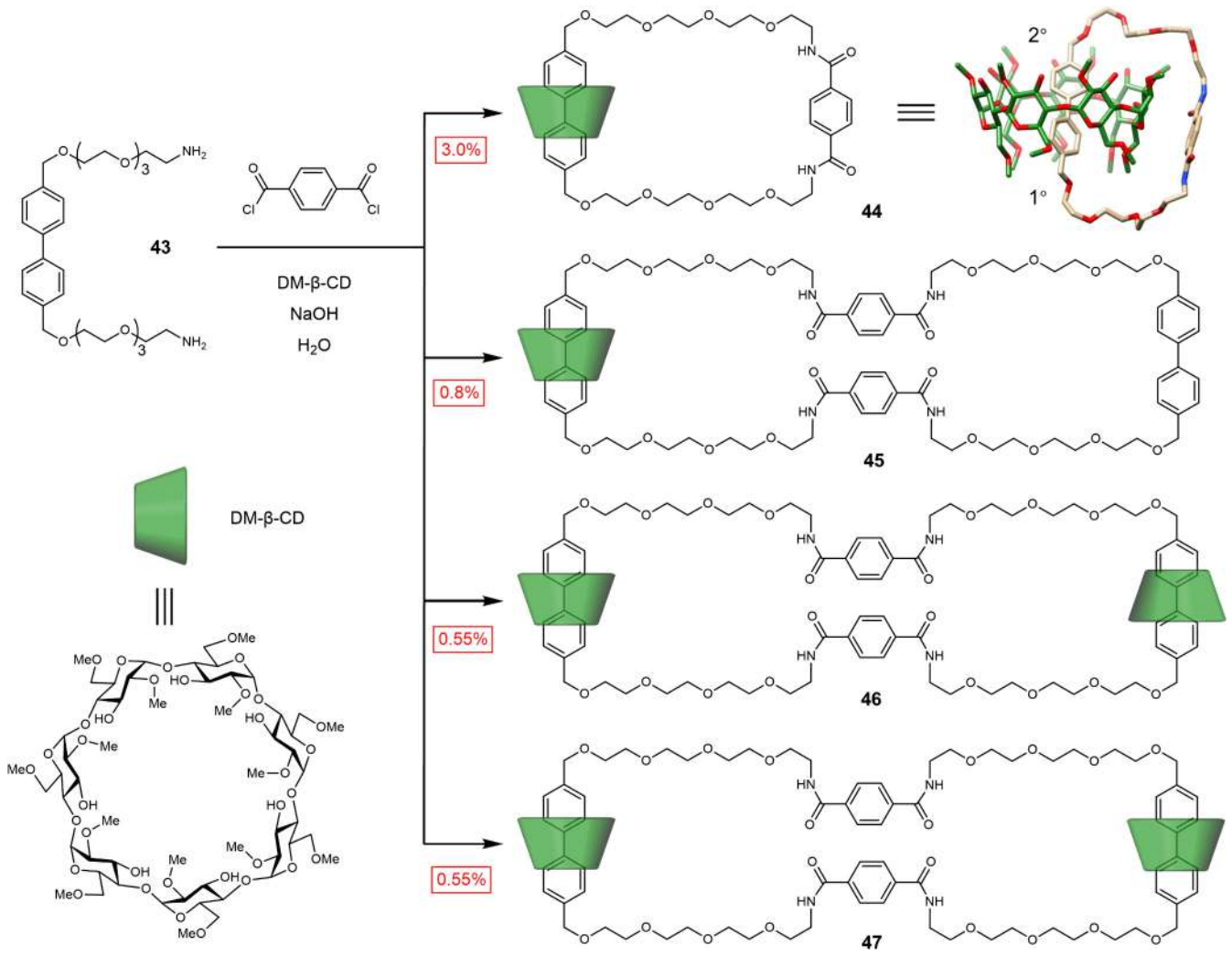

Figure 18 | *Catenation of DM-β-CD under Schotten–Baumann reaction conditions resulting in four heterocatenanes—namely, [2]catenanes **44** and **45**, isomeric [3]catenanes **46** and **47**. The crystal superstructure of [2]catenane **44** has been redrawn from CCDC deposition number 1299449. Hydrogen atoms and solvent molecules have been omitted for the sake of clarity. C green or brown, O red, N blue.*

crystallographic analysis. The solid-state structure revealed that the bitolyl unit of the macrocyclic bis(lactam) moiety is positioned inside the CD's cavity, with no hydrogen bonding interactions between the oxygen atoms on the PEG spacers and the free C-3 OH groups on the 2° face of the CD. In addition, the bis(lactam) moiety lies against the outer surface of the CD torus. These catenated CDs exhibited quite remarkable solubility in halogenated and aromatic hydrocarbons as well as in hydroxylic solvents. It has been suggested that these compounds provide valuable insights into the NCIs that CDs employ to bind substrate molecules in aqueous solutions.

Recently, the Stoddart group developed[275] a cooperative capture strategy, in which CDs were used to accelerate a cucurbituril-assisted azide-alkyne cycloaddition (CB-AAC). While the CB-AAC, which was pioneered by Mock et al.,[276,277] has been employed in the syntheses of rotaxanes and polyrotaxanes by Steinke and coworkers,[278–280] the reaction rate is relatively slow, and the yields of the reaction are far from satisfactory. To overcome these drawbacks, Chenfeng Ke in the Stoddart group at NU introduced[281] CDs as cofactors in the CB-AAC. CDs contain numerous OH groups at their rims, which can serve as hydrogen-bonding donors that are able to form a complementary hydrogen-bonding network with the carbonyl groups of the CB rings, leading to further stabilizing the substrate-CB complexation and accelerating the CB-AAC.

By employing the cooperative capture strategy, a number of sequence-controlled oligo- and polyrotaxanes were synthesized[281] with 100% threading efficiencies of recognition sites on dumbbells by rings. Specifically, polypseudorotaxanes **PPR1** and **PPR2**, which bear

DOI: 10.31635/ccschem.025.202505711
Citation: *CCS Chem.* **2025**, 7, 1935–1971
Link to VoR: https://doi.org/10.31635/ccschem.025.202505711

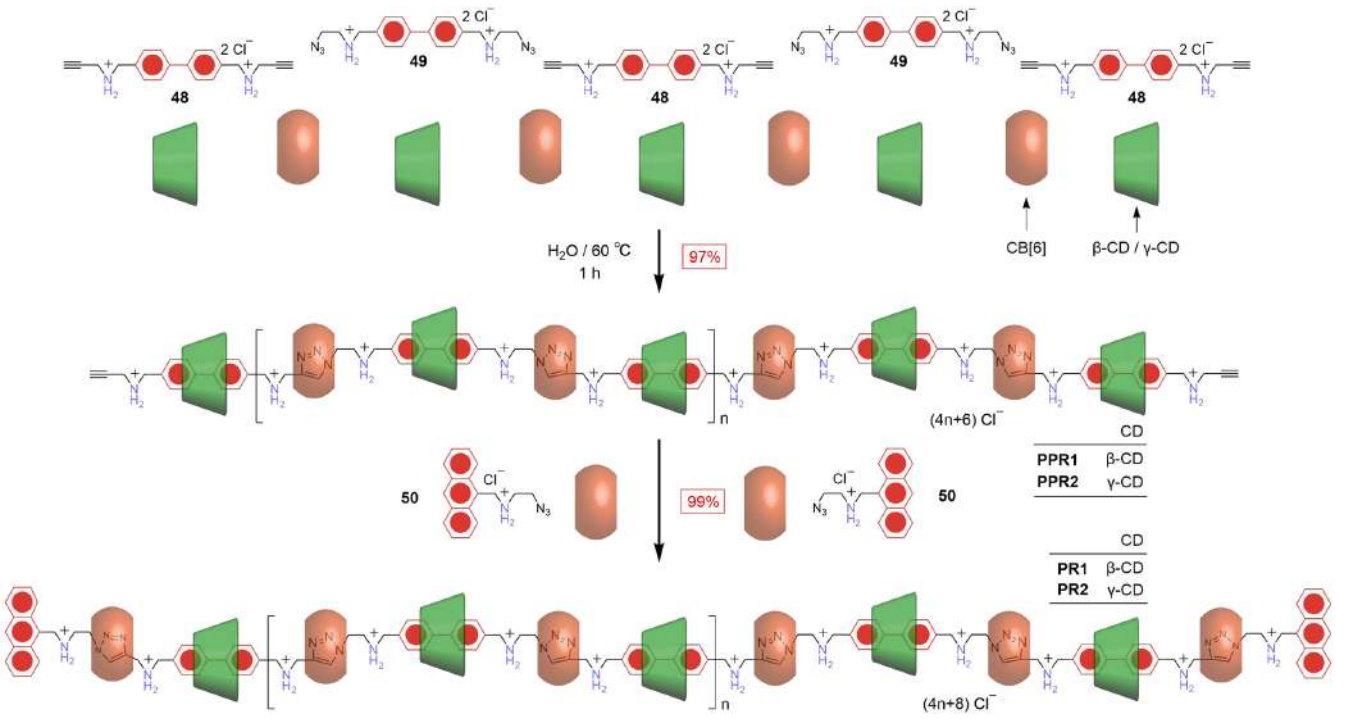

Figure 19 | *Syntheses of the polypseudorotaxanes **PPR1** and **PPR2** by polymerizing **48** and **49** in the presence of CB[6] and CD rings and subsequent capping with the stopper precursor **50** to form the corresponding polyrotaxanes **PR1** and **PR2**.*

alternating CB[6]/CD sequences, were formed with quantitative ring-threading efficiencies simply by heating monomers **48** and **49** in the presence of CB[6] and either β-CD or γ-CD in H_2O at 60 °C for 1 h (Figure 19). The degrees of polymerization were estimated to be 15.8 for **PPR1** and 7.5 for **PPR2**, corresponding to molecular weights of 84,800 and 45,600, respectively. The sequence-controlled polyrotaxanes **PR1** and **PR2** were obtained, respectively, by capping the polypseudorotaxanes **PPR1** and **PPR2** with anthracenyl stopper precursors **50**, yielding the two polyrotaxanes in near-quantitative yields. To the best of our knowledge, these polyrotaxanes are among the few examples of sequence-controlled main-chain polyrotaxanes reported[282] in the chemistry literature.

The cooperative capture strategy was also applied[283] to the facile synthesis (Figure 20a) of a γ-CD-containing hetero[4]rotaxane **53**•4Cl with tunable solid-state fluorescent properties. Rotaxane **53**•4Cl exhibits (Figure 20b) an aggregation behavior (K_{agg} = 1.4 × 10^4 M^{-1}) in the solid state wherein a pyrene end of one molecule stacks alongside the diazaperopyrenium unit of another molecule to form an exciplex in the excited state upon irradiation, resulting in a red fluorescence emission. The aggregated rotaxanes (**53**$_{agg}^{n+}$) can be disassembled in an aqueous solution by addition of γ-CD rings, which encapsulate (K_{CD} = 0.9 × 10^4 M^{-1}) the pyrene units of **53**$_{agg}^{n+}$, preventing aggregation. The γ-CD-mediated disassembly process can be reversed by introducing a competitive binding agent (CBA), for example, 2-adamantylamine hydrochloride (Ad•Cl) or 1-adamantanemethylamine hydrochloride (AdMe•Cl), which competes for the γ-CD rings and regenerates the aggregated rotaxane **53**$_{agg}^{n+}$. This dynamic supramolecular network (Figure 20b) allows[283] us the opportunity to manipulate the aggregation/deaggregation behavior of **53**$^{4+}$, not only in solution, but also in the solid state, so as to tune the fluorescence emission (Figure 20c) over a wide color range from red to green in a dynamic and reversible manner.

By loading **53**$^{4+}$-, γ-CD-, and Ad^+-containing aqueous solutions as inks into fountain pens, information (Figure 21a), which is only revealed under UV light, can be written, added, and erased. **53**$^{4+}$-based inks are also compatible with inkjet printing technology (Figure 21b,e). By loading **53**•4Cl, γ-CD, and AdMe•Cl inks into the three channels, respectively, of a tricolor inkjet cartridge, polychromic images can be printed (Figure 21c,f) with good color resolution. Supramolecular equilibration among the three components is established rapidly during the printing process, even before the inks dry. The fluorescence color range of the output images can be expanded to accommodate red–green–blue printing (Figure 21d,g,h)

DOI: 10.31635/ccschem.025.202505711
Citation: *CCS Chem.* **2025**, 7, 1935–1971
Link to VoR: https://doi.org/10.31635/ccschem.025.202505711

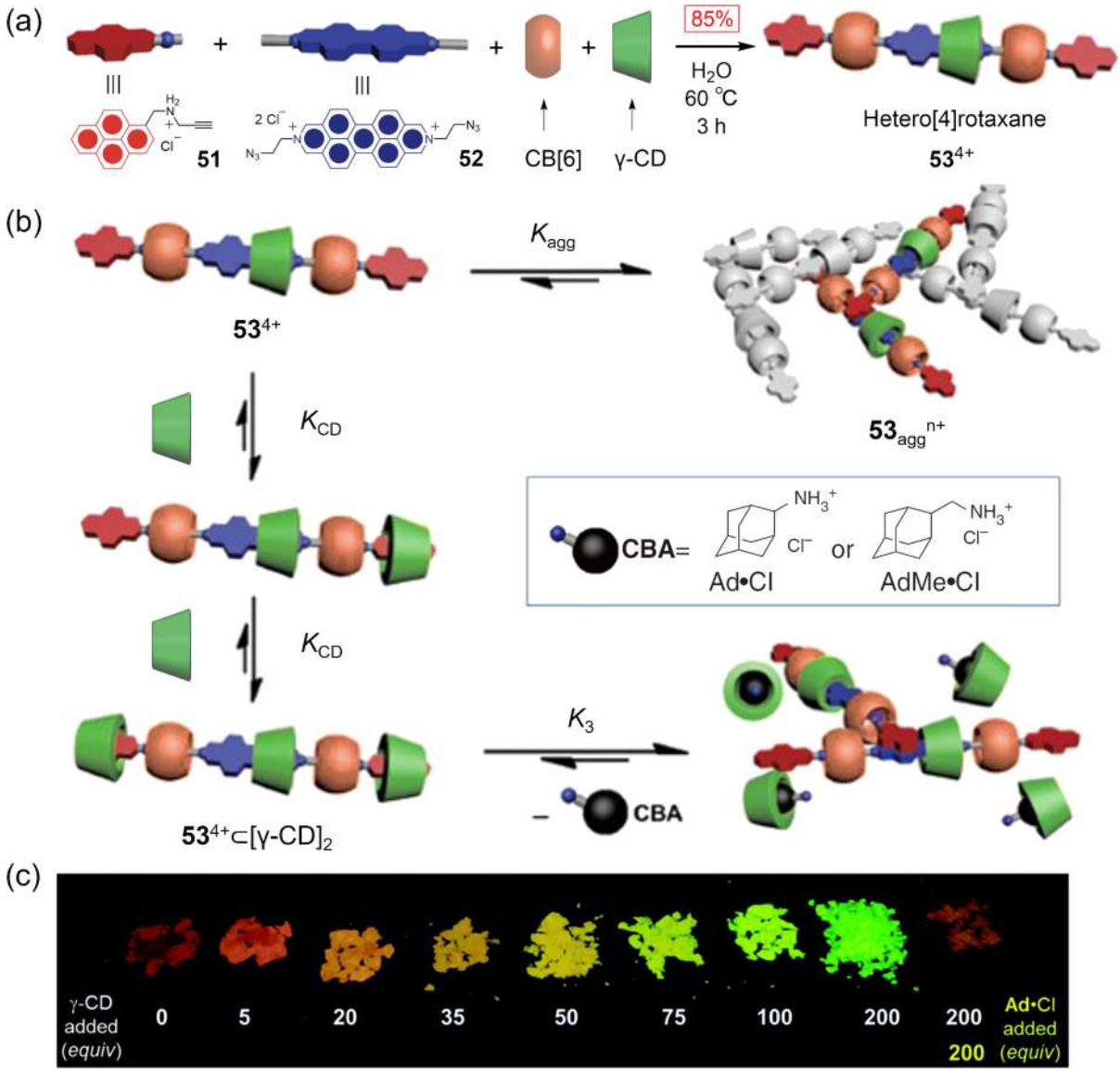

Figure 20 | *(a) Cooperative capture synthesis of heter[4]rotaxane **53**•4Cl. (b) Graphical representation of the equilibria involving **53**$^{4+}$ as its Cl^- salt in the presence of γ-CD and CBAs. (b) Powders obtained by lyophilisation of homogeneous aqueous mixtures of **53**•4Cl and varying amounts of γ-CD and Ad•Cl under UV light. Adapted with permission from ref 283. Copyright 2015 Springer Nature.*

by employing a fluorescent CBA, for example, PyMe•4Cl, which happens to constitute the ends of **53**$^{4+}$.

Cyclodextrin-Based Polypseudorotaxanes as Multivalency Mimicry

Polypseudorotaxanes, which consist of carbohydrate ligand-modified CDs as the ring component, are useful tools for mimicking and investigating multivalent[284,285] protein–carbohydrate interactions. The dynamic multivalent presentation of carbohydrate ligands in these polypseudorotaxanes allows the ligands to orient themselves in a way that maximizes their overall binding interactions with dispersed and orientation-specific receptors. The Stoddart group's adventure in this particular research direction began[286] with the syntheses of polypseudorotaxanes from both lactose-appended α- and β-CD threaded onto hydrophobic polymers such as poly(tetrahydropyran) and poly(propylene) glycol.

In order to improve the stability of the resulting polypseudorotaxanes, which is crucial when it comes to using them as dynamic water-soluble multivalent (supra)molecular polymers for binding to lectins (Figure 22), a stable polypseudorotaxane **PPR3** comprised of lactoside-displaying α-CD (Lac-α-CD) "beads" threaded onto a linear polyviologen "string" was assembled.[287,288] The

DOI: 10.31635/ccschem.025.202505711
Citation: *CCS Chem.* **2025**, 7, 1935–1971
Link to VoR: https://doi.org/10.31635/ccschem.025.202505711

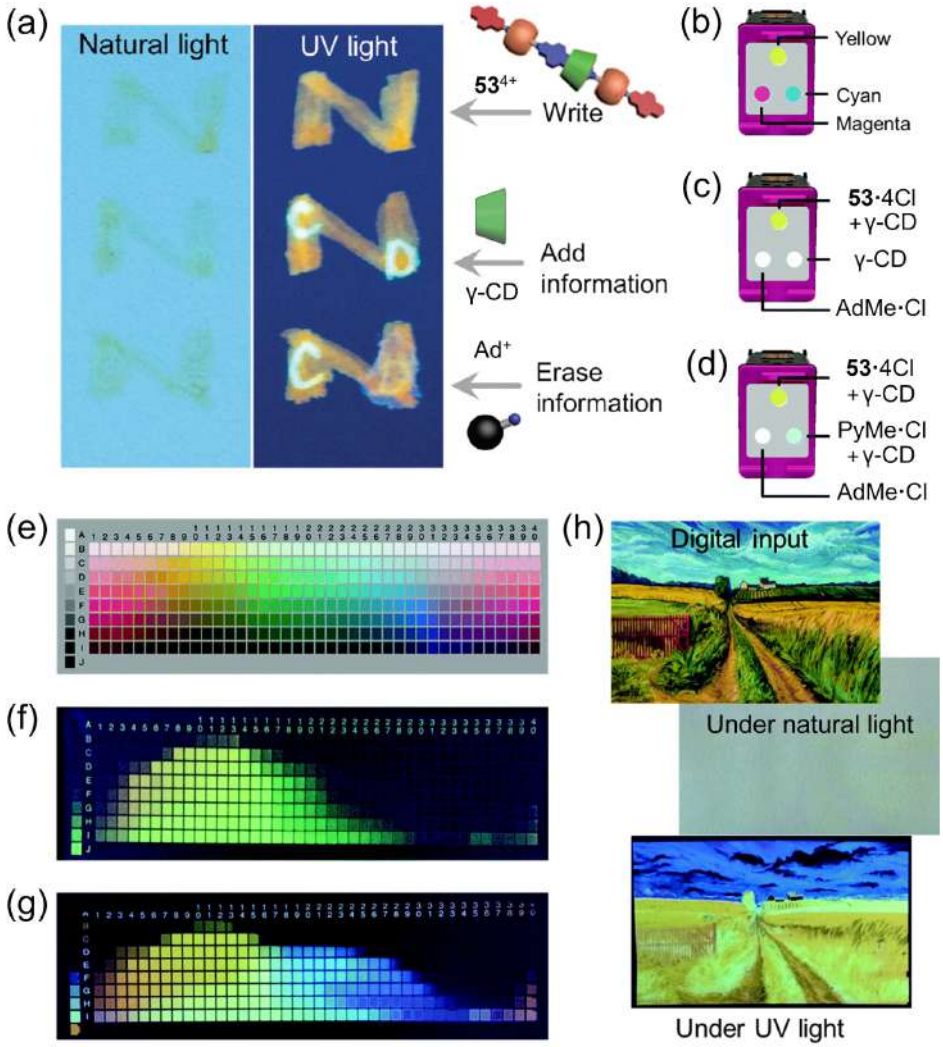

Figure 21 | *(a) Adding and erasing information reversibly on the top of the surface of the fluorescent ink with γ-CD and Ad•Cl aqueous solutions. Graphical representations of (b) a standard tricolor inkjet cartridge, (c) a customized tricolor inkjet cartridge, in which aqueous solutions of* ***53****•4Cl/γ-CD, γ-CD and AdMe•Cl occupy the yellow, cyan, and magenta color channels, respectively, and (c) a customized tricolor inkjet cartridge, in which aqueous solutions of* ***53****•4Cl/γ-CD, PyMe•Cl/γ-CD, and AdMe•Cl occupy the yellow, cyan, and magenta color channels, respectively. Graphical representations of (e) a color palette printed using the standard inkjet cartridge, (f) a fluorescent color palette printed using the customized inkjet cartridge shown in (c) under UV light, and (g) a fluorescent color palette printed using the customized inkjet cartridge shown in (d) under UV light. (h) A digital input and a fluorescent image printed using the customized inkjet cartridge in (d) under natural and UV light. Adapted with permission from ref 283. Copyright 2015 Springer Nature.*

CD rings of **PPR3** are able to spin around the axis of the polyviologen chain as well as to move back and forth along the polymeric backbone to alter their presentation to the lactoside ligands. This polypseudorotaxane exhibited remarkable inhibition of galectin-1 (Gal-1)-mediated T-cell agglutination, in which a valency-corrected 10-fold enhancement over native lactose was observed. Importantly, the 10-fold enhancement was greater than those observed for lactoside-bearing trivalent glycoclusters and a lactoside-bearing chitosan polymer tested using the same assay, demonstrating the advantages of the dynamic presentation of carbohydrate ligands in polypseudorotaxanes.

In addition, the dynamic multivalent interactions between these lactoside-displaying polypseudorotaxanes and Gal-1 were further investigated[289] by using T-cell agglutination and quantitative precipitation assays in order to evaluate polypseudorotaxanes with different degrees of threading and different polyviologen chain lengths. Among seven polypseudorotaxanes,[289] one assembly, designated [**5:21**], which was obtained from five equivalents of Lac-α-CD with a polyviologen containing,

DOI: 10.31635/ccschem.025.202505711
Citation: *CCS Chem.* **2025**, 7, 1935–1971
Link to VoR: https://doi.org/10.31635/ccschem.025.202505711

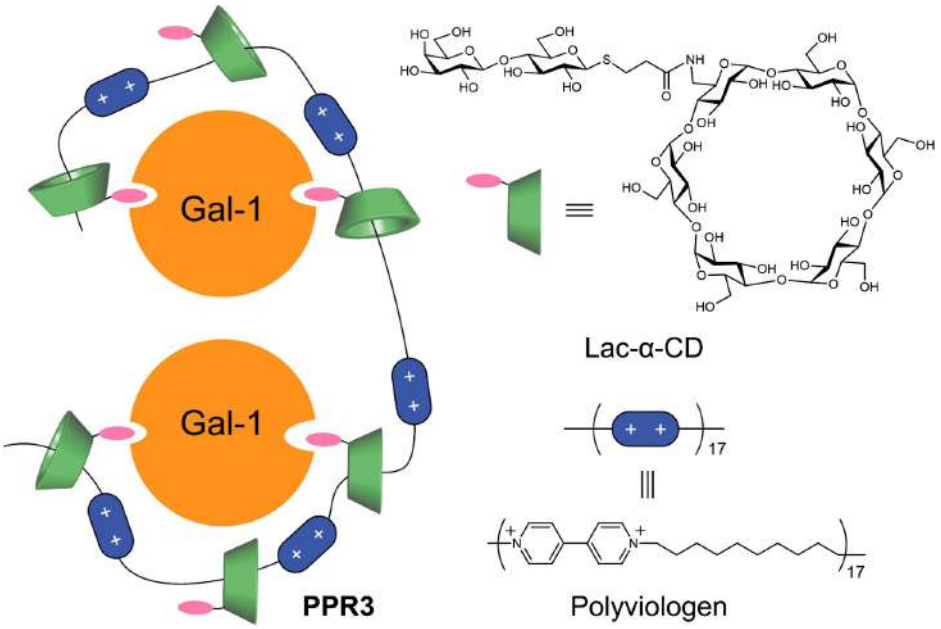

Figure 22 | *Schematic representations of multivalent interactions between bivalent Gal-1 and a polypseudorotaxane consisting of Lac-α-CD "beads" threaded onto a polyviologen-based copolymer "string".*

on average, 21 repeating units, provided valency-corrected enhancement of a 30-fold compared to native lactose and a 20-fold over free Lac-α-CD in T-cell agglutination assays. These innovative CD-based polypseudorotaxanes, which are capable of binding specific receptors with enhanced multivalent interactions, constitute a promising alternative for targeting therapeutically relevant receptors.

Cyclodextrin-Based (Pseudo) rotaxanes as Nanovalves

In 2005, in collaboration with Jeff Zink, the Stoddart group at UCLA, pioneered[290] the integration of mesoporous silica nanoparticles (SNPs) with redox-activated bistable [2]rotaxanes that function as nanovalves. The resulting organic–inorganic hybrid nanoparticles, referred to as mechanized silica nanoparticles (MSNPs), are capable of trapping and releasing guest molecules in a highly controlled manner when exposed to specific stimuli.

One representative protype of MSNPs contains (Figure 23a) three primary components: they are (1) a solid support such as mesoporous SNPs, (2) a payload of small molecules, and (3) a monolayer of external machinery usually in the form of rotaxanes. When the ring components remain close to the particle surface because the nanovalves are closed, the guest molecules are trapped inside the pores of MSNPs. In response to a specific stimulus, which leads to the cleavage of the stoppers, the ring components can move away from the surface because the nanovalves are open, allowing a controlled release of a payload of small molecules.

The first example[291] of using biocompatible CD as the ring component to construct a rotaxane-type nanovalve was described by the Stoddart-Zink team in 2008. A cargo molecule (rhodamine B)-loaded SNP was functionalized (Figure 23b) with a pseudorotaxane in which α-CD and the SNP itself act as the ring component and one stopper, respectively. The existence of α-CD close to the surfaces of SNPs effectively blocks the nanopores, preventing the release of encapsulated rhodamine B. An ester-linked adamantyl stopper precursor **54** with a terminal alkyne handle was attached to the pseudorotaxane using the Cu(I)-catalyzed azide-alkyne cycloaddition.[292,293] While the resulting MSNPs are chemically stable, a controlled cargo release can be triggered enzymatically by porcine liver esterase (PLE). PLE selectively catalyzes the hydrolysis of the adamantyl ester stopper, resulting in dethreading of the α-CD, followed by cargo release from the nanopores.

Following this initial work on α-CD-based enzyme-responsive MSNPs, the Stoddart-Zink team successfully developed various types of MSNPs comprised of CD-based nanovalves that can operate when exposed to different stimuli such as light,[294,295] redox reactions,[296–298] pH changes,[298–303] and sugars.[303] Over the years, these nontoxic MSNPs, which can accumulate passively in solid tumors thanks to an enhanced permeability and retention effect, have emerged as a promising platform for targeted delivery and release of therapeutic and diagnostic agents in response to preexisting biological triggers.[304,305]

DOI: 10.31635/ccschem.025.202505711
Citation: *CCS Chem.* **2025**, 7, 1935–1971
Link to VoR: https://doi.org/10.31635/ccschem.025.202505711

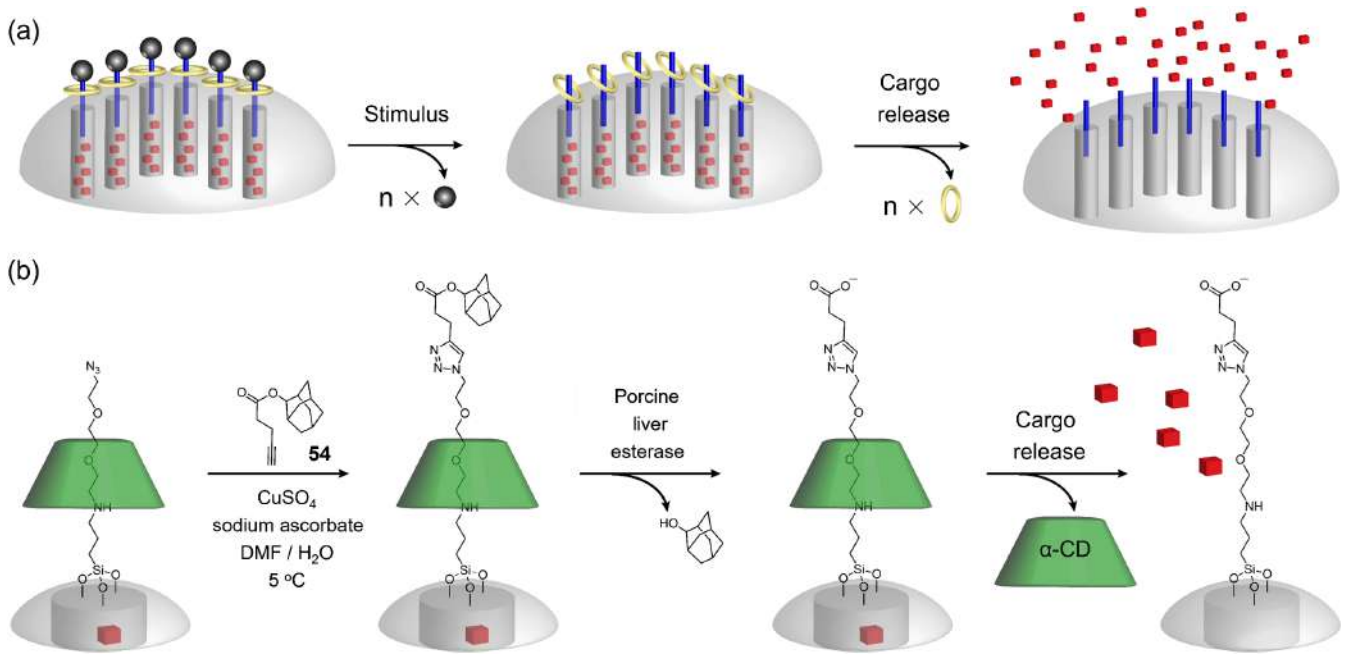

Figure 23 | *(a) Schematic representation of MSNPs functionalized with rotaxane-type nanovalves. When exposed to specific stimulus, the stoppers of nanovalves cleave, resulting in controlled cargo release. (b) Schematic representation of α-CD-based enzyme-responsive MSNPs. The adamantyl ester stopper can be hydrolyzed selectively by PLE, triggring the dethreading of α-CD and subsequent cargo release.*

Summary and Outlook

While our exploration in CD science and technology can be traced back to as early as the late 1960s, most of the research carried out by the Stoddart group did not happen until the 1980s, coinciding with the beginning of industrial production[24–27] of CDs, which made it possible to obtain high-purity CDs at relatively low costs. Our research work covers not only covalent synthesis, aiming to release CDs from their structural straightjackets, but also noncovalent synthesis wherein CDs and CD derivatives serve as nanoscale building blocks for the construction of chemically modified molecules and supermolecules. Essentially, these scientific adventures—which resulted in a number of CD derivatives, analogues, and enantiomers, as well as CD-based second-sphere coordination complexes, CD-MOFs, and CD-based MIMs—have significantly enriched the toolbox currently available for the CD community and pushed the boundaries of CD chemistry forward.

Reflecting on the origins of the Stoddart group's research in relation to CDs, it transpires that, in most cases, rational designs, which were inspired by an increasing knowledge and advances in carbohydrate and supramolecular chemistry, are the main driving forces. Nevertheless, serendipity[306] has also expressed itself twice during the past 15 years, leading to the discovery of edible CD-MOFs and the development of environmentally friendly and sustainable gold separation techniques based on second-sphere coordination wherein CDs act as second-sphere ligands. As a consequence of these serendipitous discoveries, two startup companies were launched recently, a situation that could not have been foreseen at the beginning of these curiosity-driven attempts.

Our story also emphasizes the irreplaceable importance of scientific collaboration, a dynamic that has served our CD-related research well at different stages during the past half century. For instance, our close collaboration with X-ray crystallographers David Williams[117,136,149,150,156,188,192–197,199,201,202,273,274] at the Imperial College London and Charlotte Stern[161,208,212,228,229,239,257–259,261] at NU, which have produced hundreds of solid-state structures, are prerequisites for the emergence and development of systems such as CD-based second-sphere coordination complexes and CD-MOFs. In addition, through working hand in hand with Jeff Zink[291,294–305] at UCLA, the Stoddart group pioneered the use of CD-containing MIMs as nanovalves for the controlled release of small molecular cargos including drugs. This research represents an important step towards practical applications of artificial molecular machines (AMMs) in biomedical research. Given the widely recognized superior properties of CDs such as biocompatibility and water solubility over other wholly synthetic macrocycles, we anticipate that collaborative efforts from talented scientists of different persuasions in developing

DOI: 10.31635/ccschem.025.202505711
Citation: *CCS Chem.* **2025**, 7, 1935–1971
Link to VoR: https://doi.org/10.31635/ccschem.025.202505711

biocompatible CD-based AMMs will inevitably provide the next generation of stimuli-responsive sensors, smart drugs, and adaptive biomaterials.[271,307,308]

Despite being a century-old activity, academic research into CDs and their industrial applications continue to surge, as indicated not only by the 56-year CD odyssey in the Stoddart group but also the fast growth of related publications, patents, and products on an annual basis. In the future, there is still ample room for new discoveries provided some of the major challenges facing the CD community are satisfactorily addressed.

Let us now try to foresee a few critical goals that need to be achieved in the years and decades to come. Currently, the most accessible CD homologues are still limited to medium-ring α-, β-, and γ-CDs. Although recent advances in the syntheses of small-ring,[309] large-ring,[310] and mirror-image[161] CDs have opened up new research opportunities, future efforts in scaling up while decreasing the cost of CD production are urgently needed. In addition, precise modifications[85,86] on both rims of CD tori are required in order to achieve tailored functions in diverse applications. Lastly, the average association constants[311] of CDs with organic molecules are moderate ($10^{2.5}$ M^{-1}), and it is crucial to create CD derivatives and analogues with improved binding affinities to specific guests while maintaining comparable or even improved water solubility and biocompatibility as native CDs.

Although the evolution of CD science and technology cannot be precisely predicted, one thing remains certain: CDs will continue to inspire[312] imaginative projects as long as researchers continue exploring the unknown of CDs with curiosity and zeal. We would like to conclude with what Joseph Chatt pointed[313] out three decades ago: *"If you have an exciting road to follow, do not be put off by those who say there is nothing at the end of it; they do not know. Persevere, and enjoy the excitement of exploring the unknown."*

Footnotes

[a] As a result of the three reactions, α-CD loses 18 and β-CD loses 21 stereogenic centers. The resulting compounds **1** and **2**, which belong to the point group, C_{6v} and C_{7v}, respectively, are achiral. After deacylation, achiral perhydroxymethylated polyacetals **3** (C_{6v}) and **4** (C_{7v}) were obtained.

[b] When one of the D-glucopyranosyl units has an extra substituent, the C_n symmetry is broken and every proton (and carbon) atom becomes heterotopic, leading to very complicated NMR spectra.

[c] Gatteschi and coworkers, who were close to making isostructural CD-MOFs with Na^+ ions,[220] need to be credited here. In their investigation, cubic-shaped orange-reddish single crystals of γ-Fe_2O_3/γ-CD were formed after an ethanolic solution of NaOH was added to a DMF solution of $FeCl_3$ and γ-CD, while similar colorless cubic crystals were obtained when $FeCl_3$ was replaced by NaCl. In both cases, the researchers identified a cubic cell (30.217 Å edge) of space group *I*432 but were not able to determine the crystal structure of either compound, probably on account of crystal quality issues.

[d] The preparation of CD-MOF-3 from γ-CD and CsOH was complicated by the cocrystallization of a related polymorph, which we have termed CD-MOF-4, consisting of γ-CD tori linked to one another through Cs^+ coordination to form channel-type superstructures.

[e] The mechanism of CO_2 adsorption proposed in ref 244 has been revised recently by Milner and coworkers: chemisorption of CO_2 in CD-MOFs occurs via HCO_3^- formation at nucleophilic OH^- sites within the framework pores, rather than via previously proposed pathways involving carbonic acid or alkyl carbonate formation.

[f] The first reported attempt, although not successful, to synthesize catenated CDs was done by Lüttringhaus, Cramer, Prinzbach, and Henglein.

Conflict of Interest

The authors declare no conflict of interest.

Acknowledgments

This work was supported by the Fundamental Research Funds for the Central Universities. The authors thank Sichuan University, the University of Hong Kong, and the Institute of Chemistry of the Chinese Academy of Sciences for financial support.

References

1. Liu, Z.; Nalluri, S. K. M.; Stoddart, J. F. Surveying Macrocyclic Chemistry: From Flexible Crown Ethers to Rigid Cyclophanes. *Chem. Soc. Rev.* **2017**, *46*, 2459–2478.
2. Cram, D. J.; Cram, J. M. Host-Guest Chemistry: Complexes Between Organic Compounds Simulate the Substrate Selectivity of Enzymes. *Science* **1974**, *183*, 803–809.
3. Lehn, J.-M. Supramolecular Chemistry. *Science* **1993**, *260*, 1762–1763.
4. Johnson, E. R.; Keinan, S.; Mori-Sánchez, P.; Contreras-García, J.; Cohen, A. J.; Yang, W. Revealing Noncovalent Interactions. *J. Am. Chem. Soc.* **2010**, *132*, 6498–6506.
5. Pedersen, C. J. The Discovery of Crown Ethers (Nobel Lecture). *Angew. Chem. Int. Ed. Engl.* **1988**, *27*, 1021–1027.
6. Lehn, J.-M. Supramolecular Chemistry—Scope and Perspectives Molecules, Supermolecules, and Molecular Devices (Nobel Lecture). *Angew. Chem. Int. Ed. Engl.* **1988**, *27*, 89–112.
7. Cram, D. J. The Design of Molecular Hosts, Guests, and Their Complexes (Nobel lecture). *Angew. Chem. Int. Ed. Engl.* **1988**, *27*, 1009–1020.
8. Pedersen, C. J. Cyclic Polyethers and Their Complexes with Metal Salts. *J. Am. Chem. Soc.* **1967**, *89*, 2495–2496.

DOI: 10.31635/ccschem.025.202505711
Citation: *CCS Chem.* **2025**, 7, 1935–1971
Link to VoR: https://doi.org/10.31635/ccschem.025.202505711

9. Pedersen, C. J. Cyclic Polyethers and Their Complexes with Metal Salts. *J. Am. Chem. Soc.* **1967**, *89*, 7017–7036.
10. Gutsche, C. D. Calixarenes. *Acc. Chem. Res.* **1983**, *16*, 161–170.
11. Freeman, W. A.; Mock, W. L.; Shih, N.-Y. Cucurbituril. *J. Am. Chem. Soc.* **1981**, *103*, 7367–7368.
12. Ogoshi, T.; Kanai, S.; Fujinami, S.; Yamagishi, T.-A.; Nakamoto, Y. *para*-Bridged Symmetrical Pillar[5]arenes: Their Lewis Acid Catalyzed Synthesis and Host–Guest Property. *J. Am. Chem. Soc.* **2008**, *130*, 5022–5023.
13. Wang, M.-X. Nitrogen and Oxygen Bridged Calixaromatics: Synthesis, Structure, Functionalization, and Molecular Recognition. *Acc. Chem. Res.* **2012**, *45*, 182–195.
14. Xue, M.; Yang, Y.; Chi, X.; Zhang, Z.; Huang, F. Pillararenes, a New Class of Macrocycles for Supramolecular Chemistry. *Acc. Chem. Res.* **2012**, *45*, 1294–1308.
15. Kim, S. K.; Sessler, J. L. Calix[4]pyrrole-Based Ion Pair Receptors. *Acc. Chem. Res.* **2014**, *47*, 2525–2536.
16. Chen, C.-F.; Han, Y. Triptycene-Derived Macrocyclic Arenes: From Calixarenes to Helicarenes. *Acc. Chem. Res.* **2018**, *51*, 2093–2106.
17. Liu, C.; Ni, Y.; Lu, X.; Li, G.; Wu, J. Global Aromaticity in Macrocyclic Polyradicaloids: Hückel's Rule or Baird's Rule? *Acc. Chem. Res.* **2019**, *52*, 2309–2321.
18. Yang, L.-P.; Wang, X.; Yao, H.; Jiang, W. Naphthotubes: Macrocyclic Hosts with a Biomimetic Cavity Feature. *Acc. Chem. Res.* **2019**, *53*, 198–208.
19. Guo, Q.-H.; Qiu, Y.; Wang, M.-X.; Stoddart, J. F. Aromatic Hydrocarbon Belts. *Nat. Chem.* **2021**, *13*, 402–419.
20. Wu, J.-R.; Wu, G.; Yang, Y.-W. Pillararene-Inspired Macrocycles: From Extended Pillar[n]arenes to Geminiarenes. *Acc. Chem. Res.* **2022**, *55*, 3191–3204.
21. Pan, Y.-C.; Tian, J.-H.; Guo, D.-S. Molecular Recognition with Macrocyclic Receptors for Application in Precision Medicine. *Acc. Chem. Res.* **2023**, *56*, 3626–3639.
22. Chen, X.-Y.; Chen, H.; Stoddart, J. F. The Story of the Little Blue Box: A Tribute to Siegfried Hünig. *Angew. Chem. Int. Ed.* **2023**, *62*, e202211387.
23. Stoddart, J. F. A Century of Cyclodextrins. *Carbohydr. Res.* **1989**, *192*, xii–xv.
24. Szejtli, J. Introduction and General Overview of Cyclodextrin Chemistry. *Chem. Rev.* **1998**, *98*, 1743–1753.
25. Crini, G. Review: A History of Cyclodextrins. *Chem. Rev.* **2014**, *114*, 10940–10975.
26. Morin-Crini, N.; Fourmentin, S.; Fenyvesi, É.; Lichtfouse, E.; Torri, G.; Fourmentin, M.; Crini, G. History of Cyclodextrins. In *The History of Cyclodextrins*; Crini, G., Fourmentin, S., Lichtfouse, E., Eds.; Springer Nature: Cham, Switzerland, **2020**; pp 1–93.
27. Morin-Crini, N.; Fourmentin, S.; Fenyvesi, É.; Lichtfouse, E.; Torri, G.; Fourmentin, M.; Crini, G. 130 Years of Cyclodextrin Discovery for Health, Food, Agriculture, and the Industry: A Review. *Environ. Chem. Lett.* **2021**, *19*, 2581–2617.
28. Villiers, A. Sur la Fermentation de la Fécule par L'action du Ferment Butyrique. *C. R. Hebd. Acad. Sci. Paris* **1891**, *112*, 536–538.
29. Crini, G. The Contribution of Franz Schardinger to Cyclodextrins: A Tribute on the Occasion of the Centenary of His Death. *J. Incl. Phenom. Macrocycl. Chem.* **2020**, *97*, 19–28.
30. Crini, G. Twenty Years of Dextrin Research: A Tribute to Professor Hans Pringsheim (1876–1940). *J. Incl. Phenom. Macrocycl. Chem.* **2020**, *98*, 11–27.
31. Crini, G. The Contribution of Professor Paul Karrer (1889–1971) to Dextrins. *J. Incl. Phenom. Macrocycl. Chem.* **2021**, *99*, 155–167.
32. Freudenberg, K. Beiträge zur Chemie der Stärke und der Cycloglucane (Schardinger-Dextrine). *Angew. Chem.* **1957**, *69*, 419–422.
33. Crini, G.; French, A. D.; Kainuma, K.; Jane, J.-L.; Szente, L. Contributions of Dexter French (1918–1981) to Cycloamylose/Cyclodextrin and Starch Science. *Carbohydr. Polym.* **2021**, *257*, 117620.
34. Cramer, F. Einschlußverbindungen. *Angew. Chem.* **1952**, *64*, 437–447.
35. Torri, G.; Naggi, A.; Lichtfouse, E.; Crini, G. Professor Casu's Contribution to Cyclodextrins, the Remarkable Cage-Shaped Molecules: A Review. *Environ. Chem. Lett.* **2022**, *20*, 2085–2095.
36. Bender, H. Production, Characterization and Applications of Cyclodextrins. In *Advances in Biotechnological Processes*; Liss, A. R., Ed.; Wiley: New York, **1986**; pp 31–71.
37. Saenger, W. Cyclodextrin Inclusion Compounds in Research and Industry. *Angew. Chem. Int. Ed. Engl.* **1980**, *19*, 344–362.
38. Joseph, V.; Levine, M. Ronald C.D. Breslow (1931–2017): A Career in Review. *Bioorg. Chem.* **2021**, *115*, 104868.
39. Crini, G.; Fenyvesi, É.; Szente, L. Professor József Szejtli: The Godfather of Cyclodextrins. In *The History of Cyclodextrins*; Crini, G., Fourmentin, S., Lichtfouse, E., Eds.; Springer Nature: Cham, Switzerland, **2020**; pp 95–155.
40. Biedermann, F.; Nau, W. M.; Schneider, H.-J. The Hydrophobic Effect Revisited—Studies with Supramolecular Complexes Imply High-Energy Water as a Noncovalent Driving Force. *Angew. Chem. Int. Ed.* **2014**, *53*, 11158–11171.
41. Xu, C.; Tran, Q. G.; Liu, D.; Zhai, C.; Wojtas, L.; Liu, W. Charge-Assisted Hydrogen Bonding in a Bicyclic Amide Cage: An Effective Approach to Anion Recognition and Catalysis in Water. *Chem. Sci.* **2024**, *15*, 16040–16049.
42. Hermann, J.; DiStasio, R. A. Jr.; Tkatchenko, A. First-Principles Models for van der Waals Interactions in Molecules and Materials: Concepts, Theory, and Applications. *Chem. Rev.* **2017**, *117*, 4714–4758.
43. Stoddart, J. F. Tate and Lyle Lecture. From Carbohydrates to Enzyme Analogues. *Chem. Soc. Rev.* **1979**, *8*, 85–142.
44. Breslow, R. Artificial Enzymes. *Science* **1982**, *218*, 532–537.
45. D'Souza, V. T.; Bender, M. L. Miniature Organic Models of Enzymes. *Acc. Chem. Res.* **1987**, *20*, 146–152.
46. Ji, J.; Wei, X.; Wu, W.; Yang, C. Asymmetric Photoreactions in Supramolecular Assemblies. *Acc. Chem. Res.* **2023**, *56*, 1896–1907.

DOI: 10.31635/ccschem.025.202505711
Citation: *CCS Chem.* **2025**, 7, 1935–1971
Link to VoR: https://doi.org/10.31635/ccschem.025.202505711

47. Easton, C. J.; Lincoln, S. F. Chiral Discrimination by Modified Cyclodextrins. *Chem. Soc. Rev.* **1996**, *25*, 163–170.
48. Hinze, W. L. Application of Cyclodextrins in Chromatographic Separations and Purification Methods. *Sep. Purif. Methods* **1981**, *10*, 159–237.
49. Armstrong, D. W.; Ward, T. J.; Armstrong, R. D.; Beesley, T. E. Separation of Drug Stereoisomers by the Formation of β-Cyclodextrin Inclusion Complexes. *Science* **1986**, *232*, 1132–1135.
50. Szente, L.; Szemán, J. Cyclodextrins in Analytical Chemistry: Host–Guest Type Molecular Recognition. *Anal. Chem.* **2013**, *85*, 8024–8030.
51. Portillo, A.; Berthod, A.; Armstrong, D. W. Chromatographic Separations and Analysis: Cyclodextrin-Mediated High-Performance Liquid Chromatography, Gas Chromatography and Capillary Electrophoresis Enantiomeric Separations. In *Comprehensive Chirality*; Cossy, J., Ed.; Academic Press: Cambridge, Massachusetts, **2024**; pp 184–199.
52. Xu, Y.; Rashwan, A. K.; Osman, A. I.; Abd El-Monaem, E. M.; Elgarahy, A. M.; Eltaweil, A. S.; Omar, M.; Li, Y.; Mehanni, A.-H. E.; Chen, W.; Rooney, D. W. Synthesis and Potential Applications of Cyclodextrin-Based Metal–Organic Frameworks: A Review. *Environ. Chem. Lett.* **2023**, *21*, 447–477.
53. Antlsperger, G.; Schmid, G. Toxicological Comparison of Cyclodextrins. In *Proceedings of the Eighth International Symposium on Cyclodextrins: Budapest, Hungary, March 31–April 2, 1996*; Szejtli, J., Szente, L., Eds.; Kluwer Academic Publishers: Dordrecht, **1996**; pp 149–155.
54. Braga, S. S. Cyclodextrins: Emerging Medicines of the New Millennium. *Biomolecules* **2019**, *9*, 801.
55. Kovacs, T.; Nagy, P.; Panyi, G.; Szente, L.; Varga, Z.; Zakany, F. Cyclodextrins: Only Pharmaceutical Excipients or Full-Fledged Drug Candidates? *Pharmaceutics* **2022**, *14*, 2559.
56. Puskás, I.; Szente, L.; Szőcs, L.; Fenyvesi, É. Recent List of Cyclodextrin-Containing Drug Products. *Period. Polytech. Chem. Eng.* **2023**, *67*, 11–17.
57. Bom, A.; Bradley, M.; Cameron, K.; Clark, J. K.; Van Egmond, J.; Feilden, H.; MacLean, E. J.; Muir, A. W.; Palin, R.; Rees, D. C.; Zhang, M.-Q. A Novel Concept of Reversing Neuromuscular Block: Chemical Encapsulation of Rocuronium Bromide by a Cyclodextrin-Based Synthetic Host. *Angew. Chem. Int. Ed.* **2002**, *41*, 265–270.
58. Kalydi, E.; Sebák, F.; Fiser, B.; Minofar, B.; Moussong, É.; Malanga, M.; Bodor, A.; Kardos, J.; Béni, S. Exceptional Stability of the Sugammadex-Solasodine Complex: Insights from Experimental and Theoretical Studies. *Carbohydr. Polym.* **2025**, *348*, 122819.
59. Zhang, Y.; Jiang, Y.; Lei, Q.; Li, C.; Wang, Q.; Huang, Y.; Li, Y.; Hong, Y.; Wang, S.; Lin, H.; Li, H.; Ou, Y.; Zou, X.; Sun, Q.; Guo, Q.; Chen, Z.; Min, S.; Qi, Y.; Jie, Q.; Liu, J.; Liu, B.; Zhang, W. Phase III Clinical Trial Comparing the Efficacy and Safety of Adamgammadex with Sugammadex for Reversal of Rocuronium-Induced Neuromuscular Block. *Br. J. Anaesth.* **2024**, *132*, 45–52.
60. Liu, Y.-Y.; Yu, X.-Y.; Pan, Y.-C.; Yin, H.; Chao, S.; Li, Y.; Ma, H.; Zuo, M.; Teng, K.-X.; Hou, J.-L.; Chen, Y.; Guo, D.-S.; Wang, R.; Pei, Y.; Pei, Z.; Xu, J.-F.; Hu, X.-Y.; Li, C.; Yang, Q.-Z.; Wang, L.; Liu, Y.; Li, Z.-T. Supramolecular Systems for Bioapplications: Recent Research Progress in China. *Sci. China Chem.* **2024**, *67*, 1397–1441.
61. Ory, D. S.; Ottinger, E. A.; Farhat, N. Y.; King, K. A.; Jiang, X.; Weissfeld, L.; Berry-Kravis, E.; Davidson, C. D.; Bianconi, S.; Keener, L. A.; Rao, R.; Soldatos, A.; Sidhu, R.; Walters, K. A.; Xu, X.; Thurm, A.; Solomon, B.; Pavan, W. J.; Machielse, B. N.; Kao, M.; Silber, S. A.; McKew, J. C.; Brewer, C. C.; Vite, C. H.; Walkley, S. U.; Austin, C. P.; Porter, F. D. Intrathecal 2-Hydroxypropyl-β-Cyclodextrin Decreases Neurological Disease Progression in Niemann-Pick disease, Type C1: A Non-Randomised, Open-Label, Phase 1–2 Trial. *The Lancet* **2017**, *390*, 1758–1768.
62. Clemens, D.; Anderson, A.; Dinh, D.; Bhargava, P.; Sadrerafi, K.; Malanga, M.; Garcia-Fandiño, R.; Piñeiro, Á.; O'Connor, M. Reversing Atherosclerosis by the Specific Removal of Oxidized Cholesterol with Cyclodextrin Dimer. *Atherosclerosis* **2023**, *379*, S34–S35.
63. Ramamurthy, V.; Eaton, D. F. Photochemistry and Photophysics within Cyclodextrin Cavities. *Acc. Chem. Res.* **1988**, *21*, 300–306.
64. Shigemitsu, H.; Kawakami, K.; Nagata, Y.; Kajiwara, R.; Yamada, S.; Mori, T.; Kida, T. Cyclodextrins with Multiple Pyrenyl Groups: An Approach to Organic Molecules Exhibiting Bright Excimer Circularly Polarized Luminescence. *Angew. Chem. Int. Ed.* **2022**, *61*, e202114700.
65. Tu, C.; Wu, W.; Liang, W.; Zhang, D.; Xu, W.; Wan, S.; Lu, W.; Yang, C. Host–Guest Complexation-Induced Aggregation Based on Pyrene-Modified Cyclodextrins for Improved Electronic Circular Dichroism and Circularly Polarized Luminescence. *Angew. Chem. Int. Ed.* **2022**, *61*, e202203541.
66. Alsbaiee, A.; Smith, B. J.; Xiao, L.; Ling, Y.; Helbling, D. E.; Dichtel, W. R. Rapid Removal of Organic Micropollutants from Water by a Porous β-Cyclodextrin Polymer. *Nature* **2016**, *529*, 190–194.
67. Bao, K.; Zhang, A.; Cao, Y.; Xu, L. Achievements in Preparation of Cyclodextrin-Based Porous Materials for Removal of Pollutants. *Separations* **2024**, *11*, 143.
68. Lin, Q.; Li, L.; Tang, M.; Uenuma, S.; Samanta, J.; Li, S.; Jiang, X.; Zou, L.; Ito, K.; Ke, C. Kinetic Trapping of 3D-Printable Cyclodextrin-Based Poly(pseudo)rotaxane Networks. *Chem* **2021**, *7*, 2442–2459.
69. Qiao, B.; Zeng, Q.; Li, L. Efficient Synthesis of Metastable Cyclodextrin-Based Polyrotaxanes with Tunable Threading Ratios. *Angew. Chem. Int. Ed.* **2024**, *63*, e202412839.
70. Liu, J.; Ikura, R.; Yamaoka, K.; Sugawara, A.; Takahashi, Y.; Kure, B.; Takenaka, N.; Park, J.; Uyama, H.; Takashima, Y. Exploring Enzymatic Degradation, Reinforcement, Recycling, and Upcycling of Poly(ester)-Poly(urethane) with Movable Crosslinks. *Chem* **2025**, *11*, 102327.
71. Huang, J.; Li, J.; Lyu, Y.; Miao, Q.; Pu, K. Molecular Optical Imaging Probes for Early Diagnosis of Drug-Induced Acute Kidney Injury. *Nat. Mater.* **2019**, *18*, 1133–1143.
72. d'Orchymont, F.; Holland, J. P. Supramolecular Rotaxane-Based Multi-Modal Probes for Cancer Biomarker Imaging. *Angew. Chem. Int. Ed.* **2022**, *61*, e202204072.

DOI: 10.31635/ccschem.025.202505711
Citation: *CCS Chem.* **2025**, 7, 1935–1971
Link to VoR: https://doi.org/10.31635/ccschem.025.202505711

73. Evenou, P.; Rossignol, J.; Pembouong, G.; Gothland, A.; Colesnic, D.; Barbeyron, R.; Rudiuk, S.; Marcelin, A.-G.; Ménand, M.; Baigl, D.; Calvez, V.; Bouteiller, L.; Sollogoub, M. Bridging β-Cyclodextrin Prevents Self-Inclusion, Promotes Supramolecular Polymerization, and Promotes Cooperative Interaction with Nucleic Acids. *Angew. Chem. Int. Ed.* **2018**, *57*, 7753–7758.
74. Wen, Y.; Bai, H.; Zhu, J.; Song, X.; Tang, G.; Li, J. A Supramolecular Platform for Controlling and Optimizing Molecular Architectures of siRNA Targeted Delivery Vehicles. *Sci. Adv.* **2020**, *6*, eabc2148.
75. Saenger, W.; Jacob, J.; Gessler, K.; Steiner, T.; Hoffmann, D.; Sanbe, H.; Koizumi, K.; Smith, S. M.; Takaha, T. Structures of the Common Cyclodextrins and Their Larger Analogues Beyond the Doughnut. *Chem. Rev.* **1998**, *98*, 1787–1802.
76. Harata, K. Structural Aspects of Stereodifferentiation in the Solid State. *Chem. Rev.* **1998**, *98*, 1803–1827.
77. Engeldinger, E.; Armspach, D.; Matt, D. Capped Cyclodextrins. *Chem. Rev.* **2003**, *103*, 4147–4174.
78. Connors, K. A. The Stability of Cyclodextrin Complexes in Solution. *Chem. Rev.* **1997**, *97*, 1325–1358.
79. Lipkowitz, K. B. Applications of Computational Chemistry to the Study of Cyclodextrins. *Chem. Rev.* **1998**, *98*, 1829–1874.
80. Schneider, H.-J.; Hacket, F.; Rüdiger, V.; Ikeda, H. NMR Studies of Cyclodextrins and Cyclodextrin Complexes. *Chem. Rev.* **1998**, *98*, 1755–1786.
81. Rekharsky, M. V.; Inoue, Y. Complexation Thermodynamics of Cyclodextrins. *Chem. Rev.* **1998**, *98*, 1875–1918.
82. Lebrilla, C. B. The Gas-Phase Chemistry of Cyclodextrin Inclusion Complexes. *Acc. Chem. Res.* **2001**, *34*, 653–661.
83. Hapiot, F.; Tilloy, S.; Monflier, E. Cyclodextrins as Supramolecular Hosts for Organometallic Complexes. *Chem. Rev.* **2006**, *106*, 767–781.
84. Douhal, A. Ultrafast Guest Dynamics in Cyclodextrin Nanocavities. *Chem. Rev.* **2004**, *104*, 1955–1976.
85. Khan, A. R.; Forgo, P.; Stine, K. J.; D'Souza, V. T. Methods for Selective Modifications of Cyclodextrins. *Chem. Rev.* **1998**, *98*, 1977–1996.
86. Bellia, F.; La Mendola, D.; Pedone, C.; Rizzarelli, E.; Saviano, M.; Vecchio, G. Selectively Functionalized Cyclodextrins and Their Metal Complexes. *Chem. Soc. Rev.* **2009**, *38*, 2756–2781.
87. Tabushi, I. Cyclodextrin Catalysis as a Model for Enzyme Action. *Acc. Chem. Res.* **1982**, *15*, 66–72.
88. Takahashi, K. Organic Reactions Mediated by Cyclodextrins. *Chem. Rev.* **1998**, *98*, 2013–2033.
89. Breslow, R.; Dong, S. D. Biomimetic Reactions Catalyzed by Cyclodextrins and Their Derivatives. *Chem. Rev.* **1998**, *98*, 1997–2012.
90. Harada, A.; Osaki, M.; Takashima, Y.; Yamaguchi, H. Ring-Opening Polymerization of Cyclic Esters by Cyclodextrins. *Acc. Chem. Res.* **2008**, *41*, 1143–1152.
91. Chen, Y.; Liu, Y. Cyclodextrin-Based Bioactive Supramolecular Assemblies. *Chem. Soc. Rev.* **2010**, *39*, 495–505.
92. Chen, G.; Jiang, M. Cyclodextrin-Based Inclusion Complexation Bridging Supramolecular Chemistry and Macromolecular Self-Assembly. *Chem. Soc. Rev.* **2011**, *40*, 2254–2266.
93. Liu, Z.; Liu, Y. Multicharged Cyclodextrin Supramolecular Assemblies. *Chem. Soc. Rev.* **2022**, *51*, 4786–4827.
94. Nepogodiev, S. A.; Stoddart, J. F. Cyclodextrin-Based Catenanes and Rotaxanes. *Chem. Rev.* **1998**, *98*, 1959–1976.
95. Harada, A. Cyclodextrin-Based Molecular Machines. *Acc. Chem. Res.* **2001**, *34*, 456–464.
96. Wenz, G.; Han, B.-H.; Müller, A. Cyclodextrin Rotaxanes and Polyrotaxanes. *Chem. Rev.* **2006**, *106*, 782–817.
97. Harada, A.; Takashima, Y.; Yamaguchi, H. Cyclodextrin-Based Supramolecular Polymers. *Chem. Soc. Rev.* **2009**, *38*, 875–882.
98. Harada, A.; Takashima, Y.; Nakahata, M. Supramolecular Polymeric Materials via Cyclodextrin–Guest Interactions. *Acc. Chem. Res.* **2014**, *47*, 2128–2140.
99. Prochowicz, D.; Kornowicz, A.; Lewiński, J. Interactions of Native Cyclodextrins with Metal Ions and Inorganic Nanoparticles: Fertile Landscape for Chemistry and Materials Science. *Chem. Rev.* **2017**, *117*, 13461–13501.
100. Roy, I.; Stoddart, J. F. Cyclodextrin Metal–Organic Frameworks and Their Applications. *Acc. Chem. Res.* **2021**, *54*, 1440–1453.
101. Dummert, S. V.; Saini, H.; Hussain, M. Z.; Yadava, K.; Jayaramulu, K.; Casini, A.; Fischer, R. A. Cyclodextrin Metal–Organic Frameworks and Derivatives: Recent Developments and Applications. *Chem. Soc. Rev.* **2022**, *51*, 5175–5213.
102. Hedges, A. R. Industrial Applications of Cyclodextrins. *Chem. Rev.* **1998**, *98*, 2035–2044.
103. Li, S.; Purdy, W. C. Cyclodextrins and Their Applications in Analytical Chemistry. *Chem. Rev.* **1992**, *92*, 1457–1470.
104. Chankvetadze, B.; Endresz, G.; Blaschke, G. Charged Cyclodextrin Derivatives as Chiral Selectors in Capillary Electrophoresis. *Chem. Soc. Rev.* **1996**, *25*, 141–153.
105. Votava, M.; Ravoo, B. J. Principles and Applications of Cyclodextrin Liquid Crystals. *Chem. Soc. Rev.* **2021**, *50*, 10009–10024.
106. Martínez, Á.; Mellet, C. O.; Fernández, J. M. G. Cyclodextrin-Based Multivalent Glycodisplays: Covalent and Supramolecular Conjugates to Assess Carbohydrate–Protein Interactions *Chem. Soc. Rev.* **2013**, *42*, 4746–4773.
107. Villalonga, R.; Cao, R.; Fragoso, A. Supramolecular Chemistry of Cyclodextrins in Enzyme Technology. *Chem. Rev.* **2007**, *107*, 3088–3116.
108. Uekama, K.; Hirayama, F.; Irie, T. Cyclodextrin Drug Carrier Systems. *Chem. Rev.* **1998**, *98*, 2045–2076.
109. Monti, S.; Sortino, S. Photoprocesses of Photosensitizing Drugs Within Cyclodextrin Cavities. *Chem. Soc. Rev.* **2002**, *31*, 287–300.
110. Davis, M. E.; Brewster, M. E. Cyclodextrin-Based Pharmaceutics: Past, Present and Future. *Nat. Rev. Drug Discov.* **2004**, *3*, 1023–1035.
111. Mellet, C. O.; Fernández, J. M. G.; Benito, J. M. Cyclodextrin-Based Gene Delivery Systems. *Chem. Soc. Rev.* **2011**, *40*, 1586–1608.
112. Hu, Q.-D.; Tang, G.-P.; Chu, P. K. Cyclodextrin-Based Host–Guest Supramolecular Nanoparticles for Delivery:

DOI: 10.31635/ccschem.025.202505711
Citation: *CCS Chem.* **2025**, 7, 1935–1971
Link to VoR: https://doi.org/10.31635/ccschem.025.202505711

From Design to Applications. *Acc. Chem. Res.* **2014**, *47*, 2017–2025.
113. Lai, W.-F.; Rogach, A. L.; Wong, W.-T. Chemistry and Engineering of Cyclodextrins for Molecular Imaging. *Chem. Soc. Rev.* **2017**, *46*, 6379–6419.
114. Stoddart, J. F. Reminiscences of My Interactions with Walter Anthony Szarek. *Carbohydr. Res.* **2021**, *507*, 108291.
115. Stoddart, J. F.; Szarek, W. A.; Jones, J. K. N. Large Heterocyclic Rings from Carbohydrate Precursors. *Can. J. Chem.* **1969**, *47*, 3213–3215.
116. Immel, S.; Nakagawa, T.; Lindner, H. J.; Lichtenthaler, F. W. Synthesis and Molecular Geometry of an Achiral 30-Crown-12 Polyacetal from α-Cyclodextrin. *Chem. Eur. J.* **2000**, *6*, 3366–3371.
117. Alker, D.; Ashton, P. R.; Harding, V. D.; Königer, R.; Stoddart, J. F.; White, A. J.; Williams, D. J. Per-6-bromo-per-2,3-dimethyl-β-cyclodextrin. *Tetrahedron Lett.* **1994**, *35*, 9091–9094.
118. Ashton, P. R.; Hartwell, E. Y.; Philp, D.; Spencer, N.; Stoddart, J. F. The Synthesis and Structural Mapping of Unsymmetrical Chemically Modified α-Cyclodextrins by High-Field Nuclear Magnetic Resonance Spectroscopy. *J. Chem. Soc., Perkin Trans. 2* **1995**, 1263–1277.
119. Ashton, P. R.; Königer, R.; Stoddart, J. F.; Alker, D.; Harding, V. D. Amino Acid Derivatives of β-Cyclodextrin. *J. Org. Chem.* **1996**, *61*, 903–908.
120. Fulton, D. A.; Stoddart, J. F. An Efficient Synthesis of Cyclodextrin-Based Carbohydrate Cluster Compounds. *Org. Lett.* **2000**, *2*, 1113–1116.
121. Fulton, D. A.; Pease, A. R.; Stoddart, J. F. Cyclodextrin-Based Carbohydrate Clusters by Amide Bond Formation. *Isr. J. Chem.* **2000**, *40*, 325–333.
122. Fulton, D. A.; Stoddart, J. F. Synthesis of Cyclodextrin-Based Carbohydrate Clusters by Photoaddition Reactions. *J. Org. Chem.* **2001**, *66*, 8309–8319.
123. Fulton, D. A.; Stoddart, J. F. Neoglycoconjugates Based on Cyclodextrins and Calixarenes. *Bioconjugate Chem.* **2001**, *12*, 655–672.
124. Chiu, S.-H.; Myles, D. C.; Garrell, R. L.; Stoddart, J. F. Novel Ether-Linked Secondary Face-to-Face 2-2′ and 3-3′ β-Cyclodextrin Dimers. *J. Org. Chem.* **2000**, *65*, 2792–2796.
125. Casu, B.; Reggiani, M.; Gallo, G. G.; Vigevani, A. Conformation of *O*-Methylated Amylose and Cyclodextrins. *Tetrahedron* **1968**, *24*, 803–821.
126. Boger, J.; Corcoran, R. J.; Lehn, J.-M. Cyclodextrin Chemistry. Selective Modification of All Primary Hydroxyl Groups of α- and β-Cyclodextrins. *Helv. Chim. Acta* **1978**, *61*, 2190–2218.
127. Szejtli, J.; Lipták, A.; Jodál, I.; Fügedi, P.; Nánási, P.; Neszmélyi, A. Synthesis and ^{13}C-NMR Spectroscopy of Methylated beta-Cyclodextrins. *Starch-Stärke* **1980**, *32*, 165–169.
128. Spencer, C. M.; Stoddart, J. F.; Zarzycki, R. Structural Mapping of an Unsymmetrical Chemically Modified Cyclodextrin by High-Field Nuclear Magnetic Resonance Spectroscopy. *J. Chem. Soc., Perkin Trans. 2* **1987**, 1323–1336.
129. Lai, C. S.; Moody, G. J.; Thomas, J. R.; Mulligan, D. C.; Stoddart, J. F.; Zarzycki, R. Piezoelectric Quartz Crystal Detection of Benzene Vapour Using Chemically Modified Cyclodextrins. *J. Chem. Soc., Perkin Trans. 2* **1988**, 319–324.
130. Ellwood, P.; Spencer, C. M.; Spencer, N.; Stoddart, J. F.; Zarzycki, R. Conformational Mobility in Chemically-Modified Cyclodextrins. *J. Inclusion Phenom. Mol. Recognit. Chem.* **1992**, *12*, 121–150.
131. Ashton, P. R.; Boyd, S. E.; Gattuso, G.; Hartwell, E. Y.; Königer, R.; Spencer, N.; Stoddart, J. F. A Novel Approach to the Synthesis of Some Chemically-Modified Cyclodextrins. *J. Org. Chem.* **1995**, *60*, 3898–3903.
132. Tarver, G. J.; Grove, S. J.; Buchanan, K.; Bom, A.; Cooke, A.; Rutherford, S. J.; Zhang, M.-Q. 2-*O*-Substituted Cyclodextrins as Reversal Agents for the Neuromuscular Blocker Rocuronium Bromide. *Bioorg. Med. Chem.* **2002**, *10*, 1819–1827.
133. Nogami, Y.; Nasu, K.; Koga, T.; Ohta, K.; Fujita, K.; Immel, S.; Lindner, H. J.; Schmitt, G. E.; Lichtenthaler, F. W. Synthesis, Structure, and Conformational Features of α-Cycloaltrin: A Cyclooligosaccharide with Alternating $^4C_1/^1C_4$ Pyranoid Chairs. *Angew. Chem. Int. Ed. Engl.* **1997**, *36*, 1899–1902.
134. Ashton, P. R.; Ellwood, P.; Staton, I.; Stoddart, J. F. Synthesis and Characterization of Per-3,6-anhydro Cyclodextrins. *Angew. Chem. Int. Ed. Engl.* **1991**, *30*, 80–81.
135. Ashton, P. R.; Ellwood, P.; Staton, I.; Stoddart, J. F. Per-3,6-anhydro-α-cyclodextrin and Per-3,6-anhydro-β-cyclodextrin. *J. Org. Chem.* **1991**, *56*, 7274–7280.
136. Ashton, P. R.; Gattuso, G.; Königer, R.; Stoddart, J. F.; Williams, D. J. Dipotassium Complex of Per-3,6-anhydro-β-cyclodextrin. *J. Org. Chem.* **1996**, *61*, 9553–9555.
137. Gadelle, A.; Defaye, J. Selective Halogenation at Primary Positions of Cyclomaltooligosaccharides and a Synthesis of Per-3,6-Anhydro Cyclomaltooligosaccharides. *Angew. Chem. Int. Ed. Engl.* **1991**, *30*, 78–80.
138. Schmidt, R. R. New Methods for the Synthesis of Glycosides and Oligosaccharides—Are There Alternatives to the Koenigs-Knorr Method? *Angew. Chem. Int. Ed. Engl.* **1986**, *25*, 212–235.
139. Toshima, K.; Tatsuta, K. Recent Progress in *O*-Glycosylation Methods and Its Application to Natural Products Synthesis. *Chem. Rev.* **1993**, *93*, 1503–1531.
140. Boons, G.-J. Strategies in Oligosaccharide Synthesis. *Tetrahedron* **1996**, *52*, 1095–1121.
141. Gattuso, G.; Nepogodiev, S. A.; Stoddart, J. F. Synthetic Cyclic Oligosaccharides. *Chem. Rev.* **1998**, *98*, 1919–1958.
142. Endo, H.; Sun, Y.-C.; Sasakia, N.; Nokami, T. Recent Advancements in Synthesis of Cyclic Oligosaccharides. *Chem. Commun.* **2025**, *61*, 4483–4494.
143. Mori, M.; Ito, Y.; Ogawa, T. A Highly Stereoselective and Practical Synthesis of Cyclomannohexaose, Cyclo{→4)-[α-D-Man*p*-(1→4)-]$_5$-α-D-Man*p*-(1→}, a *manno* Isomer of Cyclomaltohexaose. *Carbohydr. Res.* **1989**, *192*, 131–146.
144. Mori, M.; Ito, Y.; Ogawa, T. A Highly Efficient and Stereoselective Cycloglycosylation. Synthesis of Cyclo{→4)-[α-Man-(1→4)]$_5$-α-Man-(1→}, a *manno* Isomer of α-Cyclodextrin. *Tetrahedron Lett.* **1989**, *30*, 1273–1276.
145. Mori, M.; Ito, Y.; Uzawa, J.; Ogawa, T. Stereoselectivity of Cycloglycosylation in Mannooligose Series Depends on

DOI: 10.31635/ccschem.025.202505711
Citation: *CCS Chem.* **2025**, 7, 1935–1971
Link to VoR: https://doi.org/10.31635/ccschem.025.202505711

Carbohydrate Chain Length: Syntheses of *manno* Isomers of β- and γ-Cyclodextrins. *Tetrahedron Lett.* **1990**, *31*, 3191–3194.
146. Nishizawa, M.; Imagawa, H.; Kan, Y.; Yamada, H. Total Synthesis of Cyclo-L-Rhamnohexaose by a Stereoselective Thermal Glycosylation. *Tetrahedron Lett.* **1991**, *32*, 5551–5554.
147. Nishizawa, M.; Imagawa, H.; Kubo, K.; Kan, Y.; Yamada, H. Improved Synthesis of α-Cycloawaodorin. *Synlett* **1992**, 447–448.
148. Nishizawa, M.; Imagawa, H.; Morikuni, E.; Hatakeyama, S.; Yamada, H. Synthesis of Cyclo-L-Rhamnopentaose. *Chem. Pharm. Bull.* **1994**, *42*, 1365–1366.
149. Ashton, P. R.; Brown, C. L.; Menzer, S.; Nepogodiev, S. A.; Stoddart, J. F.; Williams, D. J. Synthetic Cyclic Oligosaccharides–Syntheses and Structural Properties of a Cyclo[(1→4)-α-L-Rhamnopyranosyl-(1→4)-α-D-Mannopyranosyl]trioside and -Tetraoside. *Chem. Eur. J.* **1996**, *2*, 580–591.
150. Ashton, P. R.; Cantrill, S. J.; Gattuso, G.; Menzer, S.; Nepogodiev, S. A.; Shipway, A. N.; Stoddart, J. F.; Williams, D. J. Achiral Cyclodextrin Analogues. *Chem. Eur. J.* **1997**, *3*, 1299–1314.
151. Maiti, K.; Jayaraman, N. Synthesis and Structure of Cyclic Trisaccharide with Expanded Glycosidic Linkages. *J. Org. Chem.* **2016**, *81*, 4616–4622.
152. Kochetkov, N. K. Tetrahedron Report Number 218: Synthesis of Polysaccharides with a Regular Structure. *Tetrahedron* **1987**, *43*, 2389–2436.
153. Roy, R.; Andersson, F. O.; Letellier, M. "Active" and "Latent" Thioglycosyl Donors in Oligosaccharide Synthesis. Application to the Synthesis of α-Sialosides. *Tetrahedron Lett.* **1992**, *33*, 6053–6056.
154. Xiao, X.; Zhao, Y.; Shu, P.; Zhao, X.; Liu, Y.; Sun, J.; Zhang, Q.; Zeng, J.; Wan, Q. Remote Activation of Disarmed Thioglycosides in Latent-Active Glycosylation via Interrupted Pummerer Reaction. *J. Am. Chem. Soc.* **2016**, *138*, 13402–13407.
155. Liu, H.; Liang, Z.-F.; Liu, H.-J.; Liao, J.-X.; Zhong, L.-J.; Tu, Y.-H.; Zhang, Q.-J.; Xiong, B.; Sun, J.-S. *ortho*-Methoxycarbonylethynylphenyl Thioglycosides (MCEPTs): Versatile Glycosyl Donors Enabled by Electron-Withdrawing Substituents and Catalyzed by Gold(I) or Cu(II) Complexes. *J. Am. Chem. Soc.* **2023**, *145*, 3682–3695.
156. Gattuso, G.; Menzer, S.; Nepogodiev, S. A.; Stoddart, J. F.; Williams, D. J. Carbohydrate Nanotubes. *Angew. Chem. Int. Ed. Engl.* **1997**, *36*, 1451–1454.
157. Ghadiri, M. R.; Granja, J. R.; Milligan, R. A.; McRee, D. E.; Khazanovich, N. Self-Assembling Organic Nanotubes Based on a Cyclic Peptide Architecture. *Nature* **1993**, *366*, 324–327.
158. Harrison, K.; Mackay, A. S.; Kambanis, L.; Maxwell, J. W. C.; Payne, R. J. Synthesis and Applications of Mirror-Image Proteins. *Nat. Rev. Chem.* **2023**, *7*, 383–404.
159. Chen, J.; Chen, M.; Zhu, T. F. Directed Evolution and Selection of Biostable L-DNA Aptamers with a Mirror-Image DNA Polymerase. *Nat. Biotechnol.* **2022**, *40*, 1601–1609.
160. Welch, B. D.; VanDemark, A. P.; Heroux, A.; Hill, C. P.; Kay, M. S. Potent D-Peptide Inhibitors of HIV-1 Entry. *Proc. Natl. Acad. Sci. U. S. A.* **2007**, *104*, 16828–16833.
161. Wu, Y.; Aslani, S.; Han, H.; Tang, C.; Wu, G.; Li, X.; Wu, H.; Stern, C. L.; Guo, Q.-H.; Qiu, Y.; Chen, A. X.-Y.; Jiao, Y.; Zhang, R.; David, A. H. G.; Armstrong, D. W.; Stoddart, J. F. Mirror-Image Cyclodextrins. *Nat. Synth.* **2024**, *3*, 698–706.
162. Beeren, S. R. Synthesis of L-Cyclodextrins. *Nat. Synth.* **2024**, *3*, 671–672.
163. Nigudkar, S. S.; Demchenko, A. V. Stereocontrolled 1,2-*cis* Glycosylation as the Driving Force of Progress in Synthetic Carbohydrate Chemistry. *Chem. Sci.* **2015**, *6*, 2687–2704.
164. Huang, W.; Zhou, Y.-Y.; Pan, X.-L.; Zhou, X.-Y.; Lei, J.-C.; Liu, D.-M.; Chu, Y.; Yang, J.-S. Stereodirecting Effect of C5-Carboxylate Substituents on the Glycosylation Stereochemistry of 3-Deoxy-D-*manno*-oct-2-ulosonic Acid (Kdo) Thioglycoside Donors: Stereoselective Synthesis of α- and β-Kdo Glycosides. *J. Am. Chem. Soc.* **2018**, *140*, 3574–3582.
165. Zhang, Y.; Zhou, S.; Wang, X.; Zhang, H.; Guo, Z.; Gao, J. A New Method for α-Specific Glucosylation and Its Application to the One-Pot Synthesis of a Branched α-Glucan. *Org. Chem. Front.* **2019**, *6*, 762–772.
166. Zhang, Y.; He, H.; Chen, Z.; Huang, Y.; Xiang, G.; Li, P.; Yang, X.; Lu, G.; Xiao, G. Merging Reagent Modulation and Remote Anchimeric Assistance for Glycosylation: Highly Stereoselective Synthesis of α-Glycans up to a 30-mer. *Angew. Chem. Int. Ed.* **2021**, *60*, 12597–12606.
167. Zhu, Y.; Delbianco, M.; Seeberger, P. H. Automated Assembly of Starch and Glycogen Polysaccharides. *J. Am. Chem. Soc.* **2021**, *143*, 9758–9768.
168. Liu, X.; Song, Y.; Liu, A.; Zhou, Y.; Zhu, Q.; Lin, Y.; Sun, H.; Zhu, K.; Liu, W.; Ding, N.; Xie, W.; Sun, H.; Yu, B.; Xu, P.; Li, W. More than a Leaving Group: *N*-Phenyltrifluoroacetimidate as a Remote Directing Group for Highly α-Selective 1,2-*cis* Glycosylation. *Angew. Chem. Int. Ed.* **2022**, *61*, e202201510.
169. Huang, X.; Huang, L.; Wang, H.; Ye, X.-S. Iterative One-Pot Synthesis of Oligosaccharides. *Angew. Chem. Int. Ed.* **2004**, *43*, 5221–5224.
170. Wu, Y.; Xiong, D.-C.; Chen, S.-C.; Wang, Y.-S.; Ye, X.-S. Total Synthesis of Mycobacterial Arabinogalactan Containing 92 Monosaccharide Units. *Nat. Commun.* **2017**, *8*, 14851.
171. Yao, W.; Xiong, D.-C.; Yang, Y.; Geng, C.; Cong, Z.; Li, F.; Li, B.-H.; Qin, X.; Wang, L.-N.; Xue, W.-Y.; Yu, N.; Zhang, H.; Wu, X.; Liu, M.; Ye, X.-S. Automated Solution-Phase Multiplicative Synthesis of Complex Glycans up to a 1,080-mer. *Nat. Synth.* **2022**, *1*, 854–863.
172. Qin, X.; Xu, C.; Liu, M.; Zeng, F.; Yao, W.; Deng, Y.; Xu, T.; Sun, S.; Sun, D.; Mo, J.; Ye, X.-S. Synthesis of Branched Arabinogalactans up to a 140-mer from *Panax notoginseng* and Their Anti-Pancreatic-Cancer Activity. *Nat. Synth.* **2024**, *3*, 245–255.
173. Yao, W.; Ye, X.-S. Donor Preactivation-Based Glycan Assembly: From Manual to Automated Synthesis. *Acc. Chem. Res.* **2024**, *57*, 1577–1594.
174. Armstrong, D. W.; Aslani, S.; Nafie, J.; Wu, Y.; Stoddart, J. F. Actions and Interactions of Mirror-Image Cyclodextrins. *JACS Au* **2025**, *5*, 693–701.
175. Rojas, M. T.; Königer, R.; Stoddart, J. F.; Kaifer, A. E. Supported Monolayers Containing Preformed Binding

DOI: 10.31635/ccschem.025.202505711
Citation: *CCS Chem.* **2025**, 7, 1935–1971
Link to VoR: https://doi.org/10.31635/ccschem.025.202505711

Sites. Synthesis and Interfacial Binding Properties of a Thiolated β-Cyclodextrin Derivative. *J. Am. Chem. Soc.* **1995**, *117*, 336–343.
176. Zhao, Y.-L.; Stoddart, J. F. Noncovalent Functionalization of Single-Walled Carbon Nanotubes. *Acc. Chem. Res.* **2009**, *42*, 1161–1171.
177. Zhao, Y.-L.; Hu, L.; Stoddart, J. F.; Grüner, G. Pyrenecyclodextrin-Decorated Single-Walled Carbon Nanotube Field-Effect Transistors as Chemical Sensors. *Adv. Mater.* **2008**, *20*, 1910–1915.
178. Zhao, Y.-L.; Hu, L.; Grüner, G.; Stoddart, J. F. A Tunable Photosensor. *J. Am. Chem. Soc.* **2008**, *130*, 16996–17003.
179. Zhao, Y.-L.; Stoddart, J. F. Azobenzene-Based Light-Responsive Hydrogel System. *Langmuir* **2009**, *25*, 8442–8446.
180. Porter, M. D.; Bright, T. B.; Allara, D. L.; Chidsey, C. E. D. Spontaneously Organized Molecular Assemblies. 4. Structural Characterization of *n*-Alkyl Thiol Monolayers on Gold by Optical Ellipsometry, Infrared Spectroscopy, and Electrochemistry. *J. Am. Chem. Soc.* **1987**, *109*, 3559–3568.
181. Dubois, L. H.; Nuzzo, R. G. Synthesis, Structure, and Properties of Model Organic Surfaces. *Annu. Rev. Phys. Chem.* **1992**, *43*, 437–463.
182. He, M.; Zhang, S.; Zhang, J. Horizontal Single-Walled Carbon Nanotube Arrays: Controlled Synthesis, Characterizations, and Applications. *Chem. Rev.* **2020**, *120*, 12592–12684.
183. Karousis, N.; Tagmatarchis, N.; Tasis, D. Current Progress on the Chemical Modification of Carbon Nanotubes. *Chem. Rev.* **2010**, *110*, 5366–5397.
184. Kauffman, D. R.; Star, A. Electronically Monitoring Biological Interactions with Carbon Nanotube Field-Effect Transistors. *Chem. Soc. Rev.* **2008**, *37*, 1197–1206.
185. Bortolus, P.; Monti, S. *Cis* ⇄ *Trans* Photoisomerization of Azobenzene-Cyclodextrin Inclusion Complexes. *J. Phys. Chem.* **1987**, *91*, 5046–5050.
186. Tomatsu, I.; Hashidzume, A.; Harada, A. Contrast Viscosity Changes upon Photoirradiation for Mixtures of Poly(acrylic Acid)-Based α-Cyclodextrin and Azobenzene Polymers. *J. Am. Chem. Soc.* **2006**, *128*, 2226–2227.
187. Inoue, Y.; Kuad, P.; Okumura, Y.; Takashima, Y.; Yamaguchi, H.; Harada, A. Thermal and Photochemical Switching of Conformation of Poly(ethylene glycol)-Substituted Cyclodextrin with an Azobenzene Group at the Chain End. *J. Am. Chem. Soc.* **2007**, *129*, 6396–6397.
188. Colquhoun, H. M.; Stoddart, J. F.; Williams, D. J. Second-Sphere Coordination–a Novel R le for Molecular Receptors. *Angew. Chem. Int. Ed. Engl.* **1986**, *25*, 487–507.
189. Raymo, F. M.; Stoddart, J. F. Second-Sphere Coordination. *Chem. Ber.* **1996**, *129*, 981–990.
190. Steed, J. W. First- and Second-Sphere Coordination Chemistry of Alkali Metal Crown Ether Complexes. *Coord. Chem. Rev.* **2001**, *215*, 171–221.
191. Liu, W.; Das, P. J.; Colquhoun, H. M.; Stoddart, J. F. Whither Second-Sphere Coordination? *CCS Chem.* **2022**, *4*, 755–784.
192. Colquhoun, H. M.; Stoddart, J. F.; Williams, D. J.; Wolstenholme, J. B.; Zarzycki, R. Second Sphere Coordination of Cationic Platinum Complexes by Crown Ethers—The X-Ray Crystal Structure of $[Pt(bpy)(NH_3)_2$•Dibenzo[30]crown-10$]^{2+}[PF_6]$•*x*H2O (x ≈ 0.6). *Angew. Chem. Int. Ed. Engl.* **1981**, *20*, 1051–1053.
193. Colquhoun, H. M.; Lewis, D. F.; Stoddart, J. F.; Williams, D. J. Crown Ethers as Second-Sphere Ligands. The Interactions of Transition-Metal Ammines with 18-Crown-6 and Dibenzo-18-crown-6. *J. Chem. Soc., Dalton Trans.* **1983**, 607–613.
194. Colquhoun, H. M.; Doughty, S. M.; Stoddart, J. F.; Williams, D. J. Second Sphere Coordination of Cationic Rhodium Complexes by Dibenzo[3*n*]crown-*n* Ethers. *Angew. Chem. Int. Ed. Engl.* **1984**, *23*, 235–236.
195. Alston, D. R.; Slawin, A. M. Z.; Stoddart, J. F.; Williams, D. J. Macrobicyclic Polyethers as V-Shaped Hosts for *cis*-Diammine-Transition Metal Complexes. *Angew. Chem. Int. Ed. Engl.* **1984**, *23*, 821–823.
196. Colquhoun, H. M.; Doughty, S. M.; Maud, J. M.; Stoddart, J. F.; Williams, D. J.; Wolstenholme, J. B. Second-Sphere Coordination of $[Pt(bipy)(NH_3)_2]^{2+}$ by Dibenzo-Crown Ethers. Solution Spectroscopic Studies and the Crystal and Molecular Structures of $[Pt(bipy)(NH_3)_2$•Dibenzo-30-crown-10$][PF_6]_2$•0.6 H_2O and $[Pt(bipy)(NH_3)_2$•Dibenzo-24-crown-8$][PF_6]_2$. *Isr. J. Chem.* **1985**, *25*, 15–26.
197. Alston, D. R.; Slawin, A. M. Z.; Stoddart, J. F.; Williams, D. J. Cyclodextrins as Second Sphere Ligands for Transition Metal Complexes—The X-Ray Crystal Structure of $[Rh(cod)(NH_3)_2$•α-Cyclodextrin$][PF_6]$•$6H_2O$. *Angew. Chem. Int. Ed. Engl.* **1985**, *24*, 786–787.
198. Alston, D. R.; Lilley, T. H.; Stoddart, J. F. The Binding of Cyclobutane-1,1-dicarboxylatodiamineplatinum(II) by α-Cyclodextrin in Aqueous Solution. *J. Chem. Soc., Chem. Commun.* **1985**, 1600–1602.
199. Alston, D. R.; Slawin, A. M. Z.; Stoddart, J. F.; Williams, D. J. The X-Ray Crystal Structure of a 1:1 Adduct Between α-Cyclodextrin and Cyclobutane-1,1-dicarboxylatodiammineplationum(II). *J. Chem. Soc., Chem. Commun.* **1985**, 1602–1604.
200. Ashton, P. R.; Stoddart, J. F.; Zarzycki, R. Mass Spectrometric Investigation of Adduct Formation by Methylated Cyclodextrins. *Tetrahedron Lett.* **1988**, *29*, 2103–2106.
201. Alston, D. R.; Slawin, A. M. Z.; Stoddart, J. F.; Williams, D. J.; Zarzycki, R. Second Sphere Coordination Adducts of Phosphane-Transition Metal Complexes with β-Cyclodextrin and Its Methylated Derivative. *Angew. Chem. Int. Ed. Engl.* **1988**, *27*, 1184–1185.
202. Alston, D. R.; Ashton, P. R.; Lilley, T. H.; Stoddart, J. F.; Zarzycki, R.; Slawin, A. M. Z.; Williams, D. J. Second-Sphere Co-Ordination of Carboplatin and Rhodium Complexes by Cyclodextrins (Cyclomalto-Oligosaccharides). *Carbohydr. Res.* **1989**, *192*, 259–281.
203. Stoddart, J. F.; Zarzycki, R. Cyclodextrins as Second-Sphere Ligands for Transition Metal Complexes. *Recl. Trav. Chim. Pays-Bas* **1988**, *107*, 515–528.
204. Utsuki, T.; Brem, H.; Pitha, J.; Loftsson, T.; Kristmundsdottir, T.; Tyler, B. M.; Olivi, A. Potentiation of Anticancer Effects of Microencapsulated Carboplatin by Hydroxypropyl α-Cyclodextrin. *J. Control. Release* **1996**, *40*, 251–260.

DOI: 10.31635/ccschem.025.202505711
Citation: *CCS Chem.* **2025**, 7, 1935–1971
Link to VoR: https://doi.org/10.31635/ccschem.025.202505711

205. Liu, Z.; Schneebeli, S. T.; Stoddart, J. F. Second-Sphere Coordination Revisited. *Chimia* **2014**, *68*, 315–320.
206. Liu, Z.; Frasconi, M.; Lei, J.; Brown, Z. J.; Zhu, Z.; Cao, D.; Iehl, J.; Liu, G.; Fahrenbach, A. C.; Botros, Y. Y.; Farha, O. K.; Hupp, J. T.; Mirkin, C. A.; Stoddart, J. F. Selective Isolation of Gold Facilitated by Second-Sphere Coordination with α-Cyclodextrin. *Nat. Commun.* **2013**, *4*, 1855.
207. Liu, Z.; Samanta, A.; Lei, J.; Sun, J.; Wang, Y.; Stoddart, J. F. Cation-Dependent Gold Recovery with α-Cyclodextrin Facilitated by Second-Sphere Coordination. *J. Am. Chem. Soc.* **2016**, *138*, 11643–11653.
208. Wu, H.; Wang, Y.; Tang, C.; Jones, L. O.; Song, B.; Chen, X.-Y.; Zhang, L.; Wu, Y.; Stern, C. L.; Schatz, G. C.; Liu, W.; Stoddart, J. F. High-Efficiency Gold Recovery by Additive-Induced Supramolecular Polymerization of β-Cyclodextrin. *Nat. Commun.* **2023**, *14*, 1284.
209. Ubaldini, S.; Massidda, R.; Vegliò, F.; Beolchini, F. Gold Stripping by Hydro-Alcoholic Solutions from Activated Carbon: Experimental Results and Data Analysis by a Semi-Empirical Model. *Hydrometallurgy* **2006**, *81*, 40–44.
210. Soleimani, M.; Kaghazchi, T. Gold Recovery from Loaded Activated Carbon Using Different Solvents. *J. Chin. Inst. Chem. Eng*, **2008**, *39*, 9–11.
211. Bunney, K.; Jeffrey, M. I.; Pleysier, R.; Breuer, P. L. Selective Elution of Gold, Silver and Mercury Cyanide from Activated Carbon. *Min. Metall. Explor.* **2010**, *27*, 205–211.
212. Liu, W.; Jones, L. O.; Wu, H.; Stern, C. L.; Sponenburg, R. A.; Schatz, G. C.; Stoddart, J. F. Supramolecular Gold Stripping from Activated Carbon Using α-Cyclodextrin. *J. Am. Chem. Soc.* **2021**, *143*, 1984–1992.
213. Yaghi, O. M.; Li, G.; Li, H. Selective Binding and Removal of Guests in a Microporous Metal–Organic Framework. *Nature* **1995**, *378*, 703–706.
214. Furukawa, H.; Cordova, K. E.; O'Keeffe, M.; Yaghi, O. M. The Chemistry and Applications of Metal–Organic Frameworks. *Science* **2013**, *341*, 1230444.
215. McKinlay, A. C.; Morris, R. E.; Horcajada, P.; Férey, G.; Gref, R.; Couvreur, P.; Serre, C. BioMOFs: Metal–Organic Frameworks for Biological and Medical Applications. *Angew. Chem. Int. Ed.* **2010**, *49*, 6260–6266.
216. Imaz, I.; Rubio-Martínez, M.; An, J.; Solé-Font, I.; Rosi, N. L.; Maspoch, D. Metal–Biomolecule Frameworks (MBioFs). *Chem. Commun.* **2011**, *47*, 7287–7302.
217. Rojas, S.; Devic, T.; Horcajada, P. Metal Organic Frameworks Based on Bioactive Components. *J. Mater. Chem. B* **2017**, *5*, 2560–2573.
218. Smaldone, R. A.; Forgan, R. S.; Furukawa, H.; Gassensmith, J. J.; Slawin, A. M. Z.; Yaghi, O. M.; Stoddart, J. F. Metal–Organic Frameworks from Edible Natural Products. *Angew. Chem. Int. Ed.* **2010**, *49*, 8630–8634.
219. Holman, K. T. Molecule-Constructed Microporous Materials: Long Under Our Noses, Increasingly on Our Tongues, and Now in Our Bellies. *Angew. Chem. Int. Ed.* **2011**, *50*, 1228–1230.
220. Bonacchi, D.; Caneschi, A.; Dorignac, D.; Falqui, A.; Gatteschi, D.; Rovai, D.; Sangregorio, C.; Sessoli, R. Nanosized Iron Oxide Particles Entrapped in Pseudo-Single Crystals of γ-Cyclodextrin. *Chem. Mater.* **2004**, *16*, 2016–2020.
221. Forgan, R. S.; Smaldone, R. A.; Gassensmith, J. J.; Furukawa, H.; Cordes, D. B.; Li, Q.; Wilmer, C. E.; Botros, Y. Y.; Snurr, R. Q.; Slawin, A. M. Z.; Stoddart, J. F. Nanoporous Carbohydrate Metal–Organic Frameworks. *J. Am. Chem. Soc.* **2012**, *134*, 406–417.
222. Pichon, A. Making a Meal of MOFs. *Nat. Chem.* **2010**, *2*. DOI: https://doi.org/10.1038/nchem.855
223. Gassensmith, J. J.; Smaldone, R. A.; Forgan, R. S.; Wilmer, C. E.; Cordes, D. B.; Botros, Y. Y.; Slawin, A. M. Z.; Snurr, R. Q.; Stoddart, J. F. Polyporous Metal-Coordination Frameworks. *Org. Lett.* **2012**, *14*, 1460–1463.
224. Bagabas, A. A.; Frasconi, M.; Iehl, J.; Hauser, B.; Farha, O. K.; Hupp, J. T.; Hartlieb, K. J.; Botros, Y. Y.; Stoddart, J. F. γ-Cyclodextrin Cuprate Sandwich-Type Complexes. *Inorg. Chem.* **2013**, *52*, 2854–2861.
225. Wu, Y.; Shi, R.; Wu, Y.-L.; Holcroft, J. M.; Liu, Z.; Frasconi, M.; Wasielewski, M. R.; Li, H.; Stoddart, J. F. Complexation of Polyoxometalates with Cyclodextrins. *J. Am. Chem. Soc.* **2015**, *137*, 4111–4118.
226. Hartlieb, K. J.; Peters, A. W.; Wang, T. C.; Deria, P.; Farha, O. K.; Hupp, J. T.; Stoddart, J. F. Functionalised Cyclodextrin-Based Metal–Organic Frameworks. *Chem. Commun.* **2017**, *53*, 7561–7564.
227. Patel, H. A.; Islamoglu, T.; Liu, Z.; Nalluri, S. K. M.; Samanta, A.; Anamimoghadam, O.; Malliakas, C. D.; Farha, O. K.; Stoddart, J. F. Noninvasive Substitution of K^+ Sites in Cyclodextrin Metal–Organic Frameworks by Li^+ Ions. *J. Am. Chem. Soc.* **2017**, *139*, 11020–11023.
228. Wu, Y.; Tang, C.; Lee, J. T.; Zhang, R.; Bhunia, S.; Kundu, P.; Stern, C. L.; Chen, A. X.-Y.; Shen, D.; Yang, S.; Han, H.; Li, X.; Wu, H.; Feng, Y.; Armstrong, D. W.; Stoddart, J. F. Metal-Assisted Carbohydrate Assembly. *J. Am. Chem. Soc.* **2024**, *146*, 9801–9810.
229. Shen, D.; Zhang, Z.; Kesharwani, T.; Wu, H.; Zhang, L.; Stern, C. L.; Chen, H.; Guo, Q.-H.; Cai, K.; Chen, A. X.-Y.; Stoddart, J. F. Electrostatically Dominated Pre-Organization in Cyclodextrin Metal-Organic Frameworks. *Angew. Chem. Int. Ed.* **2024**, *63*, e202415404.
230. Lu, H.; Yang, X.; Li, S.; Zhang, Y.; Sha, J.; Li, C.; Sun, J. Study on a New Cyclodextrin Based Metal–Organic Framework with Chiral Helices. *Inorg. Chem. Commun.* **2015**, *61*, 48–52.
231. Sha, J.-Q.; Wu, L.-H.; Li, S.-X.; Yang, X.-N.; Zhang, Y.; Zhang, Q.-N.; Zhu, P.-P. Synthesis and Structure of New Carbohydrate Metal–Organic Frameworks and Inclusion Complexes. *J. Mol. Struct.* **2015**, *1101*, 14–20.
232. Sha, J.-Q.; Zhong, X.-H.; Wu, L.-H.; Liu, G.-D.; Sheng, N. Nontoxic and Renewable Metal–Organic Framework Based on α-Cyclodextrin with Efficient Drug Delivery. *RSC Adv.* **2016**, *6*, 82977–82983.
233. Xu, H.; Rodríguez-Hermida, S.; Pérez-Carvajal, J.; Juanhuix, J.; Imaz, I.; Maspoch, D. A First Cyclodextrin-Transition Metal Coordination Polymer. *Cryst. Growth Des.* **2016**, *16*, 5598–5602.
234. Liu, J.; Bao, T.-Y.; Yang, X.-Y.; Zhu, P.-P.; Wu, L.-H.; Sha, J.-Q.; Zhang, L.; Dong, L.-Z.; Cao, X.-L.; Lan, Y.-Q. Controllable Porosity Conversion of Metal–Organic Frameworks

DOI: 10.31635/ccschem.025.202505711
Citation: *CCS Chem.* **2025**, 7, 1935–1971
Link to VoR: https://doi.org/10.31635/ccschem.025.202505711

Composed of Natural Ingredients for Drug Delivery. *Chem. Commun.* **2017**, *53*, 7804–7807.
235. Sha, J.; Yang, X.; Sun, L.; Zhang, X.; Li, S.; Li, J.; Sheng, N. Unprecedented α-Cyclodextrin Metal–Organic Frameworks with Chirality: Structure and Drug Adsorptions. *Polyhedron* **2017**, *127*, 396–402.
236. Yang, P.; Zhao, W.; Shkurenko, A.; Belmabkhout, Y.; Eddaoudi, M.; Dong, X.; Alshareef, H. N.; Khashab, N. M. Polyoxometalate–Cyclodextrin Metal–Organic Frameworks: From Tunable Structure to Customized Storage Functionality. *J. Am. Chem. Soc.* **2019**, *141*, 1847–1851.
237. Koshevoy, E. I.; Samsonenko, D. G.; Berezin, A. S.; Fedin, V. P. Metal–Organic Coordination Polymers Formed from γ-Cyclodextrin and Divalent Metal Ions. *Eur. J. Inorg. Chem.* **2019**, *2019*, 4321–4327.
238. Xu, L.; Xing, C.-Y.; Ke, D.; Chen, L.; Qiu, Z.-J.; Zeng, S.-L.; Li, B.-J.; Zhang, S. Amino-Functionalized β-Cyclodextrin to Construct Green Metal–Organic Framework Materials for CO_2 Capture. *ACS Appl. Mater. Interfaces* **2020**, *12*, 3032–3041.
239. Shen, D.; Cooper, J. A.; Li, P.; Guo, Q.-H.; Cai, K.; Wang, X.; Wu, H.; Chen, H.; Zhang, L.; Jiao, Y.; Qiu, Y.; Stern, C. L.; Liu, Z.; Sue, A. C.-H.; Yang, Y.-W.; Alsubaie, F. M.; Farha, O. K.; Stoddart, J. F. Organic Counteranion Co-Assembly Strategy for the Formation of γ-Cyclodextrin-Containing Hybrid Frameworks. *J. Am. Chem. Soc.* **2020**, *142*, 2042–2050.
240. Li, H.; Shi, L.; Li, C.; Fu, X.; Huang, Q.; Zhang, B. Metal–Organic Framework Based on α-Cyclodextrin Gives High Ethylene Gas Adsorption Capacity and Storage Stability. *ACS Appl. Mater. Interfaces* **2020**, *12*, 34095–34104.
241. Shahzaib, A.; Shaily; Ahmad, I.; Singh, P.; Zafar, F.; Akhtar, Y.; Bukhari, A. A.; Nishat, N. Ultrarapid and Highly Efficient Reduction of Nitroaromatic Compounds Using Cyclodextrin MOF. *Catal. Commun.* **2023**, *174*, 106569.
242. Gassensmith, J. J.; Furukawa, H.; Smaldone, R. A.; Forgan, R. S.; Botros, Y. Y.; Yaghi, O. M.; Stoddart, J. F. Strong and Reversible Binding of Carbon Dioxide in a Green Metal–Organic Framework. *J. Am. Chem. Soc.* **2011**, *133*, 15312–15315.
243. Zick, M. E.; Pugh, S. M.; Lee, J.-H.; Forse, A. C.; Milner, P. J. Carbon Dioxide Capture at Nucleophilic Hydroxide Sites in Oxidation-Resistant Cyclodextrin-Based Metal–Organic Frameworks. *Angew. Chem. Int. Ed.* **2022**, *61*, e202206718.
244. Wu, D.; Gassensmith, J. J.; Gouvêa, D.; Ushakov, S.; Stoddart, J. F.; Navrotsky, A. Direct Calorimetric Measurement of Enthalpy of Adsorption of Carbon Dioxide on CD-MOF-2, a Green Metal–Organic Framework. *J. Am. Chem. Soc.* **2013**, *135*, 6790–6793.
245. Wei, Y.; Han, S.; Walker, D. A.; Fuller, P. E.; Grzybowski, B. A. Nanoparticle Core/Shell Architectures Within MOF Crystals Synthesized by Reaction Diffusion. *Angew. Chem. Int. Ed.* **2012**, *51*, 7435–7439.
246. Shakya, S.; He, Y.; Ren, X.; Guo, T.; Maharjan, A.; Luo, T.; Wang, T.; Dhakhwa, R.; Regmi, B.; Li, H.; Gref, R.; Zhang, J. Ultrafine Silver Nanoparticles Embedded in Cyclodextrin Metal–Organic Frameworks with GRGDS Functionalization to Promote Antibacterial and Wound Healing Application. *Small* **2019**, *15*, 1901065.
247. Furukawa, Y.; Ishiwata, T.; Sugikawa, K.; Kokado, K.; Sada, K. Nano- and Microsized Cubic Gel Particles from Cyclodextrin Metal–Organic Frameworks. *Angew. Chem. Int. Ed.* **2012**, *51*, 10566–10569.
248. Han, S.; Wei, Y.; Valente, C.; Forgan, R. S.; Gassensmith, J. J.; Smaldone, R. A.; Nakanishi, H.; Coskun, A.; Stoddart, J. F.; Grzybowski, B. A. Imprinting Chemical and Responsive Micropatterns into Metal–Organic Frameworks. *Angew. Chem. Int. Ed.* **2011**, *50*, 276–279.
249. Gassensmith, J. J.; Kim, J. Y.; Holcroft, J. M.; Farha, O. K.; Stoddart, J. F.; Hupp, J. T.; Jeong, N. C. A Metal–Organic Framework-Based Material for Electrochemical Sensing of Carbon Dioxide. *J. Am. Chem. Soc.* **2014**, *136*, 8277–8282.
250. Shen, D.; Wang, G.; Liu, Z.; Li, P.; Cai, K.; Cheng, C.; Shi, Y.; Han, J.-M.; Kung, C.-W.; Gong, X.; Guo, Q.-H.; Chen, H.; Sue, A. C.-H.; Botros, Y. Y.; Facchetti, A.; Farha, O. K.; Marks, T. J.; Stoddart, J. F. Epitaxial Growth of γ-Cyclodextrin-Containing Metal–Organic Frameworks Based on a Host–Guest Strategy. *J. Am. Chem. Soc.* **2018**, *140*, 11402–11407.
251. Yoon, S. M.; Warren, S. C.; Grzybowski, B. A. Storage of Electrical Information in Metal–Organic Framework Memristors. *Angew. Chem. Int. Ed.* **2014**, *53*, 4437–4441.
252. Holcroft, J. M.; Hartlieb, K. J.; Moghadam, P. Z.; Bell, J. G.; Barin, G.; Ferris, D. P.; Bloch, E. D.; Algaradah, M. M.; Nassar, M. S.; Botros, Y. Y.; Thomas, K. M.; Long, J. R.; Snurr, R. Q.; Stoddart, J. F. Carbohydrate-Mediated Purification of Petrochemicals. *J. Am. Chem. Soc.* **2015**, *137*, 5706–5719.
253. Hartlieb, K. J.; Holcroft, J. M.; Moghadam, P. Z.; Vermeulen, N. A.; Algaradah, M. M.; Nassar, M. S.; Botros, Y. Y.; Snurr, R. Q.; Stoddart, J. F. CD-MOF: A Versatile Separation Medium. *J. Am. Chem. Soc.* **2016**, *138*, 2292–2301.
254. Nuñez-Lopez, A.; Galbiati, M.; Padial, N. M.; Ganivet, C. R.; Tatay, S.; Pardo, E.; Armentano, D.; Martí-Gastaldo, C. Direct Visualization of Pyrrole Reactivity upon Confinement within a Cyclodextrin Metal-Organic Framework. *Angew. Chem. Int. Ed.* **2019**, *58*, 9179–9183.
255. Zhao, Y.; Zhuang, S.; Liao, L.; Wang, C.; Xia, N.; Gan, Z.; Gu, W.; Li, J.; Deng, H.; Wu, Z. A Dual Purpose Strategy to Endow Gold Nanoclusters with Both Catalysis Activity and Water Solubility. *J. Am. Chem. Soc.* **2020**, *142*, 973–977.
256. Hu, L.; Li, K.; Shang, W.; Zhu, X.; Liu, M. Emerging Cubic Chirality in γCD-MOF for Fabricating Circularly Polarized Luminescent Crystalline Materials and the Size Effect. *Angew. Chem. Int. Ed.* **2020**, *59*, 4953–4958.
257. Kazem-Rostami, M.; Orte, A.; Ortuño, A. M.; David, A. H. G.; Roy, I.; Miguel, D.; Garci, A.; Cruz, C. M.; Stern, C. L.; Cuerva, J. M.; Stoddart, J. F. Helically Chiral Hybrid Cyclodextrin Metal–Organic Framework Exhibiting Circularly Polarized Luminescence. *J. Am. Chem. Soc.* **2022**, *144*, 9380–9389.
258. Chen, X.-Y.; Chen, H.; Đorđević, L.; Guo, Q.-H.; Wu, H.; Wang, Y.; Zhang, L.; Jiao, Y.; Cai, K.; Chen, H.; Stern, C. L.; Stupp, S. I.; Snurr, R. Q.; Shen, D.; Stoddart, J. F. Selective

DOI: 10.31635/ccschem.025.202505711
Citation: *CCS Chem.* **2025**, 7, 1935–1971
Link to VoR: https://doi.org/10.31635/ccschem.025.202505711

Photodimerization in a Cyclodextrin Metal–Organic Framework. *J. Am. Chem. Soc.* **2021**, *143*, 9129–9139.
259. Chen, A. X.-Y.; Kesharwani, T.; Wu, Y.; Stern, C. L.; Đorđević, L.; Wu, H.; Wang, Y.; Song, B.; Feng, L.; Zhang, L.; Zhao, X.; Jiao, Y.; Li, X.; Han, H.; Tang, C.; Zhang, R.; Chen, H.; Cai, K.; Stupp, S. I.; Chen, H.; Shen, D.; Stoddart, J. F. Site-Selective C–H Functionalization in a Cyclodextrin Metal–Organic Framework. *Chem* **2024**, *10*, 234–249.
260. Di Palma, G.; Geels, S.; Carpenter, B. P.; Talosig, R. A.; Chen, C.; Marangoni, F.; Patterson, J. P. Cyclodextrin Metal–Organic Framework-Based Protein Biocomposites. *Biomater. Sci.* **2022**, *10*, 6749–6754.
261. Hartlieb, K. J.; Ferris, D. P.; Holcroft, J. M.; Kandela, I.; Stern, C. L.; Nassar, M. S.; Botros, Y. Y.; Stoddart, J. F. Encapsulation of Ibuprofen in CD-MOF and Related Bioavailability Studies. *Mol. Pharmaceutics* **2017**, *14*, 1831–1839.
262. Li, H.; Lv, N.; Li, X.; Liu, B.; Feng, J.; Ren, X.; Guo, T.; Chen, D.; Stoddart, J. F.; Gref, R.; Zhang, J. Composite CD-MOF Nanocrystals-Containing Microspheres for Sustained Drug Delivery. *Nanoscale* **2017**, *9*, 7454–7463.
263. Hu, X.; Wang, C.; Wang, L.; Liu, Z.; Wu, L.; Zhang, G.; Yu, L.; Ren, X.; York, P.; Sun, L.; Zhang, J.; Li, H. Nanoporous CD-MOF Particles with Uniform and Inhalable Size for Pulmonary Delivery of Budesonide. *Int. J. Pharm.* **2019**, *564*, 153–161.
264. Liu, Z.; Stoddart, J. F. Extended Metal–Carbohydrate Frameworks. *Pure Appl. Chem.* **2014**, *86*, 1323–1334.
265. Han, Y.; Liu, W.; Huang, J.; Qiu, S.; Zhong, H.; Liu, D.; Liu, J. Cyclodextrin-Based Metal–Organic Frameworks (CD-MOFs) in Pharmaceutics and Biomedicine. *Pharmaceutics* **2018**, *10*, 271.
266. Rajkumar, T.; Kukkar, D.; Kim, K.-H.; Sohn, J. R.; Deep, A. Cyclodextrin-Metal–Organic Framework (CD-MOF): From Synthesis to Applications. *J. Ind. Eng. Chem.* **2019**, *72*, 50–66.
267. Hamedi, A.; Anceschi, A.; Patrucco, A.; Hasanzadeh, M. A γ-Cyclodextrin-Based Metal–Organic Framework (γ-CD-MOF): A Review of Recent Advances for Drug Delivery Application. *J. Drug Target.* **2022**, *30*, 381–393.
268. Bruns, C. J.; Stoddart, J. F. *The Nature of the Mechanical Bond: From Molecules to Machines*; Wiley: Hoboken, NJ, **2016**.
269. Stoddart, J. F. Mechanically Interlocked Molecules (MIMs)—Molecular Shuttles, Switches, and Machines (Nobel Lecture). *Angew. Chem. Int. Ed.* **2017**, *56*, 11094–11125.
270. Bruns, C. J. Exploring and Exploiting the Symmetry-Breaking Effect of Cyclodextrins in Mechanomolecules. *Symmetry* **2019**, *11*, 1249.
271. Beeren, S. R.; McTernan, C. T.; Schaufelberger, F. The Mechanical Bond in Biological Systems. *Chem* **2023**, *9*, 1378–1412.
272. Lüttringhaus, A.; Cramer, F.; Prinzbach, H.; Henglein, F. M. Cyclisationen Von Langkettigen Dithiolen. Versuche zur Darstellung sich umfassender Ringe mit Hilfe von Einschlußverbindungen. *Justus Liebigs Ann. Chem.* **1958**, *613*, 185–198.
273. Armspach, D.; Ashton, P. R.; Moore, C. P.; Spencer, N.; Stoddart, J. F.; Wear, T. J.; Williams, D. J. The Self-Assembly of Catenated Cyclodextrins. *Angew. Chem. Int. Ed. Engl.* **1993**, *32*, 854–858.
274. Armspach, D.; Ashton, P. R.; Ballardini, R.; Balzani, V.; Godi, A.; Moore, C. P.; Prodi, L.; Spencer, N.; Stoddart, J. F.; Tolley, M. S.; Wear, T. J.; Williams, D. J. Catenated Cyclodextrins. *Chem. Eur. J.* **1995**, *1*, 33–55.
275. Hou, X.; Ke, C.; Stoddart, J. F. Cooperative Capture Synthesis: Yet Another Playground for Copper-Free Click Chemistry. *Chem. Soc. Rev.* **2016**, *45*, 3766–3780.
276. Mock, W. L.; Irra, T. A.; Wepsiec, J. P.; Manimaran, T. L. Cycloaddition Induced by Cucurbituril. A Case of Pauling Principle Catalysis. *J. Org. Chem.* **1983**, *48*, 3619–3620.
277. Mock, W. L.; Irra, T. A.; Wepsiec, J. P.; Adhya, M. Catalysis by Cucurbituril. The Significance of Bound-Substrate Destabilization for Induced Triazole Formation. *J. Org. Chem.* **1989**, *54*, 5302–5308.
278. Tuncel, D.; Steinke, J. H. G. Catalytically Self-Threading Polyrotaxanes. *Chem. Commun.* **1999**, 1509–1510.
279. Tuncel, D.; Steinke, J. H. G. The Synthesis of [2], [3] and [4]Rotaxanes and Semirotaxanes. *Chem. Commun.* **2002**, 496–497.
280. Tuncel, D.; Steinke, J. H. G. Catalytic Self-Threading: A New Route for the Synthesis of Polyrotaxanes. *Macromolecules* **2004**, *37*, 288–302.
281. Ke, C.; Smaldone, R. A.; Kikuchi, T.; Li, H.; Davis, A. P.; Stoddart, J. F. Quantitative Emergence of Hetero[4]rotaxanes by Template-Directed Click Chemistry. *Angew. Chem. Int. Ed.* **2013**, *52*, 381–387.
282. Han, H.; Seale, J. S. W.; Feng, L.; Qiu, Y.; Stoddart, J. F. Sequence-Controlled Synthesis of Rotaxanes. *J. Polym. Sci.* **2023**, *61*, 881–902.
283. Hou, X.; Ke, C.; Bruns, C. J.; McGonigal, P. R.; Pettman, R. B.; Stoddart, J. F. Tunable Solid-State Fluorescent Materials for Supramolecular Encryption. *Nat. Commun.* **2015**, *6*, 6884.
284. Fulton, D. A.; Cantrill, S. J.; Stoddart, J. F. Probing Polyvalency in Artificial Systems Exhibiting Molecular Recognition. *J. Org. Chem.* **2002**, *67*, 7968–7981.
285. Badjić, J. D.; Nelson, A.; Cantrill, S. J.; Turnbull, W. B.; Stoddart, J. F. Multivalency and Cooperativity in Supramolecular Chemistry. *Acc. Chem. Res.* **2005**, *38*, 723–732.
286. Nelson, A.; Stoddart, J. F. Dynamic Multivalent Lactosides Displayed on Cyclodextrin Beads Dangling from Polymer Strings. *Org. Lett.* **2003**, *5*, 3783–3786.
287. Nelson, A.; Belitsky, J. M.; Vidal, S.; Joiner, C. S.; Baum, L. G.; Stoddart, J. F. A Self-Assembled Multivalent Pseudopolyrotaxane for Binding Galectin-1. *J. Am. Chem. Soc.* **2004**, *126*, 11914–11922.
288. Belitsky, J. M.; Nelson, A.; Stoddart, J. F. Monitoring Cyclodextrin–Polyviologen Pseudopolyrotaxanes with the Bradford Assay. *Org. Biomol. Chem.* **2006**, *4*, 250–256.
289. Belitsky, J. M.; Nelson, A.; Hernandez, J. D.; Baum, L. G.; Stoddart, J. F. Multivalent Interactions Between Lectins and Supramolecular Complexes: Galectin-1 and Self-Assembled Pseudopolyrotaxanes. *Chem. Biol.* **2007**, *14*, 1140–1151.
290. Nguyen, T. D.; Tseng, H.-R.; Celestre, P. C.; Flood, A. H.; Liu, Y.; Stoddart, J. F.; Zink, J. I. A Reversible Molecular Valve. *Proc. Natl. Acad. Sci. U. S. A.* **2005**, *102*, 10029–10034.

DOI: 10.31635/ccschem.025.202505711
Citation: *CCS Chem.* **2025**, 7, 1935–1971
Link to VoR: https://doi.org/10.31635/ccschem.025.202505711

291. Patel, K.; Angelos, S.; Dichtel, W. R.; Coskun, A.; Yang, Y.-W.; Zink, J. I.; Stoddart, J. F. Enzyme-Responsive Snap-Top Covered Silica Nanocontainers. *J. Am. Chem. Soc.* **2008**, *130*, 2382–2383.
292. Tornøe, C. W.; Christensen, C.; Meldal, M. Peptidotriazoles on Solid Phase: [1,2,3]-Triazoles by Regiospecific Copper (I)-Catalyzed 1,3-Dipolar Cycloadditions of Terminal Alkynes to Azides. *J. Org. Chem.* **2002**, *67*, 3057–3064.
293. Rostovtsev, V. V.; Green, L. G.; Fokin, V. V.; Sharpless, K. B. A Stepwise Huisgen Cycloaddition Process: Copper(I)-Catalyzed Regioselective "Ligation" of Azides and Terminal Alkynes. *Angew. Chem. Int. Ed.* **2002**, *41*, 2596–2599.
294. Ferris, D. P.; Zhao, Y.-L.; Khashab, N. M.; Khatib, H. A.; Stoddart, J. F.; Zink, J. I. Light-Operated Mechanized Nanoparticles. *J. Am. Chem. Soc.* **2009**, *131*, 1686–1688.
295. Tarn, D.; Ferris, D. P.; Barnes, J. C.; Ambrogio, M. W.; Stoddart, J. F.; Zink, J. I. A Reversible Light-Operated Nanovalve on Mesoporous Silica Nanoparticles. *Nanoscale* **2014**, *6*, 3335–3343.
296. Khashab, N. M.; Trabolsi, A.; Lau, Y. A.; Ambrogio, M. W.; Friedman, D. C.; Khatib, H. A.; Zink, J. I.; Stoddart, J. F. Redox- and pH-Controlled Mechanized Nanoparticles. *Eur. J. Org. Chem.* **2009**, *2009*, 1669–1673.
297. Ambrogio, M. W.; Pecorelli, T. A.; Patel, K.; Khashab, N. M.; Trabolsi, A.; Khatib, H. A.; Botros, Y. Y.; Zink, J. I.; Stoddart, J. F. Snap-Top Nanocarriers. *Org. Lett.* **2010**, *12*, 3304–3307.
298. Wang, C.; Li, Z.; Cao, D.; Zhao, Y.-L.; Gaines, J. W.; Bozdemir, O. A.; Ambrogio, M. W.; Frasconi, M.; Botros, Y. Y.; Zink, J. I.; Stoddart, J. F. Stimulated Release of Size-Selected Cargos in Succession from Mesoporous Silica Nanoparticles. *Angew. Chem. Int. Ed.* **2012**, *51*, 5460–5465.
299. Du, L.; Liao, S.; Khatib, H. A.; Stoddart, J. F.; Zink, J. I. Controlled-Access Hollow Mechanized Silica Nanocontainers. *J. Am. Chem. Soc.* **2009**, *131*, 15136–15142.
300. Meng, H.; Xue, M.; Xia, T.; Zhao, Y.-L.; Tamanoi, F.; Stoddart, J. F.; Zink, J. I.; Nel, A. E. Autonomous in Vitro Anticancer Drug Release from Mesoporous Silica Nanoparticles by pH-Sensitive Nanovalves. *J. Am. Chem. Soc.* **2010**, *132*, 12690–12697.
301. Zhao, Y.-L.; Li, Z.; Kabehie, S.; Botros, Y. Y.; Stoddart, J. F.; Zink, J. I. pH-Operated Nanopistons on the Surfaces of Mesoporous Silica Nanoparticles. *J. Am. Chem. Soc.* **2010**, *132*, 13016–13025.
302. Xue, M.; Cao, D.; Stoddart, J. F.; Zink, J. I. Size-Selective pH-Operated Megagates on Mesoporous Silica Materials. *Nanoscale* **2012**, *4*, 7569–7574.
303. Yilmaz, M. D.; Xue, M.; Ambrogio, M. W.; Buyukcakir, O.; Wu, Y.; Frasconi, M.; Chen, X.; Nassar, M. S.; Stoddart, J. F.; Zink, J. I. Sugar and pH Dual-Responsive Mesoporous Silica Nanocontainers Based on Competitive Binding Mechanisms. *Nanoscale* **2015**, *7*, 1067–1072.
304. Cotí, K. K.; Belowich, M. E.; Liong, M.; Ambrogio, M. W.; Lau, Y. A.; Khatib, H. A.; Zink, J. I.; Khashab, N. M.; Stoddart, J. F. Mechanised Nanoparticles for Drug Delivery. *Nanoscale* **2009**, *1*, 16–39.
305. Ambrogio, M. W.; Thomas, C. R.; Zhao, Y.-L.; Zink, J. I.; Stoddart, J. F. Mechanized Silica Nanoparticles: A New Frontier in Theranostic Nanomedicine. *Acc. Chem. Res.* **2011**, *44*, 903–913.
306. McGonigal, P. R.; Stoddart, J. F. Serendipity. In *Macrocyclic and Supramolecular Chemistry: How Izatt–Christensen Award Winners Shaped the Field*; Izatt, R. M., Ed.; Wiley: Chichester, West Sussex, **2016**; pp 388–414.
307. Liu, E.; Cherraben, S.; Boulo, L.; Troufflard, C.; Hasenknopf, B.; Vives, G.; Sollogoub, M. A Molecular Information Ratchet Using a Cone-Shaped Macrocycle. *Chem* **2023**, *9*, 1147–1163.
308. Zhang, L.; Wu, H.; Li, X.; Chen, H.; Astumian, R. D.; Stoddart, J. F. Artificial Molecular Pumps. *Nat. Rev. Methods Primers* **2024**, *4*, 13.
309. Ikuta, D.; Hirata, Y.; Wakamori, S.; Shimada, H.; Tomabechi, Y.; Kawasaki, Y.; Ikeuchi, K.; Hagimori, T.; Matsumoto, S.; Yamada, H. Conformationally Supple Glucose Monomers Enable Synthesis of the Smallest Cyclodextrins. *Science* **2019**, *364*, 674–677.
310. Hansen, K. H.; Erichsen, A.; Larsen, D.; Beeren, S. R. Enzyme-Mediated Dynamic Combinatorial Chemistry Enables Large-Scale Synthesis of δ-Cyclodextrin. *J. Am. Chem. Soc.* **2025**, *147*, 13851–13858.
311. Houk, K. N.; Leach, A. G.; Kim, S. P.; Zhang, X. Binding Affinities of Host–Guest, Protein–Ligand, and Protein–Transition–State Complexes. *Angew. Chem. Int. Ed.* **2003**, *42*, 4872–4897.
312. Stoddart, J. F. Cyclodextrins, Off-the-Shelf Components for the Construction of Mechanically Interlocked Molecular Systems. *Angew. Chem. Int. Ed. Engl.* **1992**, *31*, 846–848.
313. Chatt, J. A Half Century of Platinum Metal Chemistry. *Platin. Met. Rev.* **1985**, *29*, 126–130.

DOI: 10.31635/ccschem.025.202505711
Citation: *CCS Chem.* **2025**, 7, 1935–1971
Link to VoR: https://doi.org/10.31635/ccschem.025.202505711